SPATIAL MODELLING OF FIRE DYNAMICS IN SAVANNA ECOSYSTEMS

by

Stephen Gary Berjak

Submitted in fulfilment of the academic
requirements for the degree of

Master of Science

in the
Department of Mathematics and Applied Mathematics
University of Natal

Pietermaritzburg
1999

ABSTRACT

Fire is used in the management of ecosystems worldwide because it is a relatively inexpensive means of manipulating thousands of hectares of vegetation. Deciding how, where and when to apply fire depends primarily on the management objectives of the area concerned. The decision to ignite vegetation is generally subjective and depends on the experience of the fire manager. To facilitate this process, ancillary tools, forming a decision support system, need to be constructed.

In this study a spatial model has been developed that is capable of simulating fire dynamics in savanna ecosystems. The fire growth model integrates spatial fuel and topographic data with temporal weather, wind settings and fuel moistures to produce a time-evolving fire front. Spatial information required to operate the model was obtained through remote sensing techniques, using Landsat Thematic Mapper (TM) satellite imagery, and existing Geographic Information Systems (GIS) coverage's.

Implementation of the simulation model to hypothetical landscapes under various scenarios of fuel, weather and topography produced fire fronts that were found to be in good agreement with experience of observed fires. The model was applied actual fire events using information for prescribed burning operations conducted in Mkuze Game Reserve during 1997. Predicted fire fronts were found to accurately resemble the observed fire boundaries in all simulations.

PREFACE

The work described in this dissertation was carried out in the Department of Mathematics and Applied Mathematics, University of Natal, Pietermaritzburg, from February 1998 to October 1999, under the supervision of Professor John Hearne.

These studies represent original work by the author and have not otherwise been submitted in any form for any degree or diploma at any University. Where use has been made of the work of others it is duly acknowledged in the text.

Stephen G. Berjak
Pietermaritzburg
1999.

TABLE OF CONTENTS

TABLE OF ILLUSTRATIONS

LIST OF TABLES

ACKNOWLEDGEMENTS

I would like to take this opportunity to acknowledge all those people who have assisted me throughout the duration of this project. Without your encouragement, advice and support all that has been achieved would not have been possible.

Firstly, I would like to thank Professor John Hearne for supervising the entire project over the past two years. Your friendly and enthusiastic approach has made this study a thoroughly enjoyable experience. Your confidence in my ability has motivated and inspired me to always aim high and believe in myself.

I would like to thank Dr. Peter Goodman of the KwaZulu-Natal Nature Conservation Service for always making time available to assist and advise me with matters pertaining to Mkuze Game Reserve.

Colin Everson is thanked for providing the fire handbooks, which were an integral part of this project.

I would like to acknowledge Mr. Joe Schiller of the Satellite Application Centre (SAC) for donating the Landsat Thematic Mapper (TM) imagery used in the project. The time and effort of you and your staff in providing this information is appreciated.

The team at Enviromap GIS Consultants is thanked for the utilisation of their software and hardware. I would like to thank Mr. Chris Whyte for his assistance in interpreting the satellite images and map production. Lars Seeliger, Anna Reddy and Sabrina Manikum are thanked for providing technical assistance in compiling digital geographic information.

Lastly, I would like to thank my family for supporting me through the good and bad times. Your steadfast confidence in my ability is a constant source of inspiration. Thanks dad, mom, Leonie and Digby, Nigel, Denise and Bridget for putting up with all my little quirks and anecdotes over the past two years. And believe it or not, I will eventually move out of home!

CHAPTER 1

INTRODUCTION

1.1. BACKGROUND

Fire is an integral part of the dynamics of the Earth's surface and the world's biota has evolved to cope with the phenomenon of recurrent fires. In fire-adapted ecosystems, managers have learned the importance of this process and maintaining or manipulating the ecological balance (Bond and van Wilgen, 1996).

From an environmental perspective, the importance of fire is twofold. Firstly, fires have a profound and complex impact upon vegetation: removing species, altering soil chemistry, concentrating nitrogen, removing surface cover which prevents soil erosion, and even triggering reproduction in some species (Brown and DeByle, 1989). Secondly, fires are a major source of gases and particulates in the atmosphere including hydrocarbons, carbon dioxide, carbon monoxide, and ammonia (Clarke *et al.*, 1994).

There is growing concern about the role of fire in contributing to global atmospheric changes. In particular, large fires are thought to be major sources of gases that cause the much-publicised greenhouse effect. Despite the concerns levelled over the effects of fire on the dynamics of the atmosphere, there can be really no serious consideration eliminating it from major portions of the Earth's surface in order to alleviate the problem. It remains necessary for the maintenance of biological diversity and livestock production. Furthermore, it is an inevitable consequence of a combination of fuel, weather and sources of ignition (Bond and van Wilgen, 1996).

Significant effort has gone into the study of fire, especially into thermodynamics, chemistry, and modelling of the parameters associated with fire prediction and control. Less work, however, has gone into mathematical models for predicting the spatial behaviour of fire or into the valuable role that remote sensing and Geographic Information Systems (GIS) can play in fire monitoring, though the potential is

immense. Compared with other instruments for measuring physical properties that are expensive, difficult, and dangerous, remote sensing offers an effective monitoring tool for fires both during and after their incidence (Clarke *et al.*, 1994; Thompson, 1993). Furthermore, it provides a rapid, cost-effective means of quantifying vegetation biomass (Thompson, 1995). Recent developments in the use of GIS to support dynamic spatial modelling have resulted in an embryonic ability to simulate the growth of fires over the landscape (Bond and van Wilgen, 1996).

Much progress has been made towards developing an understanding of the effects of fire, and with increased knowledge has come the realisation that prediction of both the behaviour and effects of fire must rely on either a vast degree of experience or complex models. Models have proved useful as training aids or as aids to enhancing understanding of the complexity of ecosystems subject to fire (Andrews, 1988; Bond and van Wilgen, 1996; Catchpole and de Mestre, 1986; Rothermel 1972).

The goal of a mathematical model for the prediction of fire spread is the calculation of a time-evolving fire front in a physical landscape under various weather conditions. The fire front represents the dividing line between the burned and unburned parts of the system. Simulating fire behaviour and effects across landscapes facilitates the prediction of future vegetation and habitat conditions. Landscape conditions that result from different management policies or assumptions can be compared, helping ecosystem managers integrate fire into management decisions (Green *et al.*, 1995).

1.2. FIRE MANAGEMENT

Fire is extensively used in the management of ecosystems worldwide, primarily because it is a relatively inexpensive option by which the vegetation of an area can be manipulated. Deciding how, where, and when to apply fire depends on the management objectives of the area concerned and the constraints that apply to that case. There are many, diverse management objectives that influence the type of fire applied in a particular ecosystem (Bond and van Wilgen, 1996; Edwards, 1984). These include:

1. Reduction of fire hazard by applying frequent fires under mild conditions. This reduces the fuel load and thus the intensity and frequency of accidental or arson fires.
2. Forestry operations use fire for site preparation, fuel reduction, and manipulation of the composition of forest stands through inducing selective mortality in fire-sensitive species.
3. Fire can be used in controlling invasion by undesirable plants.
4. In livestock production, fire is used to achieve a plant composition that ensures optimal foraging conditions.
5. Fire is often applied to influence the hydrological cycle e.g. to enhance water yield from catchments or to prevent erosion.
6. Fire may be used to stimulate an out-of-season flush of growth.
7. Conservation aims are often met by applying fire, particularly in ecosystems where fire-dependent species and communities are involved. Fire may be used in nature reserves and other recreation areas to create habitats suited to certain game species and to induce game to graze otherwise non-preferred areas.

In the savanna areas of Africa, fire is recognised as having an important ecological role in the development and maintenance of productive and stable savanna communities (Trollope, 1984a). Fires are an integral part of these ecosystems, directly causing mortality, affecting individual reproductive success and serving as a selective force on organism attributes (Frost, 1984). Consequently, fire management is vital in sustaining these areas.

In savanna areas both crown and surface fires occur but the most common are surface fires burning with or against the wind as head or backfires. Crown fires develop only under very dry conditions when the fuel moisture is low and the prevailing weather is characterised by high winds, high air temperatures and low relative humidities. Surface fires are generally more frequent than crown fires in savanna because of the relatively non-flammable foliage of tropical and subtropical trees and shrubs will ignite only under extreme atmospheric conditions (Trollope 1984a).

At Mkuze Game Reserve (MGR) in KwaZulu-Natal, South Africa, both lightning and man-induced fire is believed to have played a major role in the development of the

vegetation of the area. In this African savanna park, fire is applied as a management tool with the intention that natural processes are allowed to prevail over those that are obviously artificial. For this reason no attempt is made to apply a rigidly defined burning programme with specific frequencies and block boundaries (Goodman, 1990).

Fires are simply ignited at a point and allowed to determine their own burn pattern and extents. Conceptually, this emulates the type of fire regime under which the land and all its biota have evolved. Goodman (1990) describes the primary management objectives for MGR as follows:

- Maintain or enhance spatial heterogeneity.
- Ensure fodder flow to large mammals.
- Retard woody plant growth.
- Reduce the risk of accidental or arson fires that will threaten the survival of plant species or destroy the composition or structure of a priority vegetation community.

The decision to ignite vegetation must consider whether the resultant fire will achieve the desired effect, while still remaining in the required limits of safety. To predict the potential behaviour of a fire, the many factors (Table 1.2) influencing fire behaviour need to be integrated (Bond and van Wilgen, 1996). This can be done in two ways. The first is traditional burning practices based on experience only - which is the existing policy at MGR (Goodman, 1990). The second is to supplement experience with models of fire behaviour.

Non-spatial models provide a means to predict fire behaviour based on inputs of fuels, weather, and topography for a specific location. Several models exist including mathematical and empirical models, and are available on hand-held calculators, slide rules and tables. However, short-term fire growth predictions over complex landscapes require repeated calculations (Rothermel, 1983), becoming impractical for non-spatial fire behaviour models that produce long-term projections of large fires over heterogeneous landscapes (Green *et al.*, 1995). Hence, the need exists for spatial computer models of fire growth.

Models of plant-herbivore dynamics in savanna ecosystems should incorporate the application of fire as a tool for maintaining the ecological balance. Developing a fire growth model, that can augment existing plant-herbivore models, will enable managers of these ecosystems to spatially simulate the outcomes of management and policy decisions.

Table 1.2.

Important variables in deciding to ignite a prescribed burn (Bond and van Wilgen, 1996).

Variables	Methods for Assessment	Importance for Control of Fire
Wind	Measured on site, taking into account the effects of topography, and forecast conditions for the predicted duration of the burn	One of the most, if not the most, important factors in determining the potential behaviour of a fire, and therefore its relative controllability. Increases in wind lead to exponential increases in rate of spread and intensity
Temperature	Measured on site, and should take into account forecast conditions	Temperature is important due to its influence on relative humidity
Relative Humidity	Measured on site, and should take into account forecast conditions	Important in determining the moisture content of fine dead fuel in the vegetation array. Fuel moisture, in turn, affects rate of spread and intensity
Topography	Assessed from local knowledge and available maps and aerial photographs	Slope has a direct effect on the rate of spread of fires (fires burn faster upslope than downslope). Topography also has an effect on wind
Surrounding Fuel Conditions	Assessed from local knowledge	The risk of escaped fires is related to the amount and condition of fuels surrounding an area to be burnt
Previous Rainfall	Assessed from local records	Rainfall affects the moisture content of dead fuels. In vegetation with heavy, dead fuels, the effects of rainfall can last for days or even weeks

1.3. OBJECTIVES

The preceding sections have outlined the need that exists for fire modelling to be performed. The following statement defines the project's objectives:

> The primary objective of this project is to develop a spatial model capable of simulating fire dynamics in savanna ecosystems. The model should act as a decision support system to managers of these ecosystems and have the potential to be integrated into existing systems. The application of Geographic Information Systems (GIS) and remote sensing as sources of spatial information for implementing the model should be investigated.

The project consists of the following steps:

- Reviewing existing fire prediction models, assessing relative strengths, weaknesses and applicability.
- Describing the development of a theoretical basis for a spatial simulation model of fire growth.
- Implementing the model for hypothetical landscapes and performing simulations under various scenarios.
- Applying the model to actual fire events that occurred in Mkuze Game Reserve during 1997
- Identifying potential, complementary arenas for further research.

CHAPTER 2

FIRE PREDICTION MODELS

2.1. INTRODUCTION

Current fire prediction models can be classified into three types: purely empirical, semi-physical and physical (Catchpole and De Mestre, 1986). Models that are purely empirical are those that make no attempt to incorporate any physical process and are a simple statistical description of test fires. Their results may be used to predict the outcome of similar fires. In Australia, Canada and the United States, empirical models have been developed into fire danger rating systems that use daily weather observations at fixed sites to produce general, broad-area ratings of fire danger (Andrews, 1988; Luke and McArthur, 1978; Stocks *et al.*, 1988).

Semi-physical models are part physical, part empirical and are a direct result of the difficulties associated with modelling heat transfer. The Rothermel (1972) model is a semi-physical model. It is physical in the sense that it uses physical parameters (fuel particle size, moisture, loading, depth) combined together using physical arguments to produce components of a rate of spread formula for the rate of spread. On the other hand, it is empirical, as heat transfer (radiation, conduction, and convection) is not modelled as a physical process. Instead, Rothermel introduces a single term, known as the propagating flux, to represent the transfer of heat from the flame to the unburned fuel. Statistical methods are implemented with data from laboratory fires to relate the physical parameters into a rate of spread formula.

The remaining category of fire prediction models comprises physical models. A purely physical model should account for the combustion of fuel and heat transfer as physical processes and be able to predict quantities like the rate of combustion and the height of the flame produced. However, due to the complexity involved in the actual combustion of fuel, physical models of fire propagation have assumed that the outcome of the chemical process is known and use factors such as flame height and temperature as inputs to the model.

The remainder of the chapter will be dedicated to describing fire prediction models in more detail, in particular, the development of the Rothermel (1972) mathematical fire spread model, which forms the core of all fire danger and fire behaviour models in the United States (Clarke *et al.*, 1994; Weise and Biging, 1997).

2.2. FIRE DANGER RATING SYSTEMS

Fire danger is defined as 'a general term used to express an assessment of both fixed and variable factors of the fire environment that determine the ease of ignition, rate of spread, difficulty of control and fire impact' (Merril and Alexander, 1987). The process of systematically evaluating and integrating the individual and combined factors influencing fire danger is referred to as fire danger rating. Fire danger rating systems produce qualitative and/or numerical indices of fire potential that are used as guides in a variety of fire management activities (Stocks *et al.*, 1988).

Throughout the world, different fire danger rating systems of widely varying complexity have developed which reflect both the severity of the fire climate and the requirement of management to have some relatively simple measure of the flammability of fuels for any particular day (Cheney, 1988). The simplest models consider only temperature and relative humidity to assess potential fire danger whilst more complex models use both theoretical and empirical models to combine a large number of factors into fire danger indices.

Well known fire danger rating systems include the United States National Fire Danger Rating System (NFDRS) (Deeming *et al.*, 1978), the McArthur Fire Danger Meters (for forests and grasslands) used in Australia (Luke and McArthur, 1978), and the Canadian Forest Fire Danger Rating System (CFFDRS) (Stocks *et al.*, 1988).

2.2.1. National Fire Danger Rating System

The NFDRS is a flexible fire danger rating system based on the mathematical fire spread model developed by Rothermel (1972). It was designed for pre-fire planning activities such as communicating fire danger to the public, restricting logging activities, setting pre-fire readiness levels, and automatic despatch of suppression forces (Andrews, 1988). The system is primarily a weather processor and uses observations, recorded daily at fixed weather stations, to simulate trends in the moisture content of fuel - which play an important role in fire danger. The structure of the system is shown in Figure 2.1 (Deeming *et al.*, 1978).

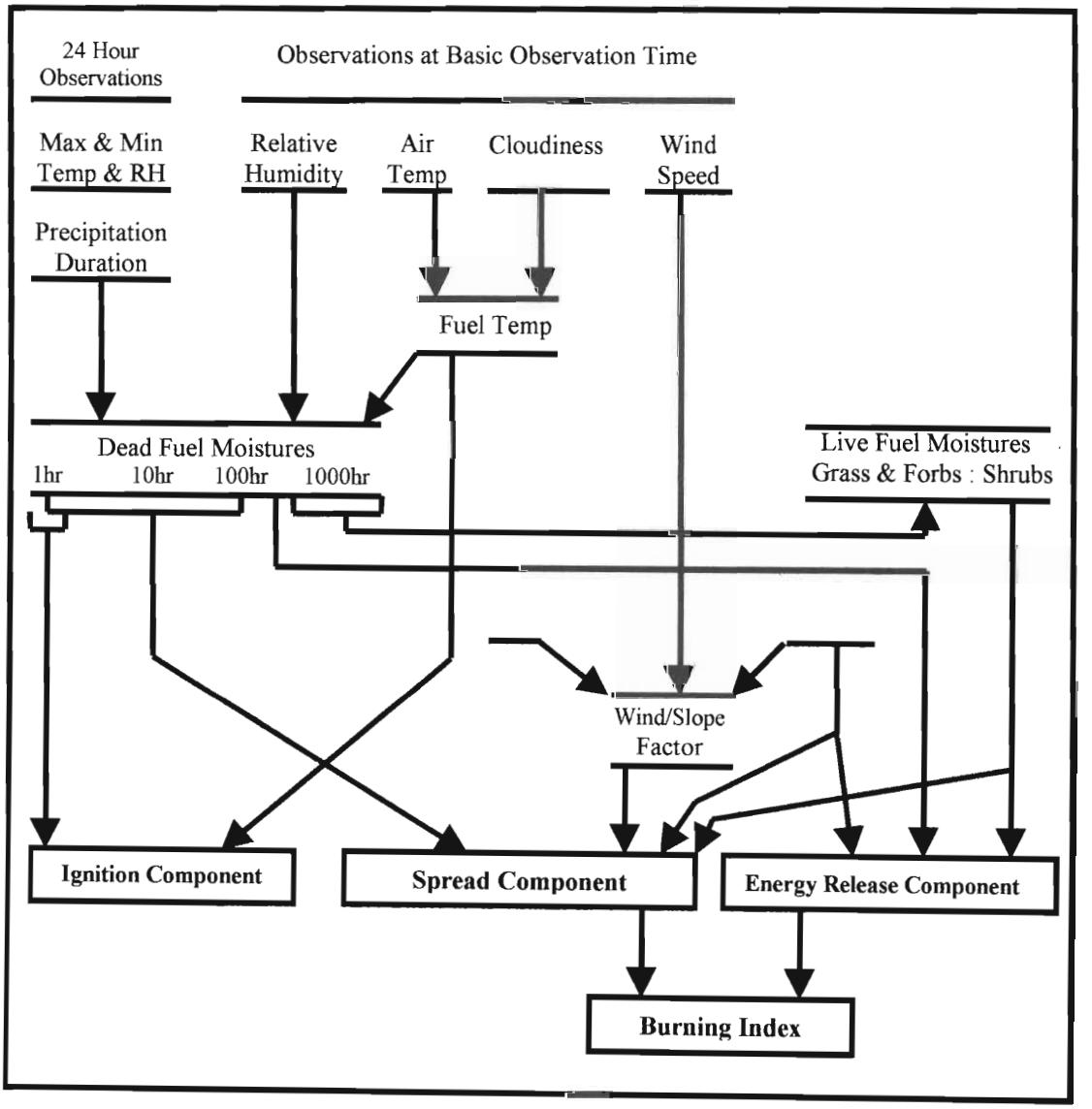

Figure 2.1. Structure of the NFDRS (from Deeming *et al.*, 1978).

The incorporation of Rothermel's (1972) fire spread model enables the expected rate of fire spread and intensity of free burning fires to be predicted. The model requires the physical and chemical composition of fuel and the environmental conditions in which it is expected to burn to be provided as inputs. These can be determined from weather data and the simulated moisture content of fuels and from the specific fuel model for the vegetation type concerned (Van Wilgen and Burgan, 1984). Because of the 'worst case' philosophy of the NFDRS, weather stations are located in the open, on level ground and readings are made in the afternoon when fire danger is usually at its highest. Fuel and slope are assumed to be constant over the rating area.

Four fire danger indices are generated by the NFDRS namely:

- Spread Component - rates the forward rate of spread of a head fire.
- Energy Release Component - rates the available energy per unit area within the flaming front at the head of the fire.
- Ignition Component - rates the probability that a firebrand will cause a fire requiring suppression.
- Burning Index - combines the spread and energy release components into a number related to the contribution of fire behaviour to the effort of containing a fire.

Indices and components are classified into one of five categories: low, moderate, high, very high and extreme. Figure 2.2 compares the Energy Release Component for a timbered area in the western United States over a two-year period. This component of fire danger is low in spring; rises with warm, dry weather; dips when it rains; tapers off in autumn and displays how the NFDRS reflects the differences in the weather pattern over the two years (Andrews, 1988).

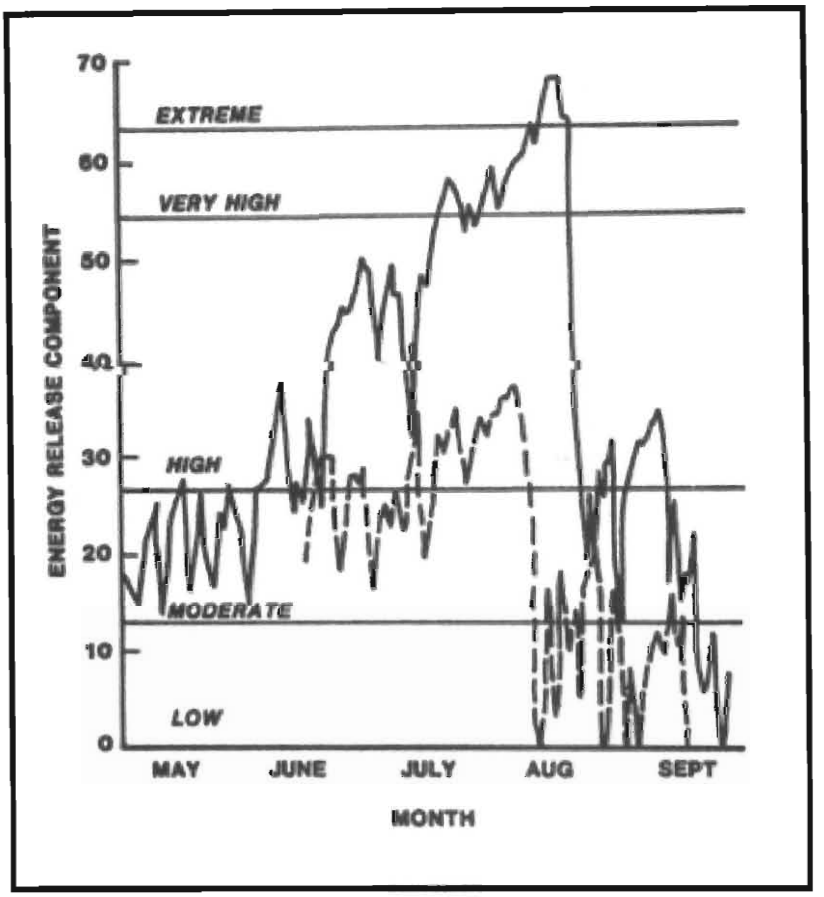

Figure 2.2. Comparison of energy release components for 2 fire seasons for a timbered area in the western United States (from Andrews, 1988).

Figure 2.3 is a map summarising fire danger conditions on a national level that would be used by fire managers in assessing fire potential (Burgan and Hartford, 1988). At this resolution, each area is relatively uniform in terms of vegetation and climate and therefore, ratings are only appropriate for broad area planning. For more precise planning on a regional level, finer resolution maps are used.

In South Africa, the NFDRS has been adapted for use in fynbos vegetation of the South Western Cape Province (Van Wilgen, 1984; Van Wilgen and Burgan, 1984), the KwaZulu-Natal Drakensberg (Everson *et al.*, 1988) and the Hluhluwe-Umfolozi Game Reserve (Wills, 1987).

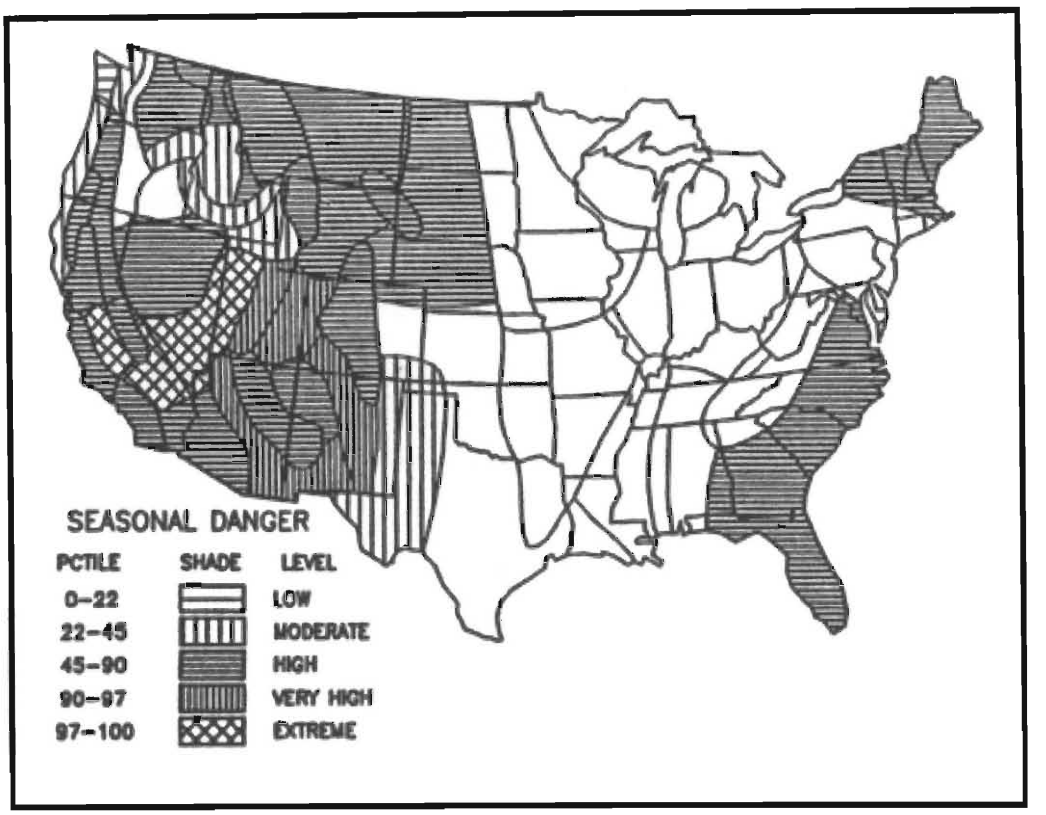

Figure 2.3. Map of relative fire danger for 6 July 1987 (from Andrews, 1988).

2.2.2. McArthur Grassland Fire Danger Meter

Climate, vegetation and ignition sources dictate that much of the Australian landscape is fire prone (Burrows and Sneeuwjagt, 1988). Consequently, there are several fire danger rating systems in Australia. Those most widely used are the McArthur fire danger rating systems for forests and grasslands and the Western Australian forest fire danger rating systems for jarrah, karri and pine forests (Cheney, 1988).

Each system predicts the rate of spread of fires propagating through a standard fuel type and provides a classification of suppression difficulty. As most fires in KwaZulu-Natal are grass-driven, it is appropriate that the McArthur Grassland Fire Danger Meter be discussed further.

The grassland fire danger meter (Figure 2.4) was designed for use in relatively fine textured annual grasslands in the temperate regions of Australia, which experience a curing process each spring and summer (Cheney, 1988; Luke and McArthur, 1978).

Variable fire danger factors of grass curing, air temperature, relative humidity and average wind speed on open ground are integrated to give a fire danger index on a logarithmic scale from 1 to 100. The rate of forward spread of a headfire is easily estimated by multiplying the danger index by:

- 0.14 if the fuel loading is 4-5 tons per hectare which is typical of a good season.
- 0.06 if a lighter fuel load of 2 tons per hectare is present.

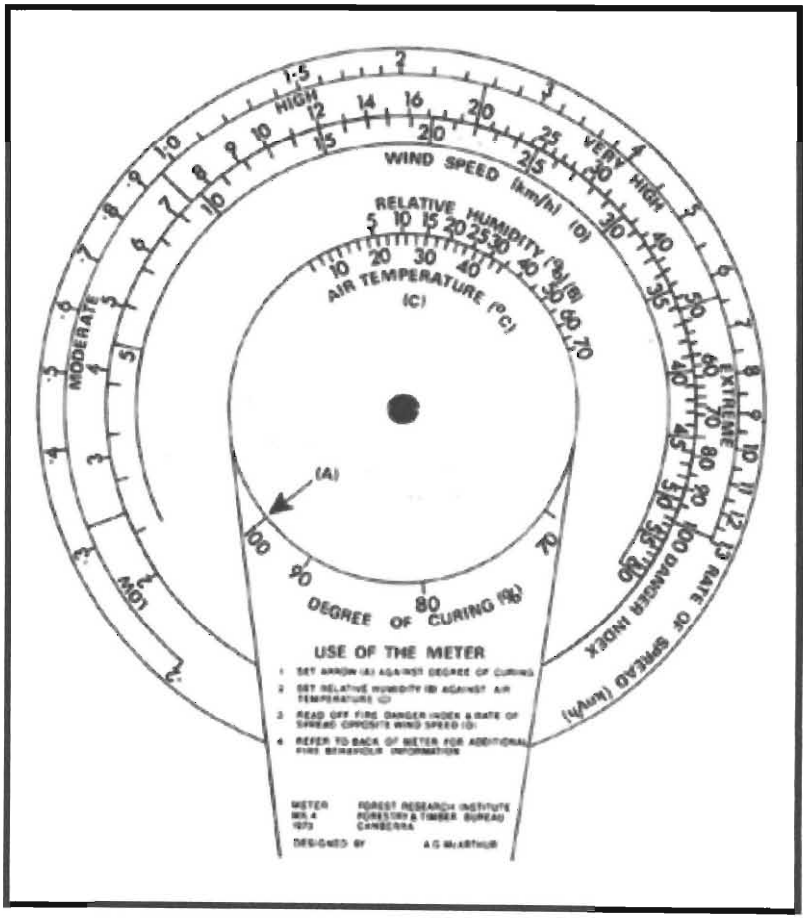

Figure 2.4. The McArthur Grassland Fire Danger Meter (from Luke and McArthur, 1978).

In drought years, fuel loads as low as 0.5-1 ton per hectare are possible. This complicates the prediction of the rate of spread as the fuel becomes discontinuous and bare patches occur. However, spread rates are generally found to range from 0.5-1 kilometre per hour, even in the most severe weather conditions (Luke and McArthur, 1978).

2.3. RADIATION, CONVECTION AND CONDUCTION MODELS

Heat transfer models, as with all physical models of fire propagation, assume that the outcome of the chemical process involved in combustion is known. A difficulty associated with these models is determining the physical processes governing heat transfer. For the transfer of heat from the flame to the unburned fuel all models include radiative heating (Catchpole and De Mestre, 1986). Some models also include convective heating - either short-range heating by hot gases emerging from the flame front (flame contact), or longer-range heating for wind-driven fires, or both.

The physics of these models are based on the energy balance of a typical fuel volume element (Figure 2.5). The cumulative effect of heat input and heat loss in a small interval of time is equated to the corresponding increase in internal energy of the fuel element. This energy balance leads to a differential equation for the average temperature of the fuel element. Solving this equation for the time of ignition of a fuel element yields a parameter for the rate of spread.

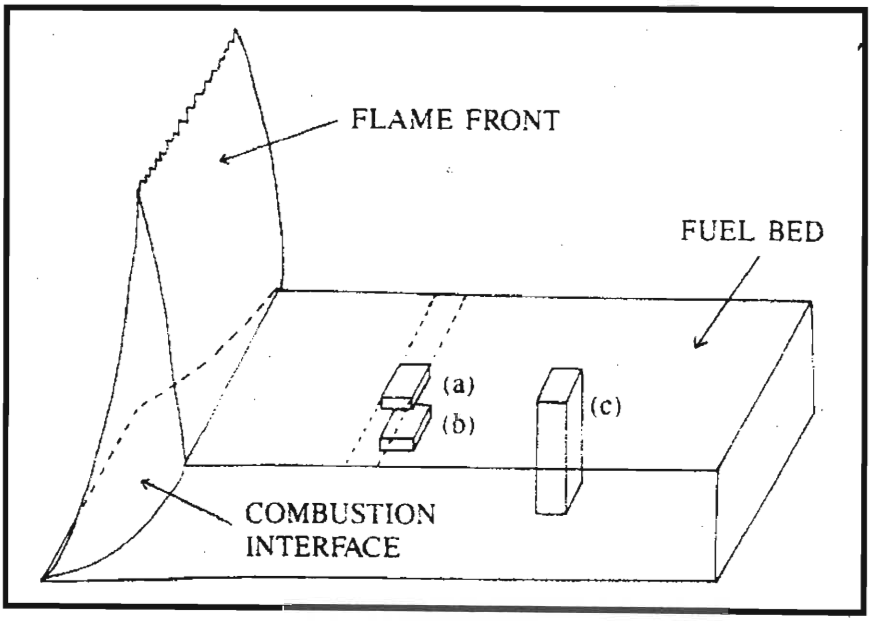

Figure 2.5. A section through the fuel bed, showing the small volume elements within the fuel bed considered by different physical models: (a) a surface element, (b) a volume element, (c) a total-depth element (from Catchpole and De Mestre, 1986).

2.3.1. Fons' Model

The pioneering mathematical fire spread modelling in the United States was by Fons (1946) (Catchpole and De Mestre, 1986). Fons conducted an extensive series of fires in a low velocity wind tunnel, with the objective of establishing the effect of compactness in pine litter on the spread of surface fires with varying wind and moisture content (Anderson, 1983).

Fons focused his attention on the head of the fire where the fine fuels carry the fire and where there is sufficient oxygen to maintain combustion. He reasoned that fire spread in a fuel bed can be visualised as proceeding by a series of successive ignitions and that its rate of spread is controlled primarily by the ignition time and the distance between particles (Rothermel, 1972).

Fons considered the fuel as an array of equally spaced vertical rods that are at ambient temperature prior to the arrival of the fire. The ignition temperature is taken at the instant that the $(n-1)^{st}$ row of rods ignites, and the temperature of the adjacent n^{th} row is an intermediate value between the ignition and ambient temperatures. The flame produced by the $(n-1)^{st}$ row then heats the n^{th} row by conduction, convection and radiation to the point of ignition.

For mathematical convenience, Fons assumed that the radiation input depended linearly on the difference between flame temperature and the temperature of the n^{th} rod. The correct physical description of the radiation input should be the difference in the fourth power of each of these temperatures (Catchpole and De Mestre, 1986).

The most serious deficiency in Fons model is that no method is provided to calculate the intermediate temperature of fuel directly ahead of the flame - a critical value in determining the rate of spread (Catchpole and De Mestre, 1986). Furthermore, the process by which a rod is heated is not specified.

2.3.2. Albini's Model

Albini (1985a, b) developed a sophisticated model for the propagation of a line fire by radiative heating. The model viewed fire spread as being a two-dimensional problem, with the temperature of fuel ahead of the flame being allowed a vertical dependence as well as a dependence on distance ahead of the flame.

Heat transfer is modelled by considering a volume element inside the fuel bed. The element is heated indirectly by radiation, from the combustion interface, travelling through the fuel and from the flame front, travelling partly through the air and fuel bed (Figure 2.5). Radiative cooling is automatically accounted for through the use of the full radiative transfer equations (Catchpole and De Mestre, 1986). Cooling by free convection (assuming no wind) to the surrounding air is included but there is no additional convective cooling at the fuel surface.

A differential equation describing the temperature field ahead of the fire front is obtained by applying the energy balance principle. A boundary condition to the problem is that the temperature at the combustion interface must reach ignition, however, the position of the combustion interface is unknown. The problem becomes one of determining a combustion interface that will propagate through the fuel at a constant speed without changing its shape (Catchpole and De Mestre, 1986). This is solved using an iterative technique.

The model has been tested on laboratory fires and the predicted shape of the combustion interface corresponded with that observed (Catchpole and De Mestre, 1986; Weise and Biging, 1997). Albini and Stocks (1986) extended the model to fit data from nine crown fires propagating through pine forest, and predictions were found to agree reasonably well with the data.

2.4. PROPAGATING FLUX MODELS

Physical models attempt to predict the propagating flux by a physical process, the flux being determined by observable properties of the flame front such as flame height, inclination and temperature. Propagating flux models do not model heat transfer as a physical process. Rather, a single term - called the propagating flux - is assumed to represent the combined effects of radiation, convection and conduction. Frandsen (1971) developed the initial propagating flux model, which was later used as the basis for the Rothermel (1972) model.

2.4.1. Frandsen's Model

Frandsen (1971) applied the conservation of energy principle to a volume element in a homogeneous fuel bed ahead of an advancing flame. Although the model assumes that radiation emanates from the combustion zone only, it remains applicable to the case where there is a significant contribution from the flame front (Catchpole and De Mestre, 1986). Analysis of the global energy balance yielded the following rate of spread formula (Rothermel, 1972):

$$R = \frac{I_{x_{ig}} + \int_{-\infty}^{0} \left(\frac{\partial I_z}{\partial z} \right)_{z_c} dx}{\rho_{be} Q_{ig}} \tag{2.1}$$

where:

R = quasi-steady rate of spread (m/min)

$I_{x_{ig}}$ = horizontal heat flux absorbed by a unit volume of fuel at the time of ignition (kJ/m^2.min)

ρ_{be} = effective bulk density (amount of fuel per unit volume of the fuel bed raised to ignition ahead of the advancing fire) (kg/m^3)

Q_{ig} = heat of pre-ignition (the heat per unit mass required to bring fuel to ignition) (kJ/kg)

$\left(\frac{\partial I_z}{\partial z}\right)_{z_c}$ = the gradient of the vertical intensity evaluated at a plane at a constant depth, z_c, of the fuel bed (kJ/m^3.min).

The horizontal and vertical co-ordinates are x and z respectively. In Frandsen's analysis, the fuel volume element is moving, relative to the combustion zone interface that is fixed, at a constant depth, z_c, from x=-∞ toward the interface at x=0 (Rothermel, 1972). The volume element ignites at the interface.

Basically, equation (2.1) shows that the rate of spread during the quasi-steady state is a ratio between the heat source (the combustion zone) and the heat sink (the fuel). The numerator in equation (2.1) represents the propagating heat flux as it contains heat flux terms for which the mechanisms of heat transfer are not known.

2.4.2. Rothermel's Model

The mathematical fire model developed by Rothermel (1972) and amended by Albini (1976) provides a means to estimate the rate at which a fire will spread through a uniform fuel array that may contain fuel particles of mixed sizes (Burgan and Rothermel, 1984). Frandsen (1971) developed the theoretical basis for the model. The terms of Frandsen's equation could not be solved analytically, however, so it was necessary to define new terms, reformulate the equation, and design experimental methods to evaluate the individual terms (Rothermel, 1972).

The fire model was designed for fires that are burning steadily in surface fuels such as grass, brush, timber litter, and so on (Burgan, 1979). The model was not designed to predict the behaviour of crown fires or the influence of spot fires on fire growth. Out of all the physically based rate of spread models (heat transfer models and propagating flux models) that have been developed, only Rothermel's (1972) model has been implemented operationally (Weise and Biging, 1997). In the United States, it is used for predicting the spread and intensity of a going wildfire or prescribed fire, or for planning activities that are based on expected fire behaviour under a range of conditions.

The basic inputs required by Rothermel's model are a description of the fuel, fuel moisture for each size class of fuel (live and dead), wind speed and slope. For ease of use, fuel descriptions are usually assembled into fuel models, which can be selected as needed (Anderson, 1982). The most important fuel descriptors include fuel bed depth, load in each size class and surface-area-to-volume ratio of the fine dead fuel. The model is applied to real landscapes by classifying natural fuels into various types according to the 13 fuel models (Table 2.1) that have been developed (Andrews, 1986).

The original Rothermel model, described below, is non-spatial and is particularly useful for calculating fire behaviour parameters such as rate of spread, intensity, flame length, and so forth. The basis of the model is adapted into a spatial context for the purposes of this project.

Table 2.1.

Parameters for the standard 13 fuel models developed by Anderson (1982)[1].

Fuel Model	Typical Fuel Complex	Surface-area-to-volume Ratio (cm^{-1}) / Fuel Loading ($kg.ha^{-1}$) 1h	10h	100h	Live	Fuel Bed Depth	Moisture of Extinction Dead Fuels
						m	Percent
	Grass and Grass Dominated Models						
1	Short grass (<30cm)	114 / 1828	-	-	-	0.305	12
2	Timber (grass and understory)	98 / 4942	4 / 2471	1 / 1235	49 / 1235	0.305	15
3	Tall grass(75cm+)	49 / 7437	-	-	-	0.762	25
	Chaparral and Shrub Fields						
4	High pocosin, chaparral (180cm+)	65 / 12379	4 / 9908	1 / 4942	49 / 12379	1.829	20
5	Brush (60cm)	65 / 2471	4 / 1235	-	49 / 4942	0.610	20
6	Dormant brush, hardwood slash	57 / 3706	4 / 6177	1 / 4942	-	0.762	25
7	Southern rough, low pocosin (60-180cm)	57 / 2792	4 / 4620	1 / 3706	49 / 914	0.762	40
	Timber Litter						
8	Closed timber litter	65 / 3706	4 / 2471	1 / 6177	-	0.061	30
9	Hardwood litter	82 / 7215	4 / 1013	1 / 370	-	0.061	25
10	Heavy timber litter and understory	65 / 7437	4 / 4942	1 / 12379	49 / 4942	0.305	25
	Slash						
11	Light logging slash	49 / 3706	4 / 11144	1 / 13615	-	0.305	15
12	Medium logging slash	49 / 9908	4 / 34668	1 / 40845	-	0.701	20
13	Heavy logging slash	49 / 17321	4 / 56931	1 / 69311	-	0.914	25

[1] Heat content = 18610 kJ/kg for all fuel models

The final form of the rate of spread formula, derived by Rothermel (1972), is defined as follows[2] (Burgan and Rothermel, 1984):

$$R=\frac{I_r\xi\left(1+\phi_w+\phi_s\right)}{\rho_b\varepsilon Q_{ig}} \tag{2.2}$$

where:

R = the forward rate of spread of the flaming front

I_r = the reaction intensity - a measure of the energy release rate per unit area of the fire front

ξ = the propagating heat flux ratio - a measure of the proportion of the reaction intensity that heats the adjacent fuel particles to ignition

ϕ_w = a dimensionless multiplier that accounts for the effect of wind in increasing the propagating flux ratio

ϕ_s = a dimensionless multiplier that accounts for the effect of slope in increasing the propagating ratio

ρ_b = the bulk density - measure of the amount of fuel per cubic metre of fuel bed

ε = the effective heating number - a measure of the proportion of a fuel particle that is heated to ignition temperature at the time flaming combustion starts

Q_{ig} = the heat of pre-ignition - a measure of the amount of heat required to ignite 1 kilogram of fuel.

Equation (2.2) shows that the rate at which fire spreads is a ratio of the heat received by the potential fuel ahead of the flame to the heat required to ignite this fuel. The numerator represents the amount of heat actually received by the potential fuel, while the denominator represents the amount of heat required to raise this fuel to the point of ignition.

[2] The full set of equations is provided in Appendix 1.

The heating of fuel ahead of the flame front is modelled by a propagating flux that is assumed to be proportional to the reaction intensity. The constant of proportionality, ξ, determines what proportion of the heat generated by combustion actually reaches the adjacent fuel. Only a small portion of the heat produced actually reaches the unburned fuel whilst the majority is carried upward by convective activity or is radiated in other directions. The concept of this spread equation is expanded below in the definition and explanation of individual parameters that have been taken from Burgan and Rothermel (1984) unless otherwise stated.

Reaction Intensity (I_r)

Reaction intensity is a measure of the energy release rate per unit area of the fire front and is affected by:

1. Size of the individual particles. Fuel particle size strongly influences fire spread and intensity. Fire spreads easily through fine fuels such as grass, shrub and foliage. The surface-area-to-volume ratio is taken as a description of particle size. The smaller the particle, the larger its surface-area-to-volume ratio and vice versa. This can be visualised by cutting a fuel particle in half, lengthwise. The total volume remains unchanged but the surface area increases. Thus, the surface-area-to-volume ratio increases.

   When a fuel array is composed of different size particles, the fire model uses their individual surface area's, and the proportion of the total surface area contributed by each size class, to determine a characteristic size that represents the array. It is then assumed that the array would burn as if it were composed of only fuel particles of the characteristic size.

2. Fuel bed compactness. Compaction is expressed as a packing ratio - a number reflecting a ratio of the volume of fuel to the volume of fuel and air space between the fuel particles. It ranges from 0, for the case of no fuel, to 1, for the case of a solid block of wood. Open or porous fuel bed burns slowly as fuel particles are far apart and little heat transfer occurs, thus causing particles to burn individually.

Fuel beds that are very compact tend to burn slowly as air flow is impeded, and there are so many particles (in a given length of fuel bed) that need to be heated to ignition.

The maximum reaction intensity occurs at some intermediate packing ratio. The effect of fuel particle size and packing ratio on the reaction intensity is incorporated in an important intermediate value called the reaction velocity.

Rothermel (1972) defines the reaction velocity as a dynamic variable that indicates the completeness and rate of fuel consumption. Essentially, it is a ratio of how efficiently a fuel particle is consumed to the burnout time of the characteristic fuel particle size. Higher reaction velocities are found when fine fuel particles are loosely packed whereas large fuel particles burn better when particles are closer together. The dependence of packing ratio on fuel particle size is illustrated in Figure 2.6.

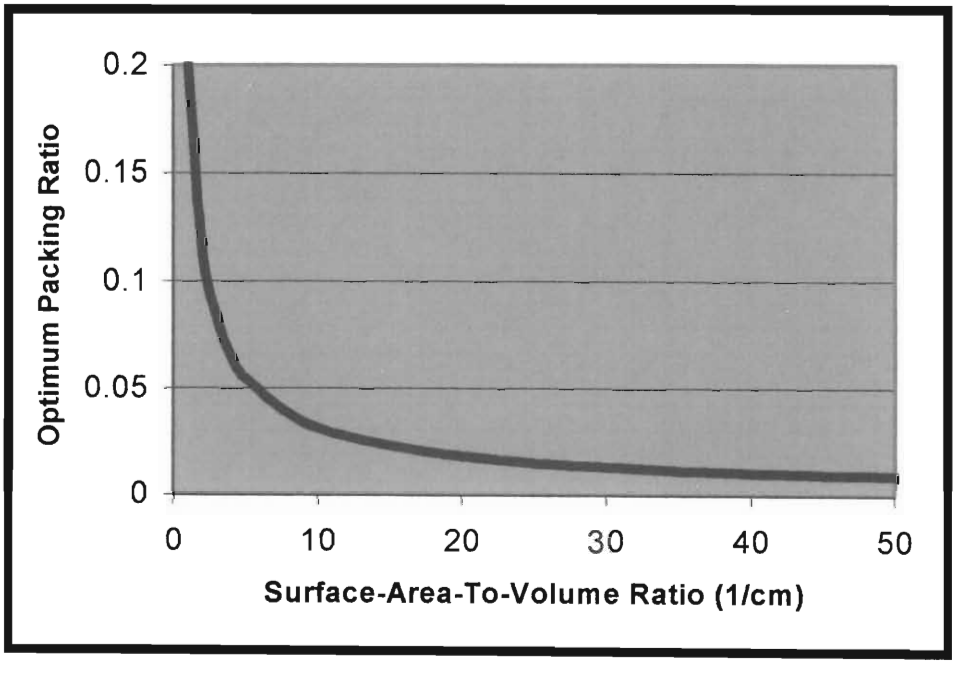

Figure 2.6. Optimum packing ratio. Fuel particle surface-area-to-volume ratio determines the optimum packing ratio for any fuel array (from Burgan and Rothermel, 1984).

The optimum packing ratio for a particle of any size, in the absence of wind, is determined empirically as follows (Wilson, 1980):

$$\beta_{op} = 0.20395\sigma_v^{-0.8189} \tag{2.3}$$

where:

β_{op} = optimum packing ratio

σ_v = surface-area-to-volume ratio.

In the presence of wind, the optimum packing ratio shifts to less tightly packed fuels (Burgan and Rothermel, 1984).

3. Moisture content of the fuel. Reaction intensity is reduced by fuel moisture, as some of the heat generated by combustion is required to evaporate the moisture and therefore, less heat is available to raise the next particle to ignition temperature. Fuel moisture is accounted for by a moisture-damping coefficient that compares the fuel moisture content to the extinction moisture.

4. Chemical composition. The quantity and type of inorganic material in the fuel affects the heat content - the energy per unit mass of fuel - and therefore the reaction intensity. The more volatile substances contained in the fuel (oil and waxes), the higher the heat content. Conversely, inorganic materials and minerals associated with salts in the fuel cause a reduction in the reaction intensity. Rothermel's model assumes that the total salt content for all fuels is 5.55 percent and the effective salt content[3] is 1.0 percent (Rothermel, 1972).

   The heat content is the only chemically oriented fuel parameter that the user can adjust. Increasing the heat content results in a 'hotter' fuel model, while decreasing it reduces the calculated fire behaviour.

The reaction intensity determines the total heat release rate per unit area of the fire front, including heat that is radiated, conducted, and convected in all directions, and not just in the direction of the adjacent potential fuel. A propagating flux ratio is

[3] The effective salt content is measure of the silica-free ash content of the fuel.

introduced that adjusts this total energy release rate down to that portion that is effective in propagating the fire.

Propagating Flux Ratio (ξ)

The propagating flux ratio determines what portion of the total heat produced actually reaches the adjacent fuel and raises its temperature to ignition. It is calculated under the assumption that the fire is burning on a flat surface in the absence of wind. Wind and slope effects are discussed later. Mathematically, the propagating flux ratio is defined according to the no slope, no wind, propagating flux $(I_p)_0$ and the reaction intensity I_r as:

$$\xi = \frac{(I_p)_0}{I_r} \tag{2.4}$$

This parameter expresses what proportion of the total reaction intensity actually heats the adjacent fuel particles to ignition. A value for the propagating flux ratio of 0 implies that no heat reaches adjacent fuels. A value of 1 implies that all heat produced reaches the adjacent fuel mass. Realistically, values are found to range from 1 percent to 20 percent. The propagating flux ratio is affected by:

- The average size of the fuel particles in the fuel bed i.e. the characteristic surface-area-to-volume-ratio.
- The compactness of the fuel bed i.e. the packing ratio.

Wind Coefficient (ϕ_w)

The effect of wind and slope on the propagation of the fire is accounted for by the introduction of a wind coefficient (ϕ_w) and a slope coefficient (ϕ_s). On flat terrain, wind increases radiant and convective heat transfer because the flame is tilted toward the unburned fuel (Rothermel, 1972; Burgan and Rothermel, 1984; Weise and Biging, 1997) (Figures 2.7 and 2.8).

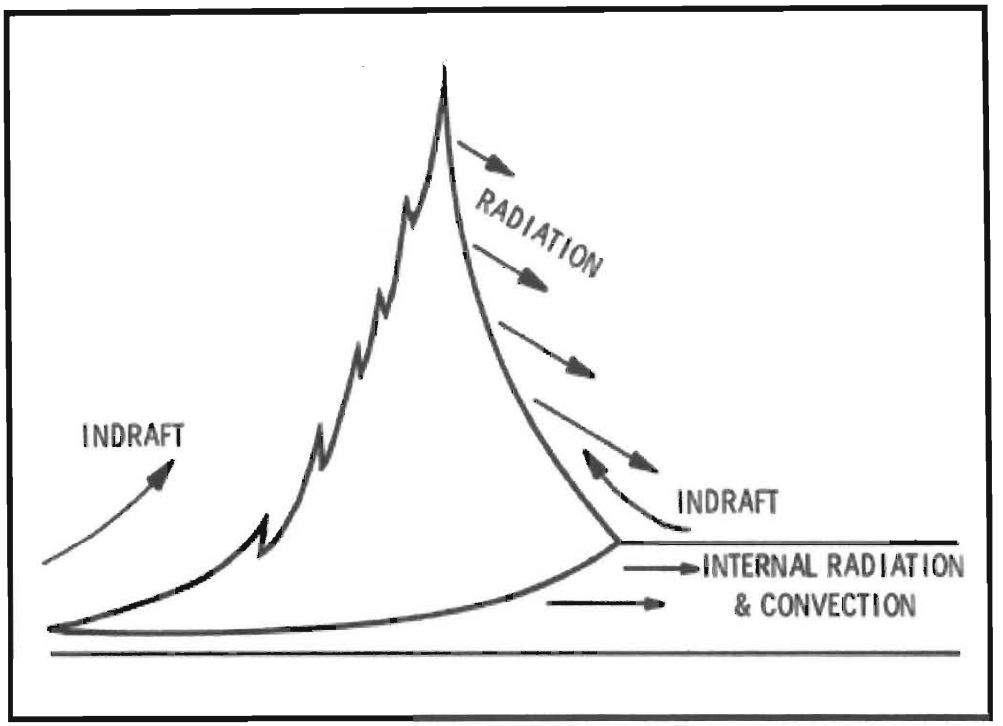

Figure 2.7. Schematic of a no wind fire (from Rothermel, 1972).

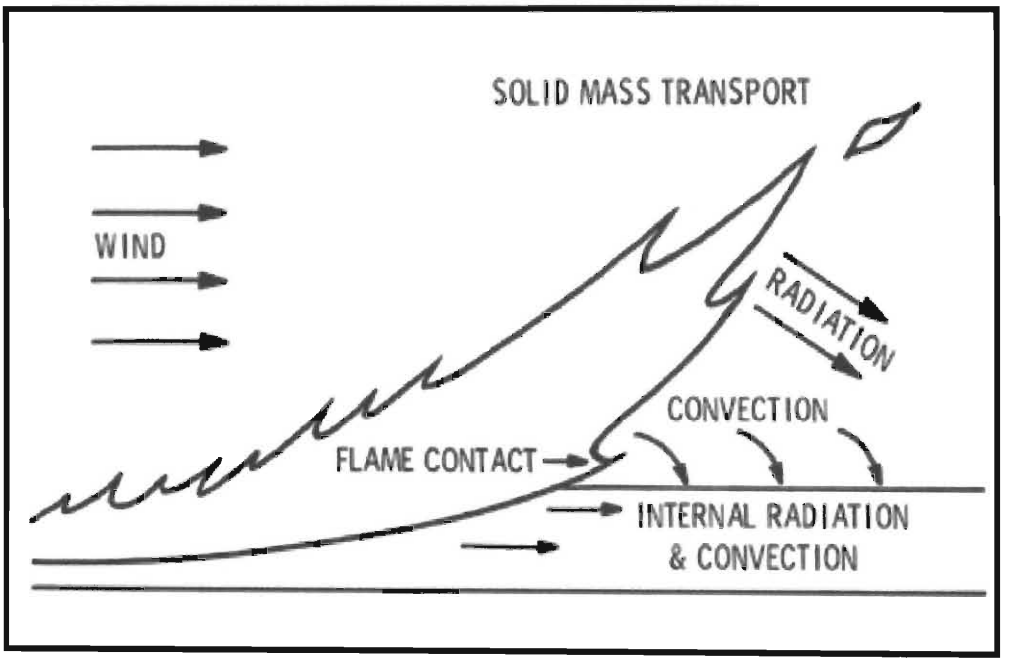

Figure 2.8. Schematic of a wind-driven fire (from Rothermel, 1972).

The wind coefficient is affected by the:

- Fuel bed's characteristic surface-area-to-volume ratio.
- Packing ratio of the fuel bed. The wind coefficient decreases rapidly as the fuel bed is more tightly packed.
- Wind speed. Obviously an increase in wind speed will produce an increase in the wind coefficient.

Slope Coefficient (ϕ_s)

The effect of slope is introduced by the coefficient ϕ_s in the expression $(1 + \phi_w + \phi_s)$. For a fire spreading upslope in the absence of wind, the angle between the flame and the slope is reduced, thus affecting radiant heat transfer from the flame to the unburned fuel in advance of the flame (Rothermel, 1972; Burgan and Rothermel, 1984; Weise and Biging, 1997) (Figure 2.9).

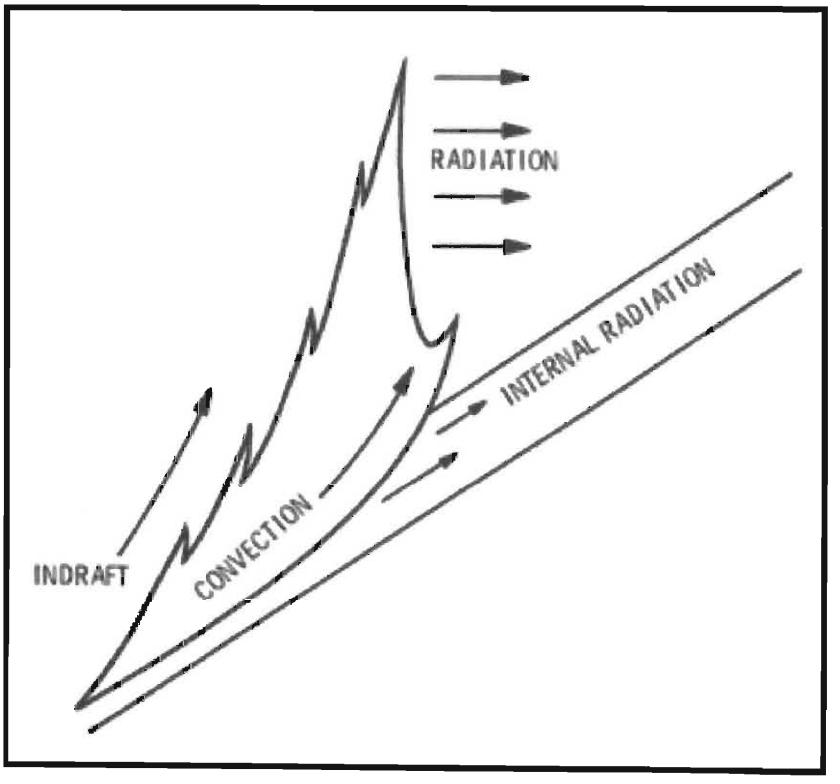

Figure 2.9. Schematic of a fire on a slope (from Rothermel, 1972).

The slope coefficient increases from 0 percent in the case of flat terrain, to some larger value. The effect of slope on fire propagation is not as pronounced as it is with wind. The slope co-efficient is affected by:

- Slope steepness. The slope coefficient increases as slope increases.
- The packing ratio of the fuel bed.

The packing ratio of the fuel model will slightly influence its sensitivity to slope steepness. The effect, however, is small relative to the magnitude of other effects produced by changes in packing ratio (Burgan and Rothermel, 1984). The slope coefficient is independent of particle size.

Bulk Density (ρ_b)

The denominator of equation (2.2) represents the heat sink i.e. the amount of heat required to raise the unburned fuel ahead of the flame to ignition temperature. The bulk density, which quantifies how much fuel is potentially available to act as a heat sink, is obtained by dividing the ovendry weight of the fuel by the fuel bed depth. Not all the fuel is necessarily heated to ignition for combustion to occur; this is discussed in the next section on the effective heating number.

An increase in the bulk density tends to result in a decrease in the rate of spread because the total heat sink is increased. This effect, however, is altered by the influence of the fuel load on the reaction intensity, and the bulk density on the propagating flux ratio. As such, no definitive conclusions can be drawn with regard to the altering of the fuel load or bulk density.

Effective Heating Number (ε)

The effective heating number represents the proportion of a fuel particle that must be heated to ignition temperature to result in combustion. For fine fuels, nearly the entire fuel particle must be heated to ignition whereas a relatively small proportion of large fuels is heated to this degree (Figure 2.10). When logs burn, the centre of the log may

be cool relative to the surface that is on fire. Hence, only the outer shell of the log has been heated to ignition temperature.

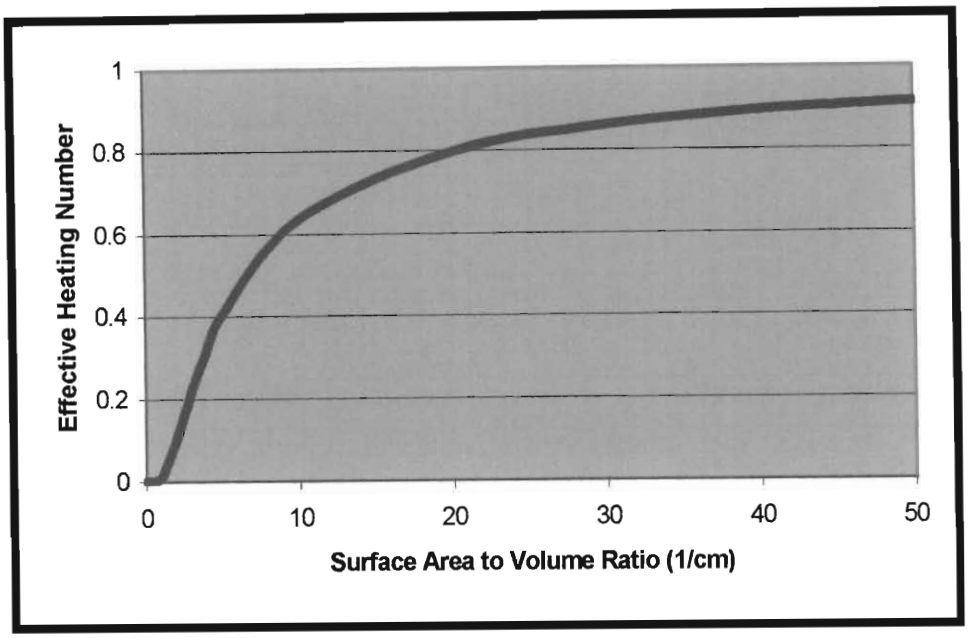

Figure 2.10. Effective heating number. As particle size decreases a greater portion of the particle has to be heated to ignition temperature at the time flaming combustion starts (from Burgan and Rothermel, 1984).

Multiplication of the bulk density by the effective heating number yields the quantity of fuel per cubic metre of fuel bed that must be heated to ignition for the fire to propagate

Heat of Pre-Ignition (Q_{ig})

The heat of pre-ignition quantifies the amount of heat required to raise the temperature of 1 kilogram of moist fuel from the ambient temperature to the ignition temperature. It includes the heat required to evaporate the moisture and to dry the fuel. Consequently, the heat of pre-ignition increases as the moisture content of the fuel increases (Figure 2.11). Whereas the product of bulk density and the effective heating number quantifies the amount of fuel weight per cubic metre of fuel bed that must be raised to ignition temperature, the heat of pre-ignition quantifies how much heat is required to do this.

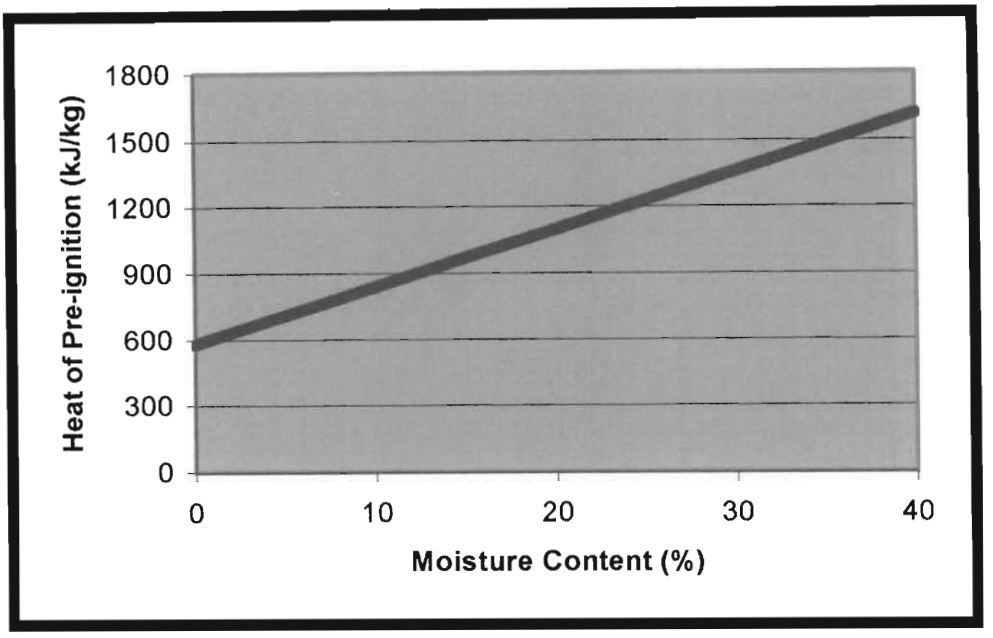

Figure 2.11. Heat of pre-ignition. The amount of heat required to ignite the fuel increases as the moisture content increases (from Burgan and Rothermel, 1984).

2.5. CONCLUSION

A review of the various fire prediction models has been provided in this chapter ranging from empirical fire danger rating systems to complex physical models. Particular emphasis has been placed on describing, in detail, the mathematical model for fire spread developed by Rothermel (1972). The basis of this model is adapted into a spatial context for the purposes of this dissertation. Further description of this topic is provided in the next chapter.

CHAPTER 3

DEVELOPING A FIRE GROWTH MODEL

3.1. INTRODUCTION

Computerised fire growth models have been the subject of research for about 25 years. Despite numerous management applications, these models still remain largely in the realm of research. Recent advances in computer technology and the increasing prevalence of Geographic Information Systems (GIS) capabilities have alleviated the problem to some extent, facilitating the transfer of fire growth modelling technology to user applications (Finney, 1994a).

Efforts to model the growth of wildland fires can be classified according to two approaches: geometric models and cellular automata (CA) models. Geometric models assume that fire burning in an undefined uniform fuel type, spread according to a well-defined growth law, and take a standard geometrical shape such as an ellipse (Kourtz and O'Regan, 1971; Anderson, 1983). If burning conditions are uniform, a single shape can be applied to estimate fire size, area, and perimeter over time, with the use of fractals to account for smaller-scale variations (Finney, 1994a). However, most fires do not burn under constant conditions as fuels, weather and topography, vary spatially, and temporally in the case of weather.

More complex geometric models use wave propagation techniques, based on Huygen's principle. The principle states that a wave can be propagated from points on its outer edge that serve as independent sources of smaller ignitions, to solve for the position of the fire front at specified times. Models based on this principle require information such as time, direction, and rate of fire spread, for points on the fire edge. These are essential components of existing models of surface fire spread, fire acceleration, crown fire and transition to crown fire, as well as spotting (Finney, 1994b). Wave-type models developed include Fire Area Simulator (FARSITE) (Finney, 1994a, 1994b) and FIRE! (Green *et al.*, 1995).

A CA model is essentially a discrete space-time-state representation of a system of many objects that simultaneously interact with other nearby objects (Gaylord and Nishidate, 1996). CA models, first introduced by von Neumann (1966), are an alternative to models of partial differential equations and have been successfully used in the modelling of physical systems and processes. Because of their discrete nature and their suitability for implementation on digital computers, CA models are appropriate for modelling fire spread (Karafyllidis and Thanailakis, 1997).

3.2. BACKGROUND

A CA consists of a regular uniform n-dimensional lattice. At each site of the lattice, or cell, a physical quantity assumes values. These physical quantities define the global state of the CA while the value of this quantity at each cell is the local state of this cell. Each cell is restricted to an interaction within a local neighbourhood only, and as a result, has no immediate global communication. The neighbourhood of a cell is taken to be the cell itself and some or all of the immediately adjacent cells. Figure 3.1 illustrates the Moore neighbourhood of the (i,j) cell. This includes the cell itself and the eight nearest neighbouring cells (Gaylord and Nishidate, 1996).

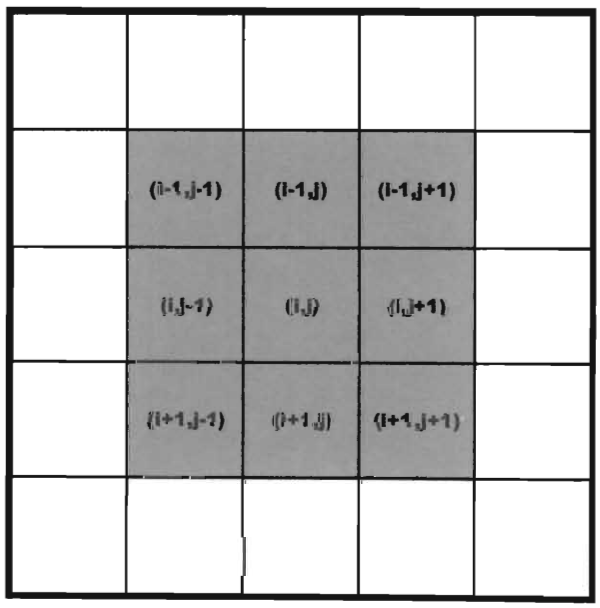

Figure 3.1. Moore neighbourhood of the (i,j) cell comprises the nine green cells.

The state of each cell is updated simultaneously at discrete time steps, based on the states in its neighbourhood at the preceding time step. The algorithm used to calculate the next state of a cell is referred to as the CA local rule.

3.3. EXISTING CA MODELS OF FIRE SPREAD

Karafyllidis and Thanailakis (1997) developed a CA model for predicting fire spread in both homogeneous and heterogeneous forests that incorporated weather conditions and topography. An algorithm constructed, based on the proposed model, was implemented to hypothetical forests, and fire fronts predicted by the model were found to agree favourably with the experience of fire spreading in real forests (Karafyllidis and Thanailakis, 1997).

However, careful review of the model proposed by Karafyllidis and Thanailakis (1997) revealed that although it was capable of predicting the pattern (or shape) of fire spread, it was unable to correctly predict the rate at which the fire spread. The fault arose from an erroneous assumption contained in the statement of the problem (Karafyllidis and Thanailakis, 1997):

> *Given a scalar field of fire spread rates R(x,y), which is the distribution of the rates of spread at every point in a forest, the forest fire front at time* t_1*, the wind speed and direction, and the height and shape of the land, determine the fire front at any time* $t_2 > t_1$.

The scalar field of fire spread rates is appropriate if fire is spreading through a homogeneous forest in the absence of wind and on level terrain. If this is not the case then a vector velocity field needs to be employed. The concept of a vector velocity field differs from a scalar field in assuming that the rate of fire spread is a function of direction. The rate of fire spread in a particular direction depends on the prevailing weather conditions and land topography, which vary spatially and temporally in the case of wind.

Karafyllidis and Thanailakis (1997) assume that wind and slope effects can be incorporated as weighting factors that modify the CA local rule. At each cell of the CA a rate of fire spread, R, is allocated which is the value of $R(x,y)$ at the central point of the cell. The value of R for a particular fuel is constant, irrespective of wind and slope conditions. Including wind and slope as weights, that have no correlation to the rate of fire spread R, leads to a miscalculation in the position of the fire front. A worked example of this point is provided in the next section.

The fire spread model of Karafyllidis and Thanailakis (1997) is described in detail in the following section, highlighting both adequacies and deficiencies. The concept of the model provides invaluable insight into spatial fire modelling using cellular automata. Cases in which the model fails to predict the rate of fire spread are illustrated.

3.3.1. The CA Model developed by Karafyllidis and Thanailakis

Karafyllidis and Thanailakis (1997) described the problem of predicting fire spread as documented in section 3.3. The forest was divided into a matrix of identical square cells, with side length a, and was represented by a CA. Each cell in the forest represents a cell in the CA lattice. The local state of a cell at any time t was defined as the ratio of the burned out cell area to the total cell area:

$$S_{i,j}^{t} = \frac{A_b}{A_t} \tag{3.1}$$

$S_{i,j}^{t}$ defines the local state of the (i,j) cell at time t, and A_b and A_t are the burned out and total cell areas respectively. Interpreting equation (3.1), the state of an unburned cell is 0 whereas a completely burned out cell is 1. Intermediate values for $S_{i,j}^{t}$ define the degree to which a cell is burned.

At each cell in the CA, a value for the rate of fire spread R, is allocated. $R_{i,j}$ is the rate of spread assigned to the (i,j) cell and it determines the time required for this cell

to be fully burned out. The rate of fire spread distribution, which is assumed to be a scalar field, is generated by some other model.

The state of the (i,j) cell after a single time step Δt, written as $S_{i,j}^{t+1}$, depends on the states of the eight neighbouring cells at time t and the state of the cell itself at time t. Expressing this concept mathematically, the general formula for the CA local rule is:

$$S_{i,j}^{t+1} = f\left(S_{i-1,j-1}^{t}, S_{i-1,j}^{t}, S_{i-1,j+1}^{t}, S_{i,j-1}^{t}, S_{i,j}^{t}, S_{i,j+1}^{t}, S_{i+1,j-1}^{t}, S_{i+1,j}^{t}, S_{i+1,j+1}^{t}\right) \tag{3.2}$$

An explicit representation for the function in equation (3.2) needs to be determined. This function controls the influence of the state of an individual neighbour on the state of the (i,j) cell. If the (i,j) cell is unburned and only one of its adjacent neighbours is completely burned out, then the (i,j) cell will be completely burned out after a time t_a given by:

$$t_a = \frac{a}{R_{ij}} \tag{3.3}$$

where a is the length of the side of a cell (m) and R is the rate of spread of the fire (m/s). Similarly, if only one diagonal cell is fully burned out, the (i,j) will be completely unburned out after a time t_d given by:

$$t_d = \frac{\sqrt{2}a}{R_{ij}} = \sqrt{2}t_a \tag{3.4}$$

where $\sqrt{2}a$ is the length of the diagonal of the cell. The effect of a fully burned out diagonal neighbour on the state of the (i,j) cell would differ from that of a burned out adjacent neighbour. If only one adjacent neighbour was burned out and the (i,j) cell was unburned, then after a time t_a the (i,j) would be fully burned. On the other hand, consider that all the cells in the neighbourhood of the (i,j) are unburned except for a single diagonal cell (Figure 3.2a). If the time step is taken to be equal to t_a, then after a single time step the (i,j) will only be partially burned out (Figure 3.2b).

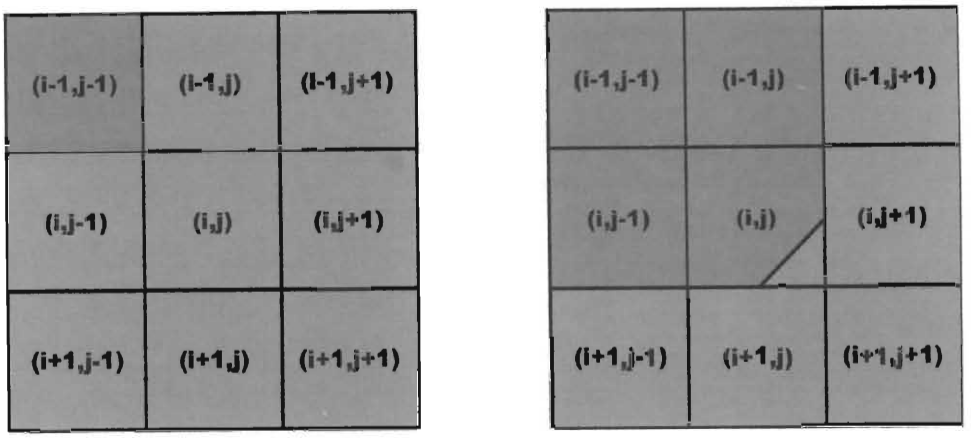

Figure 3.2 (a) The cells in the neighbourhood of the *(i,j)* cell at time *t*. Only the *(i-1,j-1)* cell is fully burned out. (b) The same cells after a single time step. The *(i-1,j-1)*, *(i-1,j)* and *(i,j-1)* cells are fully burned out. The *(i,j)* cell is partially burned out.

The state of the (i,j) cell will be (Karafyllidis and Thanailakis, 1997):

$$S_{i,j}^{t+1} = \frac{a^2 - \left(\sqrt{2}-1\right)^2 a^2}{a^2} = 2\left(\sqrt{2}-1\right) \cong 0.83 \tag{3.5}$$

The value 0.83 was in fact incorrectly calculated and should actually have been 0.17 (Karafyllidis *pers. comm.*, 1998). The correct determination of the effect of the state of a single burned out neighbour on the state (i,j) cell is presented later in the chapter. Therefore, if the state of only one diagonal neighbour is 1 then the state of the (i,j) cell at the next time step will be 0.17. Consequently the CA local rule becomes:

$$S_{i,j}^{t+1} = S_{i,j}^{t} + 1\left(S_{i-1,j}^{t} + S_{i,j-1}^{t} + S_{i,j+1}^{t} + S_{i+1,j}^{t}\right) + 0.17\left(S_{i-1,j-1}^{t} + S_{i-1,j+1}^{t} + S_{i+1,j-1}^{t} + S_{i+1,j+1}^{t}\right) \tag{3.6}$$

The basic model described above was modified to incorporate the effects of fuel heterogeneity, wind speed and direction, and topography. Heterogeneity was assumed

to result in a forest that contained values for the rate of spread that differed. The time step in the simulation was taken to be equal to the time needed for the cells with the largest value for the rate of spread to be burned. Karafyllidis and Thanailakis (1997) did not consider whether or not a specific fuel could actually ignite another, different fuel type. Rather, it was assumed - by not considering heterogeneous fuel effects - that all fuels were potentially ignitable by any other fuel type. In reality, heterogeneous effects must be accounted for as they play a significant role in restricting the spread of a fire.

Wind and slope effects were included in the proposed CA model by assigning weights to each state of the neighbouring cells in the CA local rule. The weight associated with a particular wind is dependent on the speed of the wind and its direction. Slope effects were incorporated by weighting the state of a neighbouring cell according to the height difference between the two cells. The final form of the CA local rule incorporating wind and slope effects was given by:

$$S_{i,j}^{t+1} = S_{i,j}^{t} + 1\left(nH_{i-1,j}S_{i-1,j}^{t} + wH_{i,j-1}S_{i,j-1}^{t} + eH_{i,j+1}S_{i,j+1}^{t} + sH_{i+1,j}S_{i+1,j}^{t}\right) + 0.17\left(nwH_{i-1,j-1}S_{i-1,j-1}^{t} + neH_{i-1,j+1}S_{i-1,j+1}^{t} + swH_{i+1,j-1}S_{i+1,j-1}^{t} + seH_{i+1,j+1}S_{i+1,j+1}^{t}\right) \tag{3.7}$$

$H_{k,l} = f\left(h_{i,j} - h_{k,l}\right)$ is a linear function of the height difference between the (i,j) and a neighbouring cell, (k,l), and n,e,s,w,nw,ne,sw,se are the wind weights.

3.3.2. Discussion

An algorithm of the CA model for fire spread proposed by Karafyllidis and Thanailakis (1997) was implemented using various hypothetical scenarios (Karafyllidis and Thanailakis, 1997). The shape of the fire fronts produced by the model were found to be in good agreement with the experience of fire spreading in real forests, however, the position of the fire front was miscalculated. This was particularly evident for the cases in which wind and topographic effects were examined.

The source of the problem is the assumption of a scalar field of fire spread rates, which defines the rate of fire spread in any cell in the CA lattice, that is independent of wind and slope effects. Instead, wind and slope effects are incorporated by weighting the state of a neighbouring cell in the CA local rule. This simplification ultimately results in the inability of the model to accurately predict the position of the fire front at any time – although the shape may replicate reality.

It is generally accepted that wind and slope modify the rate of fire spread in a particular direction. Fires burning with the wind, called head fires, and up a slope exhibit higher rates of spread than those spreading in the absence of wind on level ground (Weise and Biging, 1997; Rothermel, 1972; Trollope, 1984b; Luke and McArthur, 1978). Therefore, a vector velocity field should be applied in the modelling of fire spread. The rate at which the (i,j) cell spreads to the surrounding neighbours is critically affected by the speed and direction of the wind, and the underlying topography.

To illustrate how the proposed model of Karafyllidis and Thanailakis (1997) fails to predict the position of the fire front at a given time if the fire progresses in the presence of wind and slope effects, consider the following scenario:

> *A fire is spreading up a slope with the assistance of a mild breeze through a homogeneous forest. In the absence of wind and on flat terrain, the fire spreads at a rate R=1m/s. The additional effects of wind and slope cause an effective spread rate of 5m/s. The values for R are calculated using a fire behaviour model such as the Rothermel (1972) model described in chapter 2.*

As Karafyllidis and Thanailakis (1997) assume no direct correlation between R and wind and topographic effects, the simulation time step would be calculated using equation (3.3) with R=1 m/s. If the cell length a was taken to be 10m, then applying this equation yields:

$$t_a = \frac{10}{1} = 10s \tag{3.8}$$

If the (i,j) cell was burned out at time t i.e. state=1, then depending on the values for the weights for wind and slope, the states of the eight neighbouring cells could be determined using equation (3.8). The state of these cells, however, can at most be equal to 1. Hence, the model can at most predict a fire spread rate of 1m/s, regardless of wind and slope. In reality, the value for R in the direction of maximum spread – up the slope and with the wind – is 5m/s. Therefore after 10s, or one time step, the fire front should actually have spread 50m (in the direction of maximum spread) and not 10m as predicted by the model.

The CA model proposed by Karafyllidis and Thanailakis (1997) fails to accurately predict the position of the fire front because of the assumption of a scalar field of fire spread rates that is independent of wind and topographic effects. As a result, the simulation time step is calculated on a simplified value for R, which is not realistic. The simulation time step controls the degree to which a fire can spread in the CA model, and hence the position of the fire front is miscalculated.

Lastly, spatial heterogeneity in fuel composition was inadequately dealt with. The model assumed that in a heterogeneous forest, all fuels were combustible – except buildings and water that were allocated values for the spread rate R=0 – and the rate of fire spread depended on the particular fuel involved. No consideration was given to whether or not a certain fuel type was able to ignite a different fuel type e.g. fire spreading in a grassland may not be sufficiently intense to cause spread to a woodland. This simplification was reasonable for the hypothetical forests to which the model was applied. However, in reality this may not be the case.

The model of Karafyllidis and Thanailakis (1997) provides insight in terms of modelling fire spread using cellular automata. Important concepts and problematic areas identified in reviewing the proposed model served as key elements in the development of a more realistic fire spread model in this study – which is described in the next section.

3.4. DEVELOPING A CA MODEL OF FIRE SPREAD

The fundamental properties of a CA model are the definition of the state of a cell and the local rule that updates this state from one time interval to the next. If the landscape is divided into a matrix of identical cells, with side length a, and each cell represents a cell in the CA lattice, then the state of a cell at any time t is defined as a function of the heat dynamics of the cell at that time:

$$S_{i,j}^{t} = f\left(\frac{H_r}{H_0}, t\right) \tag{3.9}$$

H_r is the sum of the heat received by the cell at time t and H_0 is the total heat required to burn the cell at time t=0. From equation (3.9), the state of a cell can be one of three possibilities: unburned, burning or burned out. A cell is unburned if it requires further heat in order for combustion to occur i.e. $H_r < H_0$. The state of an unburned cell ranges from 0 to 1. A cell commences burning when sufficient heat has been received for combustion i.e. $H_r = H_0$. After a period of time, however, a burning cell extinguishes itself and therefore becomes burned out.

Each cell in the CA contains parameters describing its fuel characteristics, moisture content and height above sea level. Fuel characteristics are summarised by a fuel model (Table 2.1) containing values for the fuel load, fuel bed depth, surface area to volume ratio, extinction moisture content and heat content. Applying the parameters of the fuel model together with the fuel moisture content into equation (2.2), a value for R_0, the rate of fire spread in the absence of wind and on flat terrain, can be calculated.

If a cell is either unburned or burned out, then there is no combustion of fuel and R=0. On the other hand, if a cell is burning then it spreads to its surrounding neighbours at a rate that is a function of R_0, the prevailing wind conditions and the underlying topography. If the (i,j) cell is burning, then a vector velocity field, incorporating wind and slope effects, is defined as follows:

$$\widetilde{R}_{i,j} = R_0 \begin{bmatrix} (\phi_W \cdot \phi_S)_{i-1,j} \\ (\phi_W \cdot \phi_S)_{i,j+1} \\ (\phi_W \cdot \phi_S)_{i+1,j} \\ (\phi_W \cdot \phi_S)_{i,j-1} \\ (\phi_W \cdot \phi_S)_{i-1,j-1} \\ (\phi_W \cdot \phi_S)_{i-1,j+1} \\ (\phi_W \cdot \phi_S)_{i+1,j+1} \\ (\phi_W \cdot \phi_S)_{i+1,j-1} \end{bmatrix} \tag{3.10}$$

ϕ_w is a factor accounting for the effect, on the rate of fire spread, of the wind speed and direction. Similarly ϕ_s is a slope factor that modifies the spread rate depending on the topography. The product $R_0(\phi_w.\phi_s)_{k,l}$ determines the component of the vector velocity field for the rate of fire spread from the (i,j) cell to a neighbouring (k,l) cell. Methods of calculating explicit values for these factors are discussed in the sections to follow.

The effect of spatial variation in fuel type, or heterogeneity, is incorporated into the CA model by analysing the heat dynamics of the respective fuel types. Basically, a fire will spread from one particular fuel to another if the heat received by the unburned fuel ahead of the fire is sufficient to cause ignition. Expressing this relationship mathematically, a combustibility index, *CI*, can be defined as follows:

$$CI = \frac{(H_c)_\alpha}{(H_0)_\beta} \tag{3.11}$$

$(H_c)_\alpha$ represents the amount of heat produced by fuel α that reaches the unburned fuel and $(H_0)_\beta$ is a measure of the total heat required to ignite fuel β. If *CI* is greater than or equal to 1 then it is assumed that the fire can spread from fuel α to fuel β. Conversely, if *CI* is strictly less than 1 then the fire is unable to spread from fuel α to fuel β.

The value of the denominator in equation (3.11) can be calculated by multiplying the denominator of equation (2.2) by the fuel bed depth. Only a small portion of the heat produced by the burning fuel reaches the surrounding unburned fuel. The majority of the heat is carried away by convective activity or is radiated in other directions (Burgan and Rothermel, 1984). Furthermore, wind and topography significantly influence the degree of preheating of unburned fuel ahead of the flame by affecting the convective and radiant heat transfer processes (Luke and McArthur, 1978).

The numerator of equation (2.2) represents the rate at heat is received by the potential unburned fuel and incorporates fuel characteristics and prevailing wind and topographic conditions. An explicit value for $(H_c)_\alpha$ was obtained by multiplying the numerator of equation (2.2) by the flame residence time, t_r, which Andrews (1986) approximated as:

$$t_r = \frac{12.6}{\sigma_v} \tag{3.12}$$

where σ_v represents the surface area to volume of the burning fuel. To incorporate the effect of heterogeneity, a multiplier η_f is introduced into equation (3.10) that modifies the rate of spread from the (i,j) cell to a neighbouring (k,l) cell as follows:

$$\tilde{R}_{i,j} = R_0 \left(\phi_w . \phi_s\right)_{k,l} . \eta_f \tag{3.13}$$

The value for η_f is either 0 or 1 depending on the value obtained for CI. If $CI < 1$ then $\eta_f = 0$, indicating that the fire will not spread from the (i,j) cell to the (k,l) cell. Accordingly, the spread component in that particular direction equals zero. Similarly, if $CI \geq 1$ then $\eta_f = 1$, and the fire spreads from the (i,j) cell to the (k,l) cell at a rate determined by equation (3.13).

A basic equation incorporating the effects of wind speed and direction, topography and heterogeneity on the rate of fire spread in a particular direction has been proposed. The vector velocity field determines individual components representing the rate of spread from a cell to a neighbouring cell. The next two sections introduce explicit equations describing the relationship between the rate of fire spread and wind and topographic effects. Wind and slope are treated as independent variables affecting fire spread rate (Weise and Biging, 1997).

3.4.1. Topographic Effects

Slope has a considerable influence on the rate of spread, especially in the initial stages of a fire (Luke and McArthur, 1978). If a fire burns up a slope, then the angle between the flame and the unburned fuel is reduced (Figure 2.9). This leads to an increase in the degree of preheating of the unburned fuel immediately in front of the flames, resulting in an increase in the forward rate of spread (Burgan and Rothermel, 1984; Trollope, 1984b; Kushla and Ripple, 1997; Luke and McArthur, 1978; Weise and Biging, 1996, 1997). Conversely, the angle increases for a fire spreading down slope and the radiant heat transfer decreases, causing a decrease in the rate of spread.

Data from experimental fires in eucalypt and grass fuels in Australia indicate that the rate of forward progress of a fire on level ground doubles on a 10° slope and increases almost fourfold travelling up a 20° slope (Luke and McArthur, 1978). Spread is considerably reduced on down slopes, particularly when moving with the prevailing wind and the general relationship between slope and rate of spread is shown in Figure 3.3 (Luke and McArthur, 1978). In Figure 3.3, negative slope angles represent down slope fire spread and similarly, positive angles pertain to up slope spread.

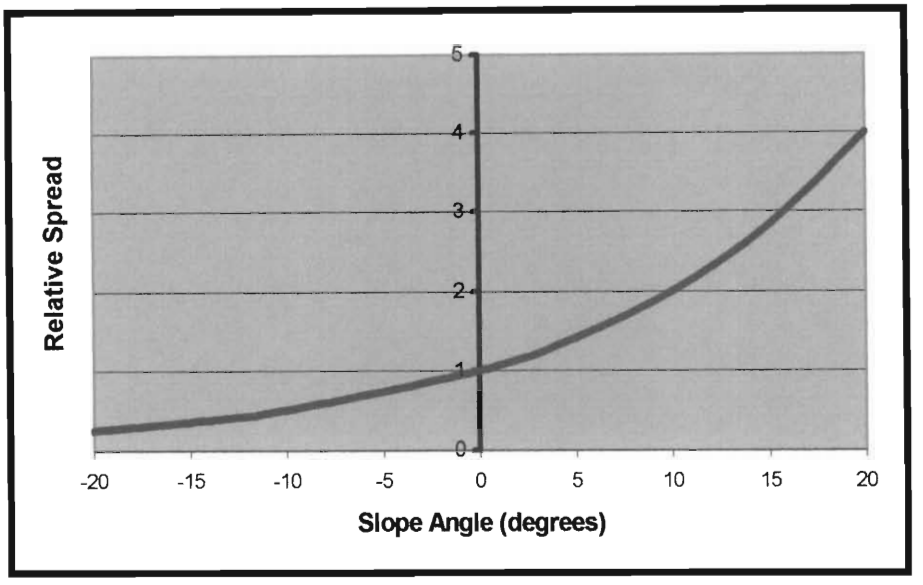

Figure 3.3. The effect of slope on increasing or decreasing the rate of spread of the headfire in forests and grasslands (from Luke and McArthur, 1978)

This relationship between spread and slope is generally accepted throughout Australia and is supported by data derived from individual fire reports for the California region by the US Forest Service (Luke and McArthur, 1978). Experience gained in the US indicates that the increasing effect of slope on the rate of spread of fires burning uphill doubles from a moderate (0° to 22°) to a steep slope (22° to 35°) and then doubles again from a steep to a very steep slope (35° to 45°) (Trollope, 1984b).

The Australian slope effect is quoted as a multiplying factor of the spread rate. Cheney (1981) proposed the following general relationship between slope and rate of spread:

$$R = R_0 \exp(\alpha \theta_s) \tag{3.14}$$

where R is the rate of spread (m/s); R_0 is the rate of spread on level ground (m/s); α is 0.0693; and θ_s is the slope angle (°).

Van Wagner (1988) derived a formula for the case of fire spreading down slope by conducting laboratory experiments using fuel beds consisting of pine needles. Results obtained showed that the spread rate decreased to 64% of the level rate as slope was raised to 22°, then gradually increased to the level rate at 45°. A least-squares regression of the experimental data yielded the following equation:

$$\phi_s = 1 - 0.330\theta_s + 0.000749\theta_s^2 \tag{3.15}$$

where ϕ_s is a downhill spread rate factor that is applied as a multiplier of the estimated level rate of spread and θ_s is the slope angle.

Rothermel (1972) proposed a slope co-efficient that modifies the propagating flux in the numerator of equation (2.2), by conducting experiments on fine fuels in a large combustion laboratory. The effect of slope on spread rate was correlated to the compaction of the fuel bed, described by the packing ratio β, and the slope angle:

$$\phi_s = 5.275\beta^{-0.3}(\tan\theta_s)^2 \tag{3.16}$$

where ϕ_s is the slope co-efficient and tan(θ_s) is the slope of the fuel bed. Rothermel's formulation for the effect of slope on the spread rate, however, assumes that a fire spreading down slope spreads at a rate equal to that on level ground. Equation (3.16) was derived for the case of fire spreading up slope only and therefore only applies to positive angles. If a fire is spreading down slope then in terms of Rothermel's formulation, $\phi_s = 0$. The foundation of this assumption is that fires spreading down slope are not heated from radiation from the flame, but rather from the combustion interface.

In South Africa, no quantitative data on the effect of slope on spread rate are available (Trollope, 1984b). Consequently, these effects were incorporated into the proposed CA model using the formulation of Cheney (1981), as the relationship between slope and spread rate was derived for conditions most similar to those occurring in South Africa i.e. grasslands and savanna ecosystems. Furthermore, Cheney (1981)

accounted for reduced rates of fire spread for the case in which down slope movement occurs.

In the CA model, each cell contains a parameter for its height. Slope is calculated by finding the difference in height between any two neighbouring cells and dividing by the horizontal distance between the two cells. If the cells are adjacent then the difference in heights is divided by a, whereas if the cells are diagonal, the horizontal distance is $\sqrt{2}a$. The slope angle, θ_s, is determined by finding the arctangent of the slope.

3.4.2. Wind Effects

Wind is generally viewed as affecting heat transfer from a flame to unburned fuel downwind of the flame primarily by changing the angle between the flame relative to the fuel. Wind increases radiant heat transfer for headfires because the flame is tilted toward the unburned fuel and decreases radiant heat transfer for backfires because the flame is tilted away from the unburned fuel (Burgan and Rothermel, 1984; Trollope, 1984b; Luke and McArthur, 1978; Nelson and Adkins, 1987; Weise and Biging, 1996, 1997).

In many respects, the effect of wind on the rate of fire spread is analogous to that of slope. Both affect the angle between the flame and the unburned fuel (Figure 3.4). Luke and McArthur (1978) found that, except at very low and very high wind speeds, the rate of spread of a fire varies approximately as the square of wind speed. Thus in a grassland situation the rate of spread under a 15 km/h wind is only one-quarter of the spread under a 30 km/h wind.

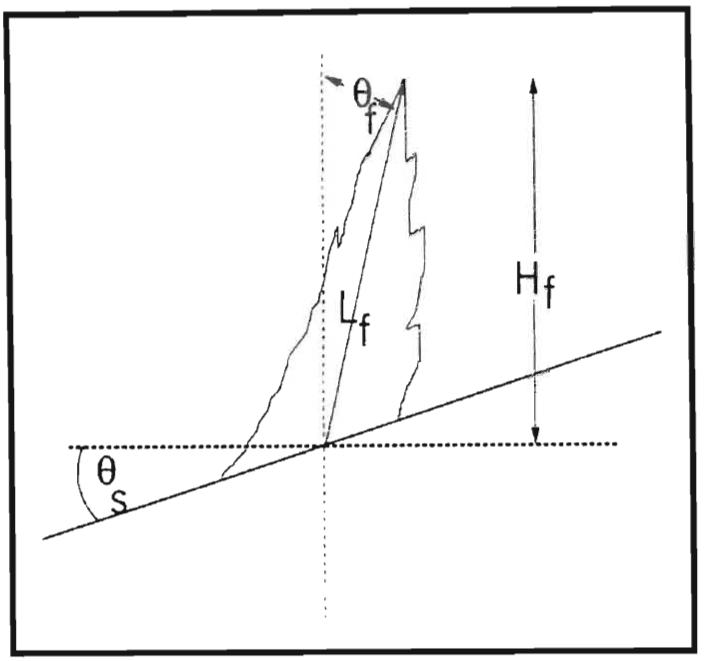

Figure 3.4. Flame geometry of a line fire. Flame angle (θ_f) is measured from the vertical in the direction of fire spread: positive values indicate that the flame is tilted in the direction of fire spread, and negative values indicate that the flame is tilted away from the direction of fire spread. Slope angle (θ_s) is measured relative to a horizontal line. H_f is the flame height and L_f the flame length (Weise and Biging, 1996).

Beaufait (1965) found that wind speeds ranging from 0 to 3.6 m/s increased the rate of spread of surface head fires exponentially but had no effect on the rate of spread of backfires. The lack of effect on backfires is, apparently, a widely observed phenomenon. The reasoning is that, in the case of a backfire, the flame is not responsible for heating the unburned fuel but rather it is heated from the combustion interface (Beaufait, 1965).

There is a strong interrelationship between fuel particle size, fuel distribution and wind speed and it is difficult to apply the same basic relationships to fine grass fuel and to heavier forest fuels (Luke and McArthur, 1978). An added complication is that once the open wind velocity exceeds 50km/h, the rate of forward spread in grasslands decreases (Figure 3.5). The chief reason for this is that the head fire becomes narrow and tends to become fragmented into a number of even narrower heads, so that a deceleration process begins to operate (Luke and McArthur, 1978; Rothermel, 1972).

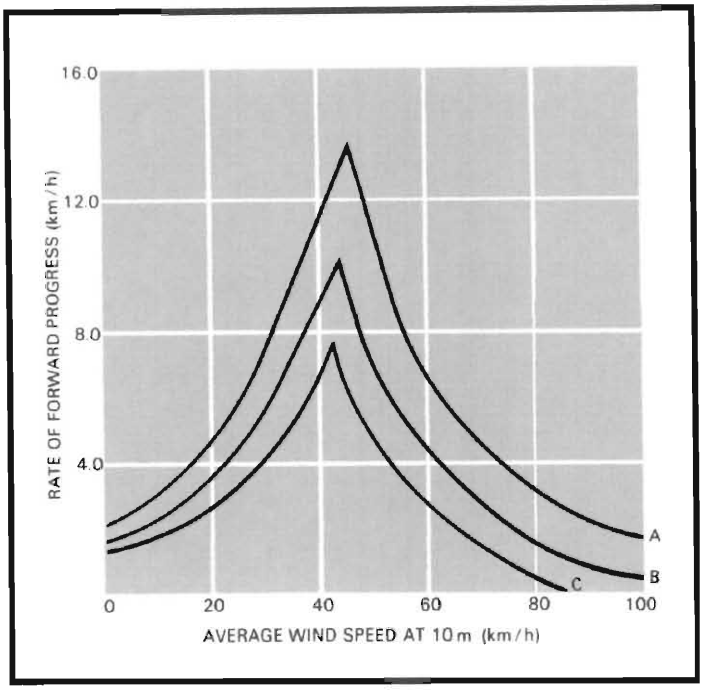

Figure 3.5. Relationship between rate of forward progress of grassfires and wind speed in varying pasture growth: (A) heavy continuous pastures; (B) moderate density pasture; (C) sparse pastures (from Luke and McArthur, 1978).

Rothermel (1972) conducted laboratory experiments to determine an empirical relationship between wind velocity, U, and a multiplication factor for the wind, ϕ_w, that included the interrelationship between and the size of the fuel particles, represented by the surface area to volume ratio σ_v, and the compaction of the fuel bed. The degree of compaction of the fuel bed was represented by the ratio of the packing ratio β, to the optimum packing ratio β_{op}. Correlating these parameters yielded the following equation (Wilson, 1980):

$$\phi_w = C\left(3.281U\right)^B \left(\frac{\beta}{\beta_{op}}\right)^{-E} \tag{3.17}$$

where $C = 7.47\exp\left(-0.8711\sigma_v^{\,0.55}\right)$

$B = 0.15988\sigma_v^{\,0.54}$

$E = 0.715\exp\left(-0.01094\sigma_v\right)$.

The wind co-efficient calculated using equation (3.17) modifies the propagating flux in the numerator of equation (2.2). The derivation of ϕ_w assumed that the rate of fire spreading on level ground against the wind equals that in which no wind occurs, as per Beaufait (1965). In the event of a backfire, U is set equal to 0 and hence, ϕ_w=0. Rothermel's formulation for backfire spreading is analogous to the case of fire spreading down slope. In this instance, heating of fuel is by radiation emitted from the combustion interface and not the flame.

An alternative method for incorporating wind effects on the spread rate deals with the influence of wind velocity on flame properties. Flame angle models assess the impact of wind on tilting the flame either toward or away from the surrounding unburned fuel (Weise and Biging, 1996). Flame angle, θ_f, is measured from the vertical in the direction of fire spread (Figure 3.4). Positive values indicate that the flame is tilted in the direction of fire spread and conversely, negative values indicate that the flame is tilted away from the direction of fire spread.

Numerous authors have derived theory relating flame angle to the ratio of a fire's buoyant force and the force of the horizontal wind (Albini, 1981; Nelson and Adkins, 1986; Putnam, 1965). Albini (1981) developed a physical model of the structure of the wind-blown flame of a turbulent wind-driven line fire that included chemical reactions. The flame angle was roughly approximated as being:

$$\tan^2 \theta_f \approx \left(\frac{3}{2}\right)\frac{U^2}{gH_f} \tag{3.18}$$

where g is the earth's gravitational acceleration (m.s^{-2}) and H_f is the flame height (Figure 3.4). The ratio (U^2/gH_f) is dimensionless and is called the Froude number (Weise and Biging, 1996). Weise and Biging (1996) found that predictions using this rough approximation matched observed data from laboratory fires somewhat better than existing empirical relations.

Putnam (1965) developed a theoretical model relating flame angle to the Froude number defined in terms of the flame length, L_f, using experimental data for natural gas flames. The model was derived for conditions of horizontal wind flow and no slope. The final form of the equation was calculated as (Putnam, 1965):

$$\theta_f = \tan^{-1}\left(1.4\left(\frac{U^2}{gL_f}\right)^{0.5}\right) \tag{3.19}$$

Nelson and Adkins (1986) examined flame length and angle using data for 22 laboratory and 8 field-scale fires. New coefficients for Byram's (1959) empirical relationship relating flame length and fire intensity were estimated that predicted flame lengths that were 70-80% of those predicted by Byram (1959). The flame angle model proposed by Nelson and Adkins (1986) is given by:

$$\theta_f = \tan^{-1}\left(1.22\left(\frac{U^2}{gH_f}\right)^{0.5}\right) \tag{3.20}$$

Weise and Biging (1996) found that equation (3.19) and (3.20) tended to underestimate flame angle for wind tunnel experiments, although the experimental data supported the theory that flame angle is a function of the square of root of the Froude number. Discrepancies were attributed to measurement difficulties (Weise and Biging, 1996).

Weise and Biging (1996) used heading fire data to estimate the parameters for both forms of the Froude model. Regression analysis of the flame height data yielded an equation that was significant in accounting for 61% of the variation of heading fire flame angle (Weise and Biging, 1996):

$$\theta_f = \tan^{-1}\left(2.35\left(\frac{U^2}{gH_f}\right)^{0.57}\right) \tag{3.21}$$

Parameter estimates for equation (3.21) were highly correlated with $r = 0.95$ (Weise and Biging, 1996). The regression model based on flame length only accounted for 48% of the variation:

$$\theta_f = \tan^{-1}\left(2.67\left(\frac{U^2}{gL_f}\right)^{0.57}\right) \tag{3.22}$$

Fire behaviour studies in South Africa have shown that wind speed has no statistically significant effect on the intensity and flame height of surface grass fires under conditions of controlled burning where wind velocity does not exceed 5.6 m/s (Trollope, 1984b). Trollope (1978) found that the average height, H_f, of surface head and backfires in grasslands were 2.8m ±0 .4m and 0.8m ± 0.1m respectively.

In contrast, McArthur (1967) found that although rates of spread are greatly increased with increasing wind speed, flame heights are correspondingly reduced (Figure 3.6). This partly explains why crown fires - fires that burn in the canopies of trees and shrubs (Trollope, 1984b) – do not always occur when wind speeds and spread rates are high. This was demonstrated in the southern Tasmanian fire of 7th February 1967 when few forest fires crowned (Luke and McArthur, 1978).

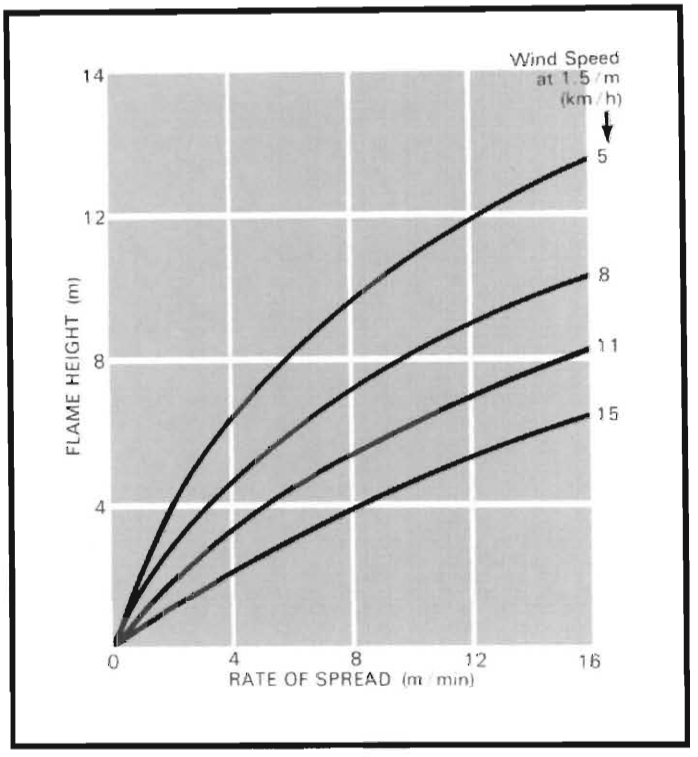

Figure 3.6. Relationship between flame height and rate of spread in dry sclerophyll eucalypt forest (from Luke and McArthur, 1978)

Wills (1987) collected data for 10 field-scale experimental fires conducted in savanna vegetation at the Hluhluwe and Umfolozi Game Reserves in northern KwaZulu-Natal. (Table 3.1). These data were used to determine a relationship between the flame angle, produced by the wind, and the resultant rate of fire spread. The flame angle models of Putnam (1965), Nelson and Adkins (1986), Weise and Biging (1996) were applied in this regard. Flame angle models requiring estimates of flame height were implemented assuming a flame height equal to 2.8m – in accordance with the findings of Trollope (1984b). The earth's gravitational acceleration, g, was approximated as $9.8 m.s^{-2}$.

Table 3.1.

Conditions of fuel and weather at 10 experimental fires in savanna vegetation in the Hluhluwe and Umfolozi Game Reserves in northern KwaZulu-Natal (from Wills, 1987)

Fire Number	Fuel Moisture	Wind		Slope	Rate of Spread	Flame Length
		Speed	Direction			
	(%)	(km/h)	(degrees)	(degrees)	(m/min)	(m)
H1	4.2	6.3	0	0	7.9	2.0
H2	5.0	12.8	90	0	5.6	1.2
H3	4.4	6.3	0	0	5.0	2.2
H4	4.4	10.1	0	0	17.5	3.0
U1	4.7	13.5	0	0	49.5	3.2
U2	4.8	16.8	0	0	60.1	4.5
U3	4.2	4.2	0	0	2.5	1.0
U4	4.2	12.0	45	0	11.0	2.0
U5	4.2	9.0	0	0	50.0	3.0
U6	4.2	7.2	45	0	9.2	1.5

*H = Hluhluwe, U=Umfolozi

Table 3.2 contains the flame angle calculated using the respective models. In fires H2, U4 and U6 the wind blew at an angle to the direction of spread. The component of the wind in the direction of fire spread was assessed using a vector approach. Letting θ_d represent the angle between the wind direction and the direction of fire spread, then magnitude of the wind component, U_e, was defined as follows:

$$U_e = U\cos(\theta_d) \tag{3.23}$$

Applying equation (3.23), the wind speed in the direction of spread for fire H2=0 and the resultant flame angle is 0 i.e. the fire spreads as if no wind existed. In the case of fire U4 and U6 the wind components were calculated as 8.5 km/h and 5.1 km/h respectively.

Table 3.2.

Flame angle in degrees generated by each of the flame angle models using the experimental data of Wills (1987)

Putnam	Nelson and Adkins	Weise and Biging (Flame Height Model)	Weise and Biging (Flame Length Model)
28.96	22.17	33.96	42.82
0.00	0.00	0.00	0.00
27.82	22.17	33.96	41.28
35.87	33.11	49.01	51.49
43.15	41.13	58.08	59.39
44.55	47.40	64.12	60.77
27.62	15.24	23.05	41.01
36.67	28.74	43.36	52.43
32.84	30.21	45.32	47.85
27.31	18.23	27.84	40.58

The wind factor, ϕ_w, was assumed to be an exponential function of the flame angle that modified the rate of fire spread in flat, windless conditions:

$$R = R_0 \exp(\beta\theta_f) \tag{3.24}$$

where $\phi_w = \exp(\beta\theta_f)$. R_0 was calculated using the Rothermel fire spread model (equation 2.2) with neither wind nor slope being present. Taking the natural logarithm of both sides of equation (3.24), the value of β for each particular flame model can be estimated by a least-squares linear regression.

Table 3.3 lists the values obtained for β and the correlation coefficient, r, of the predicted versus the observed spread rates. The correlation coefficient was significant at the 1% level for all the models except the Weise and Biging flame length model, which was significant at the 5% level.

Table 3.3.

Estimation of β by linear regression with associated correlation coefficient *r*.

	Putnam	Nelson and Adkins	Weise and Biging (Flame Height Model)	Weise and Biging (Flame Length Model)
β	0.0719	0.0835	0.0576	0.0501
r	0.80	0.85	0.87	0.77

Figure 3.7 illustrates a graph of the wind angle versus the predicted wind factor for the four regression models. In the absence of wind, $\theta_f = 0$ and $\phi_w = 1$ as expected. As the wind increases, the rate of spread of the headfire increases exponentially as a consequence of positive flame angles. Conversely, the rate of backfire spread decreases exponentially due to the flame being tilted away from the unburned fuel.

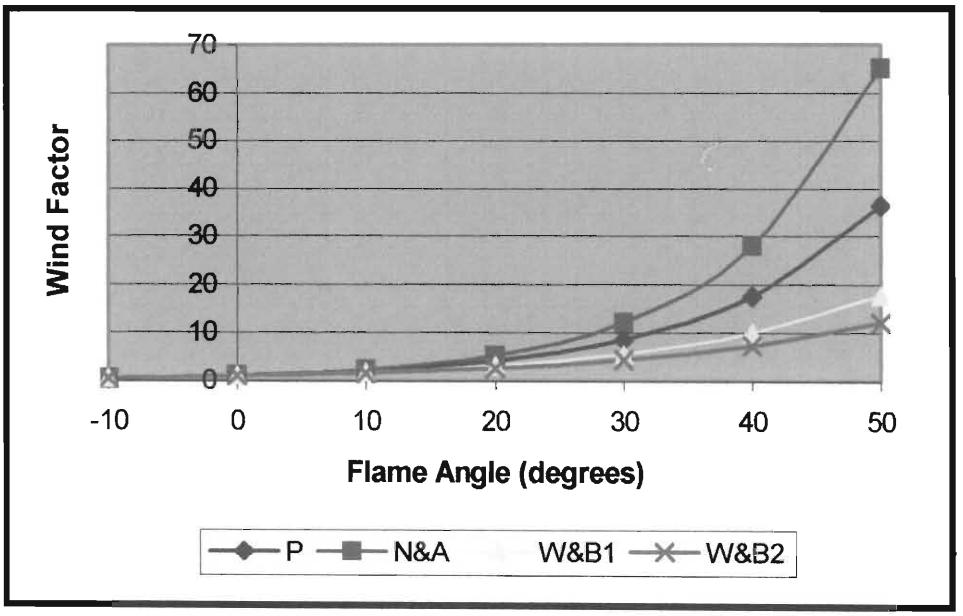

Figure 3.7. Flame angle versus wind factor for various models: Putnam (P), Nelson and Adkins (N&A), Weise and Biging (Flame Height) (W&B1) and Weise and Biging (Flame Length) (W&B2).

The regression model of Nelson and Adkins flame angle model predicts spread rates that are approximately 65 times greater than the rate of spread in windless conditions if $\theta_f = 50°$. Similarly, the regression model of the Weise and Biging flame length model only predicts a wind factor $\phi_w = 12$ for the equivalent flame angle. All regression models predict reduced rates of spread in the case of backfire spread.

An interesting feature of the four regression models was that the value of the wind coefficient parameter β is less than the respective slope parameter, i.e. 0.0693, for both models of Weise and Biging and greater than the slope parameter for the remaining two models. The implication of $\beta < 0.0693$ is that a fire spreading upslope has a greater effect on the rate of fire spread than a wind velocity for an equivalent flame angle.

Burgan and Rothermel (1984) however, found that although the mechanism producing this effect is the same as for slope – improved heat transfer because the flames are closer to the unburned fuels – the effect is accentuated in the case of wind. This is because the combustion rate of a fire is directly influenced by the rate of oxygen supply to the fire, and wind speed tends to be positively related to the rate at which energy is released by the fire.

The reason for the relatively small β parameter in the case of the Weise and Biging flame length and flame height models is that these models predict significantly larger values for the flame angle than the Putnam and Nelson and Adkins models for an equivalent wind velocity (Table 3.2). As a consequence of the inverse relationship of these parameters, smaller values for β correspond to larger flame angles and vice-versa. Further verification of the effect of slope on the rate of fire spread, however, requires investigation as the relationship applied for the purposes of this project was derived for Australian conditions. Therefore, it is impossible to conclusively relate the effect of wind and slope on flame angle, and hence spread rate, due to the lack of pertinent slope information.

Wind direction is restricted in the model to the eight major compass directions. The rate of fire spread in the direction of the wind is modified according to the flame angle

θ_f. The rate of fire spread in the opposite direction to the wind is adjusted by setting flame angle to $-\theta_f$. In all other directions, the flame angle $\theta_f = 0$.

If the wind is diagonally orientated i.e. north east, north west, south east, south west, then the wind has additional components in the two nearest major compass bearings e.g. a north east wind has components in a northerly and an easterly direction. The magnitude of the wind in these directions is calculated using equation (3.23) - which determines the vector component of the wind velocity in that particular direction. The flame angle in each particular direction can then be calculated based on the respective flame angles. Negative flame angles are applied in the direction directly opposite to the associated wind direction and its components.

3.4.3. Combined Wind and Slope Effects

Wind and slope effects are easily combined into the rate of spread formula by multiplying their respective components, in a particular direction, using equation (3.10). The general form of the spread equation for a fire spreading from the (i,j) cell to a neighbouring (k,l) cell is given by:

$$\widetilde{R}_{i,j} = R_0 \exp\left(0.0693(\theta_s)_{k,l} + (\beta\theta_f)_{k,l}\right)(\eta_f)_{k,l} \tag{3.25}$$

where the values of θ_f and β are calculated depending on the flame angle model in operation (Table 3.3). In the absence of wind and on homogeneous, flat terrain, equation (3.25) predicts $R=R_0$ as expected. The proposed equation for calculating the spread in any direction is adapted into a CA model in the next section.

3.4.4. The CA Local Rule

The CA local rule determines the influence of the state of a particular cell on some or all of the immediately adjacent neighbours. The neighbourhood of a cell consists of the eight nearest neighbouring cells and the cell itself. The state of the (i,j) cell after a single time step depends on the rate of spread from a neighbouring cell to the (i,j) cell at time t, $R^t_{k,l}$, and the state of the cell itself at time t:

$$S^{t+1}_{i,j} = f\left(S^t_{i,j}, R^t_{i-1,j-1}, R^t_{i-1,j}, R^t_{i-1,j+1}, R^t_{i,j-1}, R^t_{i,j+1}, R^t_{i+1,j-1}, R^t_{i+1,j}, R^t_{i+1,j+1}\right) \tag{3.26}$$

Unburned and burned out cells, in which no fuel combusts, have spread rates $R^t_{k,l} = 0$ and hence, have no influence on the state of the (i,j) cell at time t. Cells that are burning have vector spread rates in each direction calculated using equation (3.25). The basis for the local rule is derived for conditions in which neither wind nor slope existed. The incorporation of wind and slope factors, as described in the preceding sections, are assumed to modify the rate and pattern of fire fronts generated by the CA model.

To formulate the local rule, let a homogeneous landscape be represented by a matrix of identical cells each with side length a, where each cell represents a CA cell. In the absence of wind and on level ground, the spread rate in each cell is the same and can be calculated using equation (3.25) i.e. $R^t_{k,l} = R_0$. Furthermore, the total heat required to ignite a cell at time t=0 is represented by H_0.

If the (i,j) cell is completely unburned and only one adjacent neighbour burning, then the time taken for the fire to spread to the (i,j) cell, t_a, is given by equation (3.3). Similarly, if the (i,j) cell is completely unburned and only one diagonal cell is burning, then the (i,j) cell commences burning after t_d seconds, where t_d is calculated using equation (3.4). In this instance, the burning diagonal neighbour will first spread to two of its adjacent neighbours that are also adjacent neighbours of the (i,j) cell (Figure 3.8).

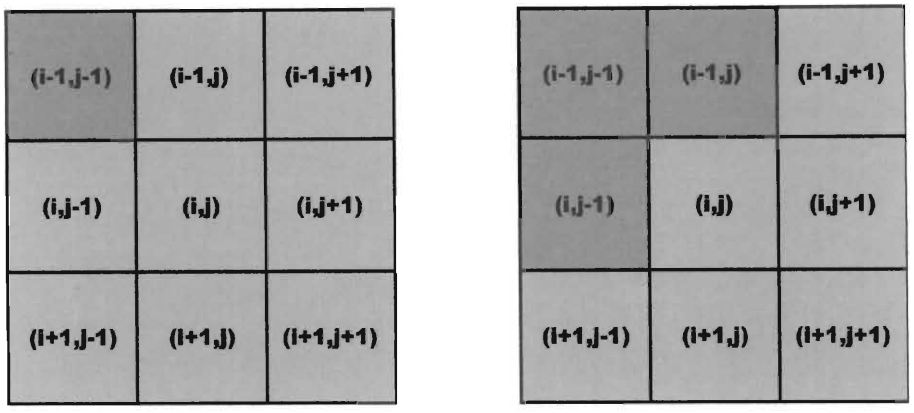

(a) **(b)**

Figure 3.8 (a) The initial CA configuration with only the (*i-1,j-1*) cell burning. (b) After a single time step the (*i-1,j*) and (*i,j-1*) cell begin burning.

Therefore, in the first t_a seconds, the (i,j) cell receives heat from diagonal neighbour only. Thereafter, additional heat is received from the two common adjacent cells. The rate at which heat is received, per second, by the (i,j) cell is given at any time t is given by:

$$\frac{dH_r}{dt} = \begin{cases} x\left(\frac{H_0}{t_d}\right) & (0 \le t \le t_a) \\ x\left(\frac{H_0}{t_d}\right) + 2\left(\frac{H_0}{t_a}\right) & (t_a \le t \le t_d) \end{cases} \tag{3.27}$$

where x represents the proportion of H_0 that is supplied by the burning diagonal neighbour. Integrating these equations over the time interval $[0,t_d]$ yields:

$$\begin{aligned} H_r &= \int_0^{t_a}\left(\frac{xH_0}{t_d}\right)dt + \int_{t_a}^{t_d}\left[\left(\frac{xH_0}{t_d}\right) + 2\left(\frac{H_0}{t_a}\right)\right]dt \\ &= \int_0^{t_d}\left(\frac{xH_0}{t_d}\right)dt + \int_{t_a}^{t_d} 2\left(\frac{H_0}{t_a}\right)dt \\ &= xH_0 + 2H_0\left(\frac{t_d - t_a}{t_a}\right) \end{aligned} \tag{3.28}$$

At time $t=t_a$, the sum of the heat received by the (i,j) cell must equal H_0 as the cell must start burning. Applying this condition and substituting equation (3.4) for t_d in terms of t_a:

$$\begin{aligned} H_0 &= H_0\left(x + 2\left(\sqrt{2}-1\right)\right) \\ \Rightarrow \quad x &\approx 0.17 \end{aligned} \tag{3.29}$$

Therefore, approximately 17% of the total heat required to burn the (i,j) cell comes from the neighbouring diagonal cell whilst the remaining 83% comes from the two adjacent cells which begin contributing heat at time $t=t_a$. The (i,j) cell is assumed to be burned out at the time when all the surrounding neighbours have commenced burning. Generally, if (i,j) cell starts burning at time t_s, then the cell is burned out after $t_s + t_d$ seconds. Consequently, the CA local rule has been verified for the homogeneous, slopeless, windless case to be of the same form as equation (3.6).

In the presence of wind, topography and heterogeneous fuels, the rate of fire spread to the (i,j) cell varies according to equation (3.25). If $R^t_{k,l}$ represents the rate of spread from the (k,l) cell to the (i,j) cell at time t, taking these additional factors into account, then in a discrete time interval Δt, the CA local rule that updates the cells in the lattice is given by:

$$\begin{aligned} S^{t+1}_{i,j} = S^t_{i,j} + &\left\{\left(\frac{1}{a}\right)\left(R^t_{i-1,j} + R^t_{i,j-1} + R^t_{i,j+1} + R^t_{i+1,j}\right)\right\}\Delta t + \\ &0.17\left\{\left(\frac{1}{\sqrt{2}a}\right)\left(R^t_{i-1,j-1} + R^t_{i-1,j+1} + R^t_{i+1,j-1} + R^t_{i+1,j+1}\right)\right\}\Delta t \end{aligned} \tag{3.30}$$

If $S^{t+1}_{i,j} < 1$ then the cell is unburned and $R^{t+1}_{i,j} = 0$. If $S^{t+1}_{i,j} \geq 1$ and $t < t_s + t_d$ then the cell is burning and spreads to its surrounding neighbours at a rate determined by equation (3.25). The cell is burned out if it is burning at time t and $\left(t + \Delta t\right) \geq \left(t_s + t_d\right)$. When a cell is burned out, there is no combustion and $R^t_{i,j} = 0$.

3.5. ALGORITHM

Figure 3.9 is a flow chart depicting the algorithm of a single time step in the fire growth model developed. The CA consists of n rows and m columns, where each cell contains parameters for its fuel characteristics, elevation, mineral and moisture content. User-defined inputs to the model include:

- The simulation time step (Δt).
- Wind speed (U) and direction (N, S, E, W, NE, SE, SW, NW).
- Topographic coverage.
- Fuel coverage with associated moisture content for each fuel type.
- Flame angle model.
- Flame height or flame length.
- Ignition point.

The output of the model is a time-evolving fire front that incorporates the spatial variation in fuel and topography with temporal wind conditions. In the next chapter the theoretical model is implemented using hypothetical landscapes under various scenarios.

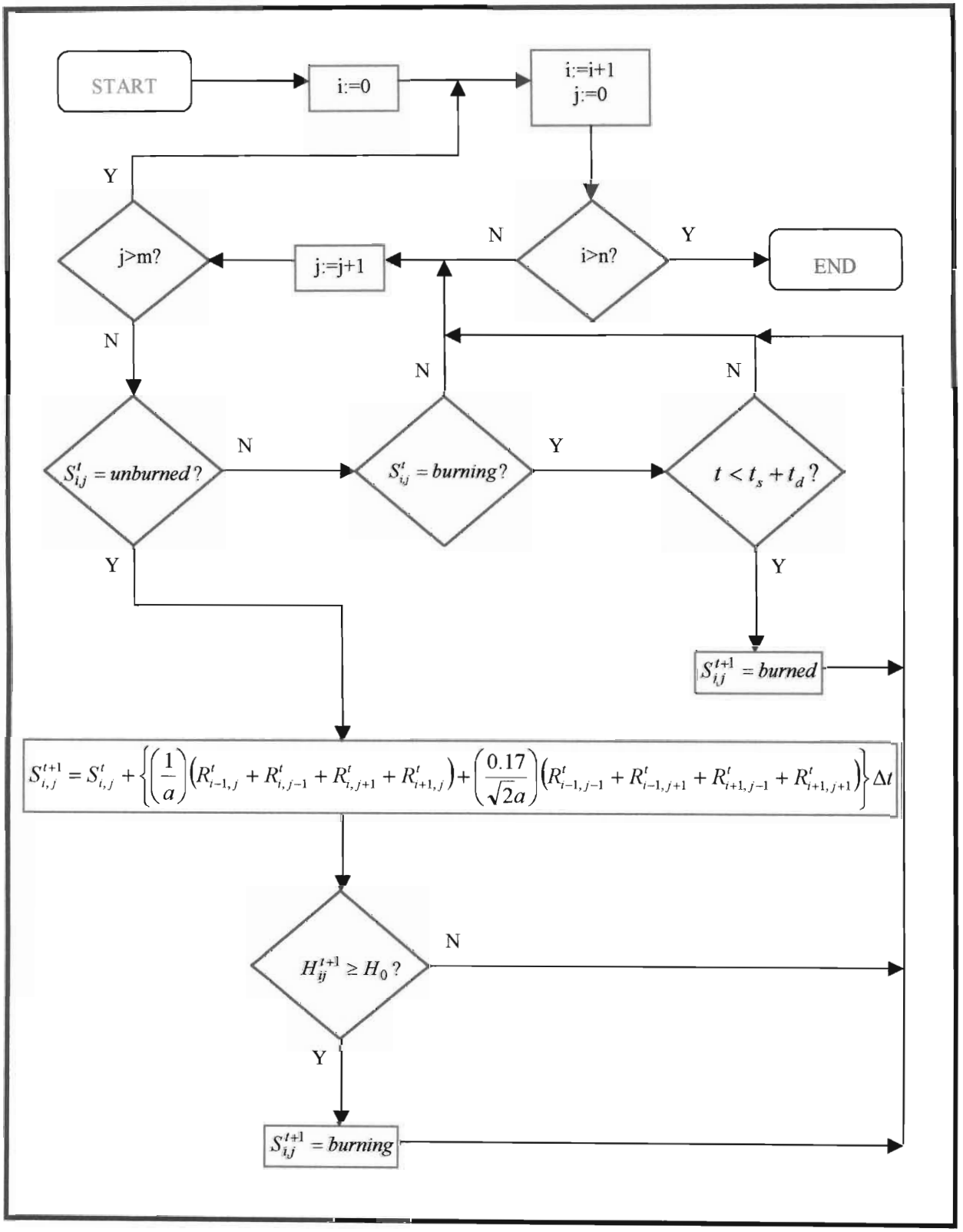

Figure 3.9. Flow chart of the algorithm of a single time-step in the CA model.

CHAPTER 4

IMPLEMENTATION

4.1. INTRODUCTION

An algorithm based on the proposed fire growth model, described in the previous chapter, has been constructed to facilitate the determination of fire fronts in a number of hypothetical landscapes. The simulation model was developed using the object-oriented programming language, Delphi, by Borland, and was designed for operation in a Windows 95/98 environment.

The objective of implementing the model to hypothetical landscapes under various scenarios of fuel, wind and topography is to assess its ability to predict the rate and pattern of fire spread and investigate its sensitivity to variations in these parameters. Predictions generated by the model are evaluated by comparing the characteristics of the fire fronts with the experience of fire spreading in reality. Statistical analysis of simulation results is performed subject to the availability of observed fire information.

Tests were performed on a 50x50 lattice consisting of square cells with a side length of 10m. Each cell contained parameters describing its fuel characteristics - fuel load, surface area to volume ratio, fuel bed depth, mean fuel energy content and moisture of extinction - moisture content and height above sea level. Values for these parameters were assigned according to the scenario implemented, which ranged from fire spreading in a homogeneous landscape on level terrain in the absence of wind to fire spreading in the presence of a uniform wind, topography and heterogeneous fuels.

4.2. HOMOGENEOUS LANDSCAPES

Fuel characteristics for an *Acacia Nilotica* savanna (Table 4.1) were assigned to each cell for scenarios involving homogeneous landscapes. Wills (1987) collected information for this fuel model from the Hluhluwe and Umfolozi Game Reserves situated in northern KwaZulu-Natal. The vegetation of the area is dominated by the

grasses *Themeda Triandra* and *Cymbopogon Excavatus*, and short (up to 2 metres) *Acacia Nilotica* trees.

Table 4.1.

Fuel model parameters for an *Acacia Nilotica* savanna in the Hluhluwe and Umfolozi Game Reserves (from Wills, 1987).

Parameters of Fuel Model for an *Acacia Nilotica* Savanna	
Fuel Loads	
Fine Dead Fuel (1 hr timelag)	312 gm^{-2}
Medium Dead Fuel (10 hr timelag)	2 gm^{-2}
Live Herbaceous Fuel	61 gm^{-2}
Live Woody Fuel	4 gm^{-2}
Surface Area To Volume Ratios	
Fine Dead Fuel (1 hr timelag)	66 cm^2cm^{-3}
Medium Dead Fuel (10 hr timelag)	3.6 cm^2cm^{-3}
Live Herbaceous Fuel	59 cm^2cm^{-3}
Live Woody Fuel	59 cm^2cm^{-3}
Heat Content	19500 kJ/kg
Fuel Bed Depth	0.44m
Moisture of Extinction	20%

4.2.1. Homogeneous Landscape with no Wind and no Slope

Hypothesis:

In the absence of wind and in flat terrain, a fire will spread at the same rate in all directions so that the spread pattern is an approximate circular area with the point of ignition in the centre (Byram, 1959; Luke and McArthur, 1978; Karafyllidis and Thanailakis, 1997).

A graphical representation of the results is shown in Figure 4.1. The fire fronts are approximately circular, with facets being present on the fronts because of the shape of the cells in the CA lattice. The fire was ignited at the centre of the successive fronts that are displayed at 20-minute intervals. The simulation time step was 60 seconds and the fuel moisture content was 1%.

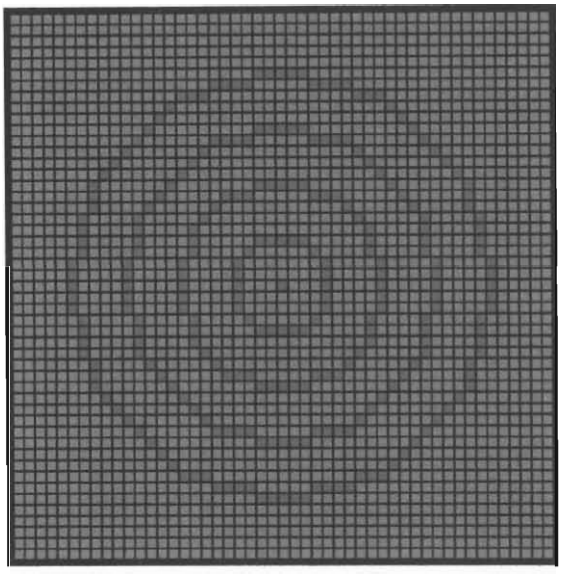

Figure 4.1. Fire fronts in a flat, homogeneous savanna when no wind blows. The fire starts at the centre of the circular fronts that are 20 minutes apart.

The rate of fire spread, which was the same in all directions, was approximated by dividing the distance covered by the fire front by the time elapsed on the simulation clock. This yielded a value for the spread rate of 2.38 $m.min^{-1}$. Increasing the moisture content of the fuel had no impact on the shape of the fire fronts, which remained circular. The position of the fire front varied however, with the rate of fire spread being inversely proportional to the moisture content (Figure 4.2). The relationship between spread rate and moisture content appeared to be of an exponential form and from a least-squares regression of the data the following equation was obtained:

$$R = 2.2437\exp(-0.0816) \tag{4.1}$$

with a correlation coefficient $r = 0.98$ that was significant at the 1% level.

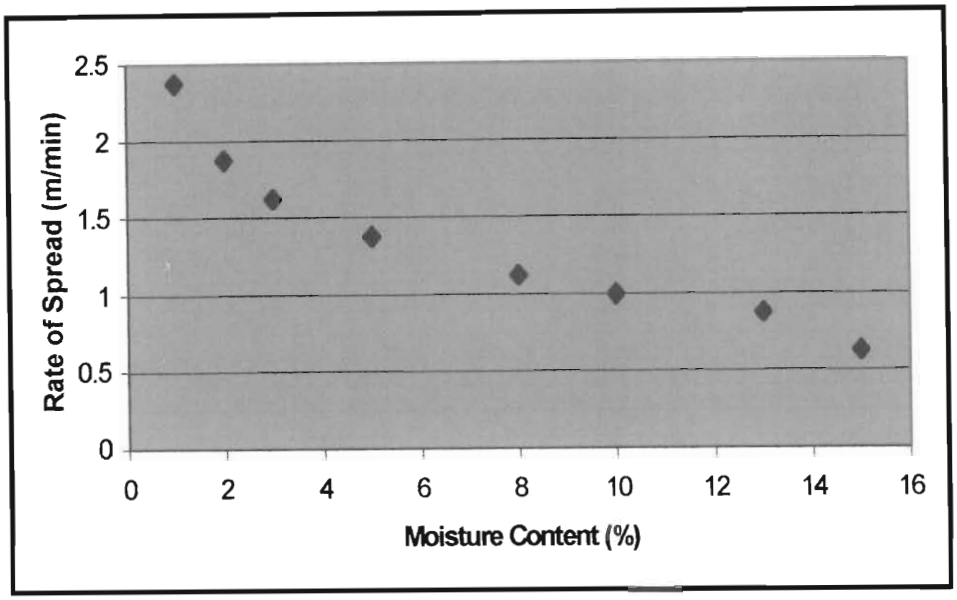

Figure 4.2. Predicted rate of fire spread versus fuel moisture content for a homogeneous landscape in which there is no slope and no wind.

4.2.2. Homogeneous Landscape with Wind and no Slope

Hypothesis:

> *If there is a wind that maintains a constant direction, then the fire front will assume the shape of an elongated ellipse, with the long-axis parallel to the direction of the wind* (Anderson, 1983; Byram, 1959; Luke and McArthur, 1978).

Simulations were performed using fuel and weather data for the 10 experimental fires conducted in the Hluhluwe and Umfolozi Game Reserves (Table 3.1) with the objective of analysing the influence of each flame angle model, discussed in the previous chapter, on the predicted rate of fire spread. These initial tests were not geared at evaluating the shape of the fire, but rather to provide an assessment of the predicted versus observed rates of headfire spread.

Table 4.2 contains the rate of fire spread predicted by the simulation model obtained using the four flame angle models discussed in the previous chapter. The height of

the flame in the Weise and Biging flame height model and the Nelson and Adkins model equalled 2.8m – which corresponded to the average height of grassland headfires recorded by Trollope (1984b). Flame length was assigned in the Weise and Biging flame length model and the Putnam model, according to the value recorded by Wills (1987) for each of the experimental fires (Table 3.1).

A surprising yet consistent feature of the simulation results was the higher correlation coefficient associated with the models requiring input for flame height compared with flame length. The Weise and Biging flame height model had a correlation coefficient $r = 0.88$; the Nelson and Adkins model had $r = 0.85$; the Putnam model had $r = 0.79$; and the Weise and Biging flame length model had $r = 0.78$. All correlation coefficients were significant at the 1% level.

Table 4.2.

Predicted rate of fire spread for each of the flame angle models versus the observed rate of fire spread for 10 experimental fires conducted in the Hluhluwe and Umfolozi Game Reserves by Wills (1987).

Case	Observed (m/min)	Weise and Biging (Flame Height) (m/min)	Nelson and Adkins (m/min)	Putnam (m/min)	Weise and Biging (Flame Length) (m/min)
H1	7.9	8.8	8.5	10.0	11.0
H2	5.6	1.4	1.4	1.4	1.4
H3	5.0	9.0	8.5	9.5	10.3
H4	17.5	20.0	20.0	17.0	17.0
U1	49.5	30.7	40.0	24.0	24.0
U2	60.1	40.0	60.0	30.0	24.0
U3	2.5	5.2	4.8	9.5	10.0
U4	11.0	15.0	15.0	17.0	17.0
U5	50.0	17.0	15.5	13.0	15.0
U6	9.2	6.8	6.2	9.5	10.0
r		0.88	0.85	0.79	0.78

The remaining simulations involving wind were conducted using the Weise and Biging flame height model, which was selected as it corresponded to the highest value of the correlation coefficient. Figure 4.3 illustrates the position of the fire front at 20-minute intervals for a fire spreading through a flat, homogeneous landscape in the presence of a northerly wind of 30m.min^{-1}. The simulation time step was 5 seconds and the fuel moisture content was 1%. The fire was ignited in the centre of the fire fronts.

The rate of headfire spread increased from 2.38 m.min^{-1}, in the case of fire spreading with neither wind nor slope, to 3.9m.min^{-1} whereas the rate of backfire spread decreased to 1.63m.min^{-1}. The shape of successive fire fronts is an approximate ellipse with the long-axis parallel to the direction of the wind.

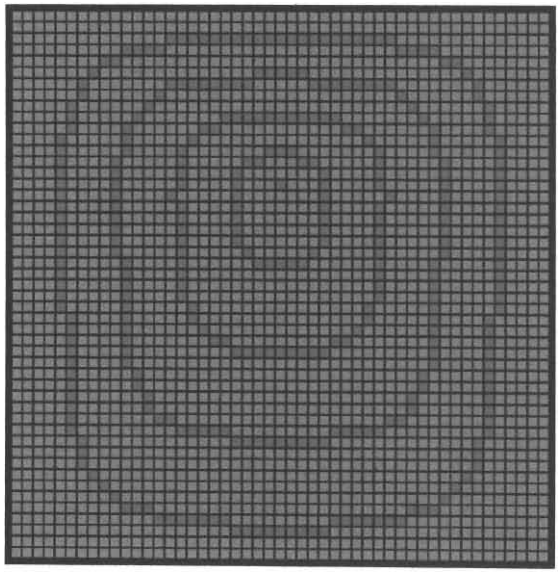

Figure 4.3. Fire fronts in a flat, homogeneous landscape with a northerly wind of 30m.min^{-1}. The fire is ignited at the centre of the fire fronts that are displayed at 20-minute intervals.

As the wind speed increased (the direction remained constant), the degree of elongation increased. This is evident in Figures 4.4a and 4.4b that depicts successive fire fronts in a flat homogeneous landscape with a northerly wind of 60 and 80m min^{-1} respectively. The rate of headfire spread in the former increased to 6.8m.min^{-1} and the rate of backfire spread decreased to 1m.min^{-1}. Similarly, the 80m.min^{-1} wind

produced a headfire spread rate of 9.75m.min^{-1} and a backfire spread rate of 0.75m.min^{-1}.

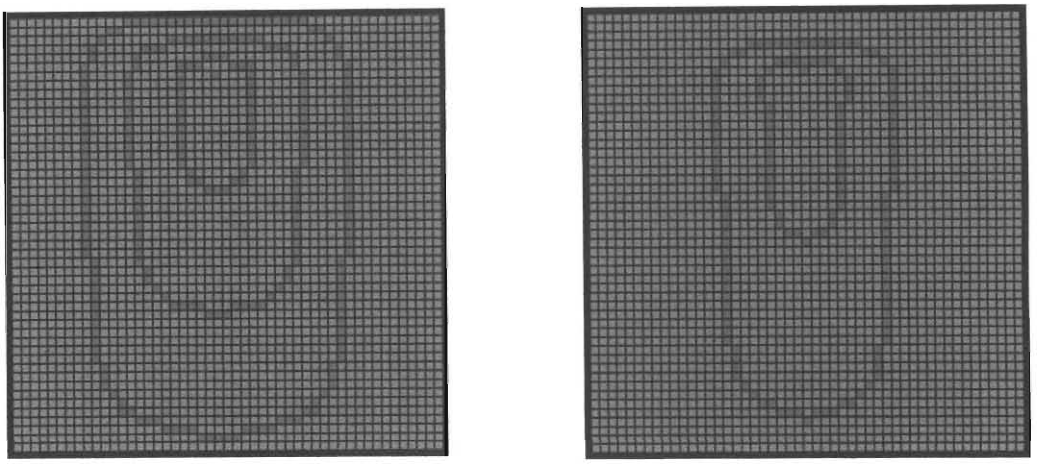

(a) (b)

Figure 4.4. Successive fire fronts in a flat, homogeneous landscape with (a) a 60m.min^{-1} wind and (b) an 80m.min^{-1} northerly wind.

The effect of wind on transforming the shape of the fire from circles – when there is no wind – to an ellipse where the degree of elongation depends on the wind speed, was a commonly observed phenomenon in all simulation tests. The effect of fuel moisture content on the rate and pattern of fire spread required further investigation.

Fons (1946) found that the shape of the burned area in any fuel type is independent of the compactness and fuel moisture content. He confirmed this by comparing the means of the ratio of angular spread distance to the maximum spread distance obtained within each wind class for the upper and lower ranges of compactness and moisture content (Anderson, 1983). The analysis found that the shape of the burned area was dependent only upon wind velocity and formulated an equation for the ratio of maximum length to width for mat beds of ponderosa pine needles as a function of the wind velocity.

Simulations were conducted using a flat, homogeneous landscape in which the fuel moisture contents were assumed to be 1%, 5% and 10% with uniform wind velocities ranging from 0m.min^{-1} to 200m.min^{-1}. The rate of head and backfire spread and the

length to width ratio of the fire fronts generated by the simulation model were evaluated for the various fuel moisture contents to determine the relationship between these parameters.

Figure 4.5 is a graphical representation of the wind speed versus the rate of headfire spread for a homogeneous landscape with a fuel moisture content of 1%, 5% and 10%. The spread rate appears to be an exponential function of the wind speed that depends on the moisture content of the fuel involved. For a 120m.min^{-1} wind, the rate of spread predicted by the model for a fuel moisture of 1%, 5% and 10% was 18, 11.3 and 8.4 m.min^{-1} respectively.

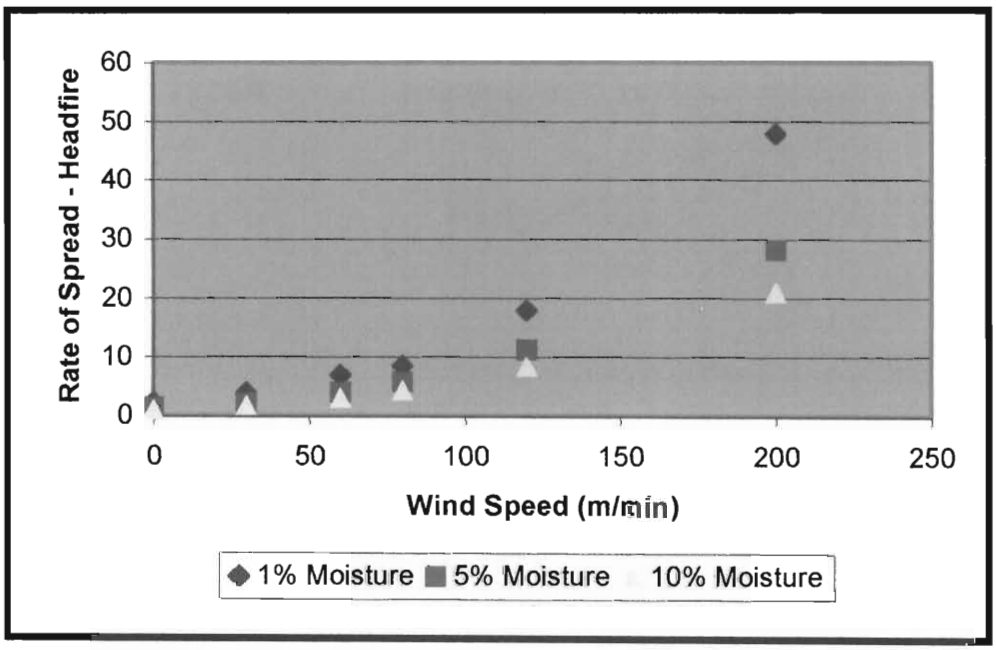

Figure 4.5. Wind speed versus spread rate for a headfire for a homogeneous fuel with a moisture content of 1%, 5% and 10%.

Similarly, the rate of backfire spread decreased exponentially as the wind speed increased for a particular fuel moisture content. The rate of backfire spread predicted by the model for a 1%, 5% and 10% moisture content decreased from 2.38, 1.38 and 1m.min^{-1} respectively when no wind existed to 0.75, 0.5 and 0.38 m.min^{-1} when a wind of 80m.min^{-1} was blowing.

An interesting result was that the length to width ratio determined by the model was in agreement with the findings of Fons (1946). Analysis of the length to width ratio of the fire fronts produced by the simulation model was independent of the moisture content of the fuel but was a function of the wind velocity. Figure 4.6 shows the wind speed versus the length to width ratio for a homogeneous landscape with fuel moisture content of 1%, 5% and 10%.

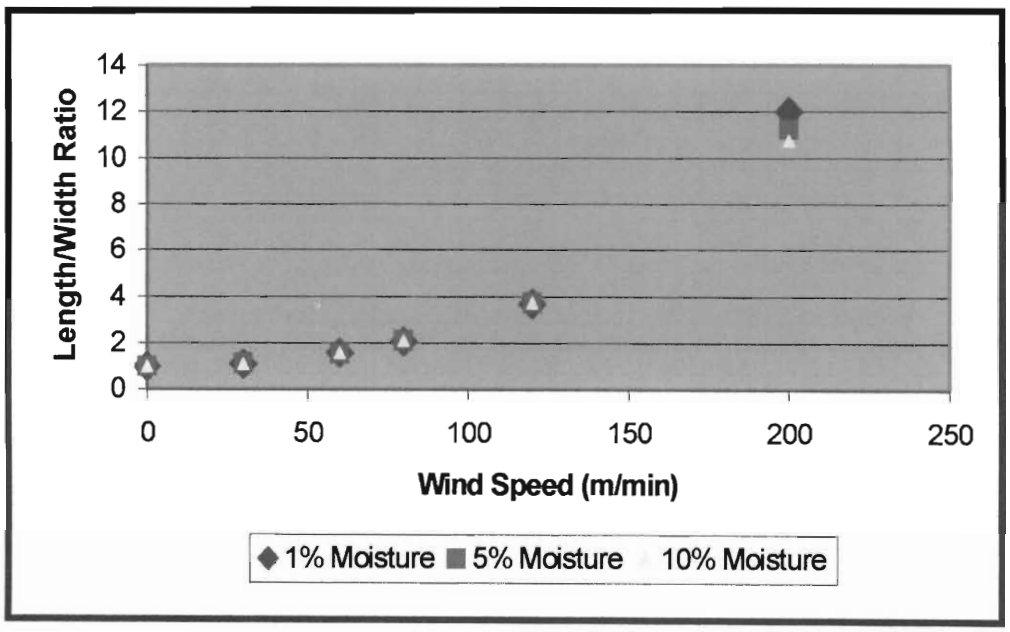

Figure 4.6. Wind speed versus length to width ratio for a fire spreading in a homogeneous landscape with fuel moisture content of 1%, 5% and 10%.

An explicit function for the length to width ratio (l/w) of a fire in terms of the wind velocity (U) measured in m.min^{-1} was obtained via a least-squares regression of the simulation results as being:

$$l/w = 0.821\exp(0.0127U) \tag{4.2}$$

The correlation coefficient $r = 0.99$ and was significant at the 1% level. Equation (4.2) is useful for predicting the dimensions of a fire spreading through a homogeneous fuel in the presence of a constant wind. Furthermore, it validates that the shape of the fire forms an elongated ellipse, with the long-axis parallel to the

direction of the wind, if a constant wind exists. This involves solving equation (4.2) for the critical parameters defining an ellipse.

4.2.3. Homogeneous Landscape with Slope and no Wind

Hypothesis:

> *In the absence of wind, fires burning up slope exhibit higher rates of spread than fires burning either down slope or on level ground due to a decrease in the angle between the flame and the unburned fuel immediately ahead of the flame* (Luke and McArthur, 1978; Trollope, 1984b; Weise and Biging, 1997).

Figure 4.7 depicts the passage of a fire front spreading in a homogeneous landscape containing a hill or mountain. The topographical feature is represented by the black contours to the north-east that are at 2m intervals. The fire spreads in the absence of wind and successive fronts are displayed at 20-minute intervals. The fuel moisture content was 1% to maintain consistency with previous simulations and facilitate comparison of results.

In the first 20 minutes, the fire spreads in a circular fashion at approximately $2.38 m.min^{-1}$ in all directions. As the fire encounters the hill, its rate of spread in that direction increases as the fire burns upslope. The rate of spread in all other directions remains unchanged. First evidence of the increased rate of spread occurs after 40 minutes as the shape of the fire front becomes more pronounced in the north-east. The rate of spread up the hill is approximately $4.12 m.min^{-1}$.

After an hour the fire reaches the summit and begins to descend the hill. As the fire spreads downslope, the rate of spread decreases to roughly $1.5 m.min^{-1}$ resulting in the retardation of the front in that direction. After 100 minutes has elapsed, the fire passes the hill and commences spreading on level terrain.

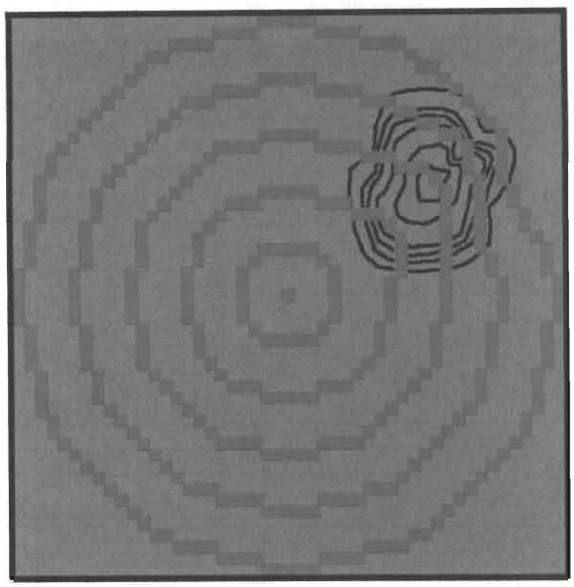

Figure 4.7. Fire spreading in a homogeneous forest containing a hill or mountain in the absence of wind. The topographical feature is represented by the black contour lines that are at 2-metre intervals. Successive fire fronts are displayed at 20-minute intervals.

As a consequence of the topographical feature, the overall shape of the fire is slightly distorted in the north-east direction. The net effect of the hill or mountain has caused the fire to spread more slowly in that particular direction compared with all other directions, resulting in the fire front becoming non-circular.

4.3. HETEROGENEOUS LANDSCAPES

To incorporate the effect of heterogeneity into the model, a second fuel model was introduced. The fuel characteristics represented a Highland Sourveld consisting of a two-year old *Themeda Triandra* grassland. The information describing this fuel model was collected by Everson *et al.* (1988) for the KwaZulu-Natal Drakensberg and is displayed in Table 4.3.

Table 4.3.

Fuel model parameters for a Highland Sourveld grassland in the KwaZulu-Natal Drakensberg (Everson *et al.*, 1988).

Parameters of Fuel Model for a Highland Sourveld Grassland	
Fuel Loads	
Fine Dead Fuel (1 hr timelag)	336 gm^{-2}
Live Herbaceous Fuel	224 gm^{-2}
Surface Area To Volume Ratios	
Fine Dead Fuel (1 hr timelag)	66 cm^2cm^{-3}
Live Herbaceous Fuel	49 cm^2cm^{-3}
Heat Content	19990 kJ/kg
Fuel Bed Depth	0.305m
Moisture of Extinction	30%

Note that grasslands do not contain woody plants or coarse dead fuel (10, 100 and 1000-hour timelag) and, therefore, these components do not appear in Table 4.3.

4.3.1. Heterogeneous Landscapes

Hypothesis:

> *Fire passing through a heterogeneous landscape will spread to a surrounding fuel type if the fire is sufficiently intense to cause ignition. The rate of fire spread is dependent on the particular fuel involved and its underlying characteristics.*

Figure 4.8a is a graphical representation of the fire fronts produced by the model for a heterogeneous landscape in which the green cells represent cells containing fuel for an *Acacia Nilotica* savanna and the yellow cells a Highland Sourveld grassland. The fuel

moisture content of the former was assigned a value of 1%, which was the same as in all previous tests, and the latter was assigned a value of 8%. The fire spread in the absence of wind and slope and successive fronts are displayed at 20-minute intervals.

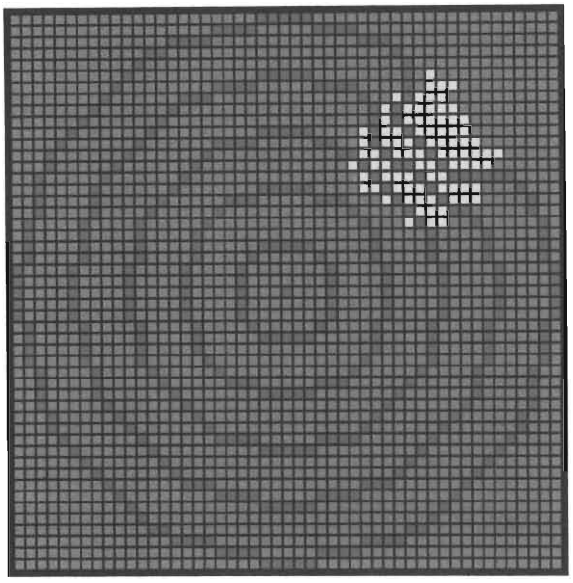

Figure 4.8(a). Fire spreading in a heterogeneous landscape with neither wind nor slope. Green cells represent an *Acacia Nilotica* savanna, with a moisture content of 1%, and yellow cells a Highland Sourveld grassland, with a moisture content of 8%. Successive fronts are displayed at 20-minute intervals.

In the first 40 minutes, the fire spreads in circles at a rate of approximately 2.38m.min^{-1} as it propagates through the *Acacia Nilotica* savanna. After an hour the fire reaches the Highland Sourveld grassland in the north-east. The fire is sufficiently intense to ignite the grassland and continues to spread in this direction. The rate of spread, however, decreases as the fire passes through the grassland to approximately 1.1m.min^{-1}. In all other directions the rate of fire spread remains constant.

As a consequence of the reduced rate of spread, the fire fronts become non-circular and begin to bend in the region of the grassland. The effect of heterogeneity is very pronounced after 100 minutes as the fire spreads more rapidly through the savanna compared with the grassland.

A second scenario was tested in which the fuel moisture content of the grassland was increased to 20%. The objective was to determine the effect on the simulation model of an increase in the level of heat required for combustion of the grassland fuel.

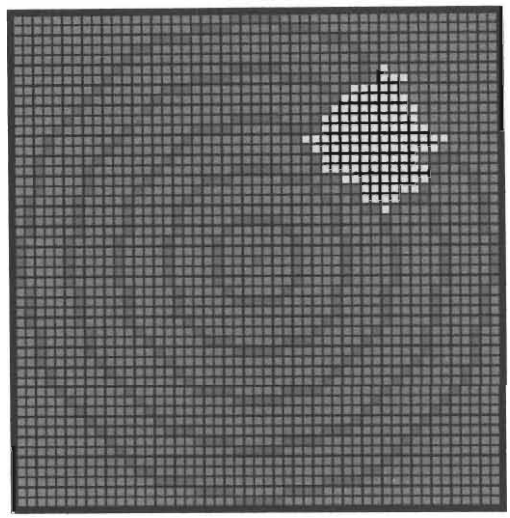

Figure 4.8(b). Fire spreading in a heterogeneous landscape with neither wind nor slope. Green cells represent an *Acacia Nilotica* savanna, with a moisture content of 1%, and yellow cells a Highland Sourveld grassland, with a moisture content of 20%. Successive fronts are displayed at 20-minute intervals.

The simulation was implemented using the same parameter settings as the previous example, except for the fuel moisture content of the grassland. The fire spread in the same manner through the savanna as previously described. However, it was unable to ignite the fuel in the grassland. This resulted in the fire fronts bending around the region occupied by the grassland while continuing to spread at a constant rate in all other directions (Figure 4.8b).

A further scenario was implemented to determine the influence of the wind on the rate and pattern of fire spread in a heterogeneous landscape. Figure 4.9 displays fire fronts at 20-minute intervals produced by the simulation model for a flat, heterogeneous landscape. The fuel moisture content of the savanna and the grassland were 1% and 20% respectively, as in the previous example. In the first 40 minutes the fire spread in the absence of wind and successive fire fronts remained unchanged from the previous two simulations. Thereafter, a gentle south westerly breeze of $30 m.min^{-1}$

was introduced. The subsequent increase in heat supplied from the savanna fuel, resulting from the presence of the wind, facilitated fire spread into the grassland fuel. An interesting feature of the simulation was that reducing the initial wind speed from 30 to 20 $m.min^{-1}$ resulted in the inability of the fire to spread into the grassland.

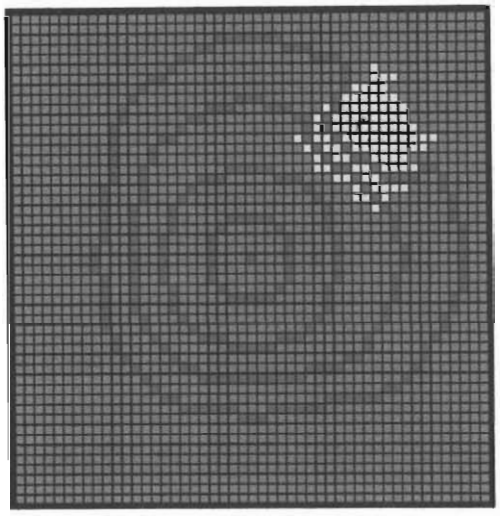

Figure 4.9. Fire fronts in a heterogeneous landscape displayed at 20-minute intervals. After 40 minutes, a south westerly wind of a 30 $m.min^{-1}$ was introduced that facilitated fire spread into the grassland fuel.

4.4. CONCLUSION

The simulation model has been implemented to hypothetical landscapes under various scenarios of fuel, wind and topography. The rate and pattern of fire spread predicted by the model is in good agreement with the experience of fire spreading in reality. In reality, however, the response of a fire is not easily isolated to individual changes in wind, topography and heterogeneous fuel. Rather, it is the collective influence of these spatially varying parameters that account for the properties of the fire.

In the next chapter, the simulation model is used to predict actual fire events that occurred in Mkuze Game Reserve during 1997. Recordings of the fire boundaries – representing the final extents of the fire – facilitate application of the model to complex scenarios incorporating the interdependence of fire spread on fuel, wind and topographical qualities.

CHAPTER 5

CASE STUDY: MKUZE GAME RESERVE

5.1. INTRODUCTION

Mkuze Game Reserve (MGR) is one of the large reserves managed by the KwaZulu-Natal Nature Conservation Services (KZNNCS). Located in northern KwaZulu-Natal (KZN) and covering an area of approximately 37 000 ha (Figure 5.1), MGR has an exceptionally high bio-diversity comprising flora and fauna (Goodman, 1982).

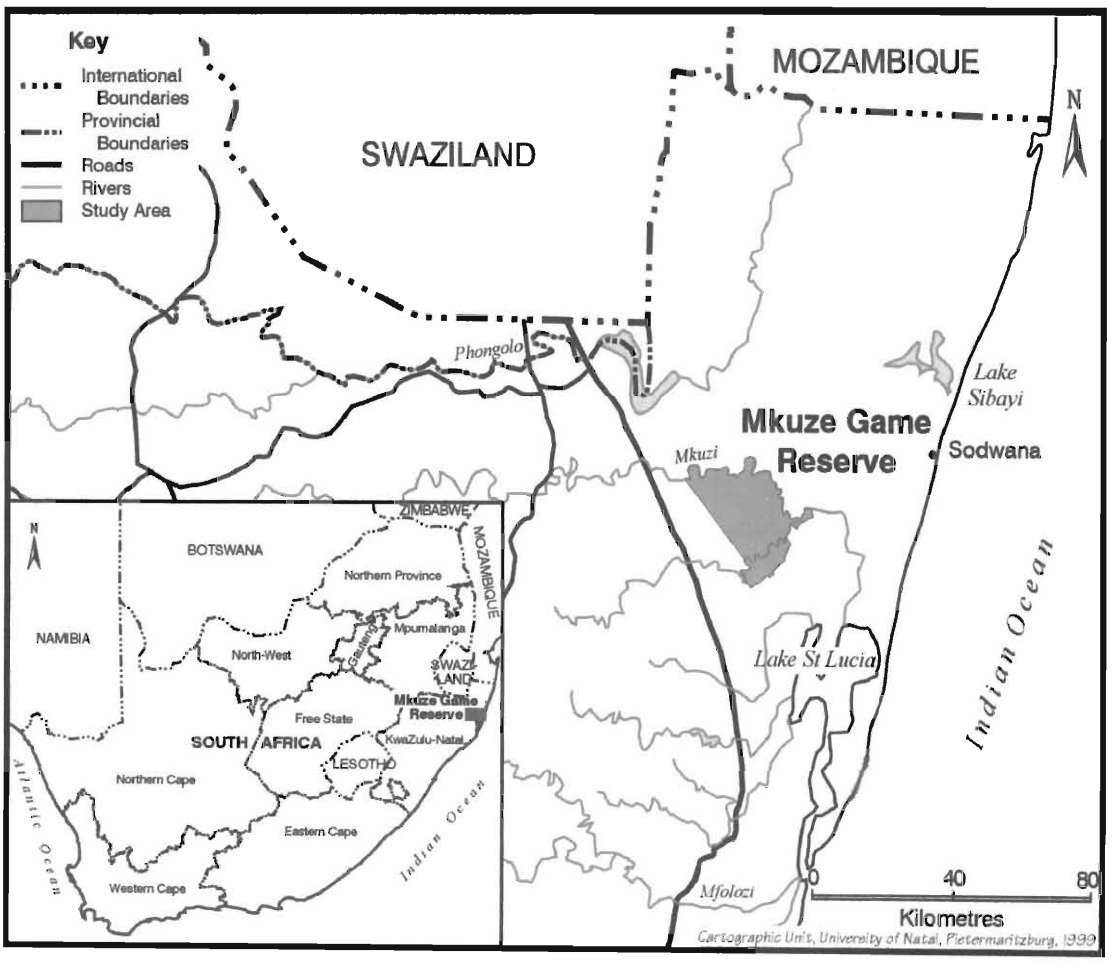

Figure 5.1. Site map of MGR in northern KwaZulu-Natal, South Africa.

The climate of MGR is described as warm to hot, humid subtropical (Schulze, 1965). According to Thornthwaite's (1948) classification, the region is semi-arid with little

or no moisture surplus in any season. Goodman (1990) found that compared with other savanna areas in South Africa the diversity of vegetation is high, largely as a result of high landscape level spatial heterogeneity. A detailed numerical classification and ordination analysis revealed the existence of 25 physiognomically and floristically distinct vegetation types within the reserve (Goodman, 1990).

The KZNNCS mission is to '*conserve the indigenous bio-diversity of KZN, which includes ecosystems and processes upon which it depends, and to assist all people in ensuring the sustainable use of the biosphere*' (Sandwith, 1996). Specific actions geared at conserving the bio-diversity of a region have been identified and form the core of the protected areas' management plan. The overall purpose of forming protected areas has been to retain the diversity of biological elements and ecological processes inherent in nature that would otherwise be lost as a result of continued habitat degradation.

Spatial heterogeneity can be practically manipulated using several management tools including fire, the distribution of water and mega-herbivore populations (Goodman, 1990). Fire is widely used in the management of ecosystems worldwide as it is a relatively inexpensive option by which vegetation can be manipulated. For the price of a box of matches, literally, it is possible to subject thousands of hectares of vegetation to a powerful modifying force.

Fire, both lightning and man induced, is believed to have played a major role in the development of vegetation in MGR. Consequently, application of fire within the reserve serves as possibly the most important tool available to management. The prescription of fire is intended to enable natural processes to prevail over those that are artificial. As a result, no attempts are made to rigidly apply burning programmes with specific frequencies and boundaries (Goodman, 1990).

Current management approaches to prescribed burning at MGR include block and patch burning methodologies. The former involves burning subdivided units of the landscape, or blocks, on a strict rotation period e.g. every 3rd year in spring. Blocks may be subdivided by either natural boundaries, including rivers and heterogeneous vegetation, or artificial boundaries, including roads and firebreaks.

Patch burning, which is more commonly practised at MGR, involves igniting a fire at a point and allowing it to determine its own burn pattern and extents. The objective of this burning strategy is the emulation of the type of fire regime under which the landscape and all its biota have evolved. Although simple in its application and relatively inexpensive, patch burning is potentially dangerous as no control is exercised over the actual fire.

Efforts to monitor burning operations, in order to improve understanding of this phenomenon and facilitate better management practice, has resulted in the collection of pertinent fire information that includes final fire extents and ignition points. The simulation model developed in this study has been applied to selected patch burning to determine the genuine predictive ability of the proposed model. This provides the real 'acid test' for any particular fire model, as verification of fire fronts generated by the model with actual fire boundaries requires the incorporation of the complex interaction of physical and environmental conditions that critically affect the rate and pattern of fire spread.

5.2. DATA COLLECTION

Spatial information for fuels, topography, ignition points and fire boundaries, required to operate the fire growth model, were captured into a Geographic Information System (GIS) using the MicroImages Image Processing System (MIPS). The information was derived from a variety of sources including:

- Landsat Thematic Mapper (TM) satellite imagery.
- Aerial photographs and orthophotographs.
- Existing GIS layers.

All GIS layers were geo-referenced using a Gauss Conformal projection with the 33° east central meridian. Maps compiled for display within this project were developed using the ArcView GIS. A brief review of the procedures implemented to compile each individual spatial layer is described in the next section.

5.2.1. Fuel Class Layer

A Landsat TM satellite image consisting of 7 distinct spectral bands with a pixel size of 25x25 metres was used in the fuels classification process. The entire area of MGR was covered in a single scene that was taken prior to the burning season.

The MGR fuel layer was mapped to the 13 fuel models developed by Anderson (1982), described in chapter 2, plus two non-fuel classes (Figure 5.2). Table 5.1 summarises the areas of the reserve occupied by each individual fuel class. Each fuel class represents a specific measure of fuel loading, surface area to volume ratio of each size group, fuel depth, heat content of fuel and moisture of extinction values.

Table 5.1.

Fuel classification system for the MGR study area.

Fuel Model/Class	Model Description	Hectares
Grass and grass-dominated models		
1	Short Grass	6197
2	Timber (grass and understory)	5175
3	Tall grass	562
Chaparral and shrub fields		
4	High pocosin, chaparral	5046
5	Brush	0
6	Dormant brush, hardwood slash	1042
7	Southern rough, low pocosin	1079
Timber Litter		
8	Closed timber litter	14
9	Hardwood litter	792
10	Heavy timber litter and understory	2942
Slash		
11	Light logging slash	0
12	Medium logging slash	0
13	Heavy logging slash	0
Non fuel		
14	Water	712
15	Bare, non-flammable	41

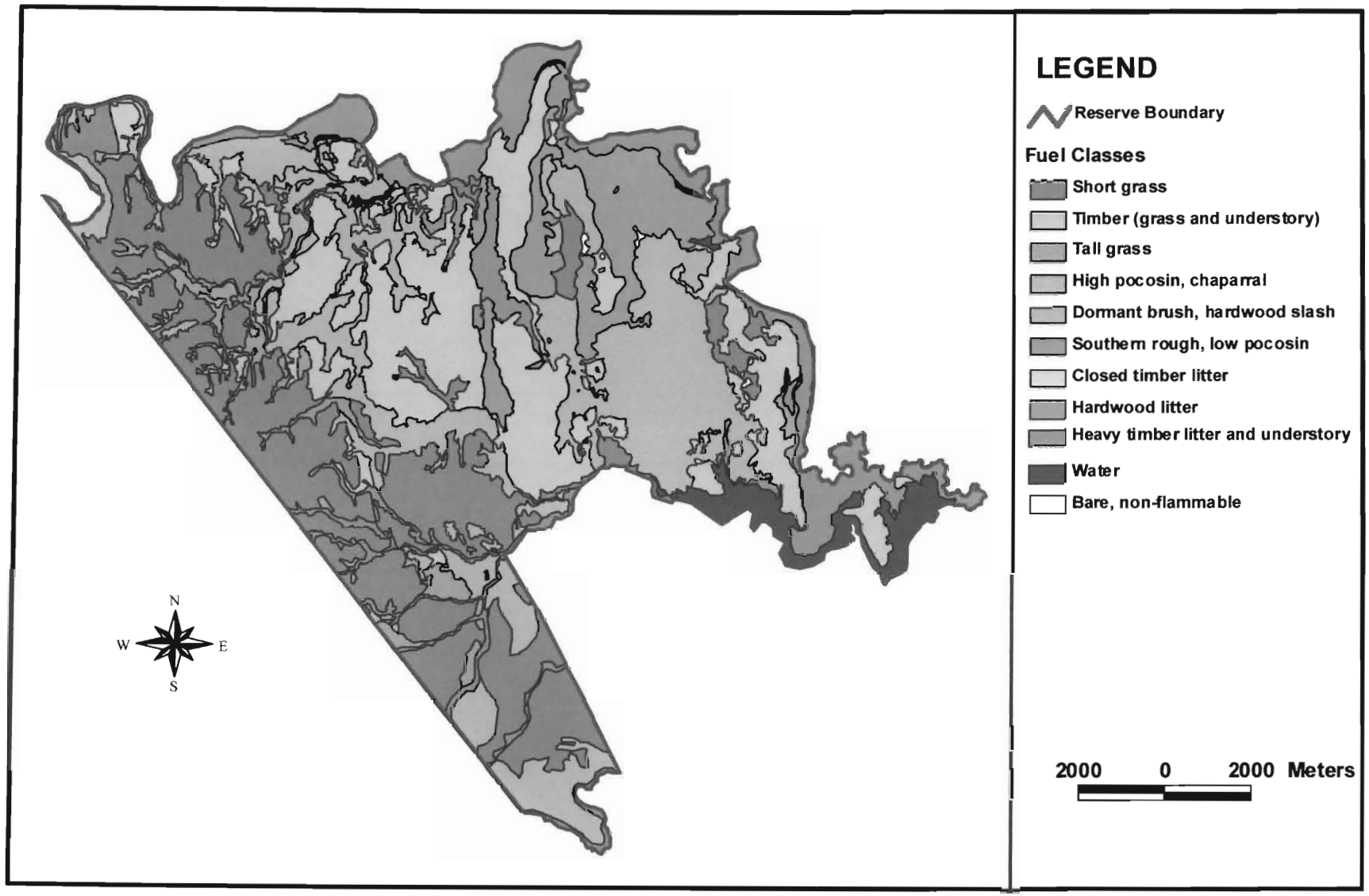

Figure 5.2. Fuel classification layer for the Mkuze Game Reserve study area.

The fuel layer was created from the Landsat TM image using a combined supervised/unsupervised approach (Congalton *et al.*, 1993; Thompson, 1993). Image classification was enhanced through the use of aerial photographs from 1975 and 1999, and ancillary GIS data layers. The latter included a detailed vegetation coverage containing fields for vegetation physiognomy, floristics, sensitivity/conservation value, soils and geology that was developed by Goodman (1990) by interpreting 1975 aerial photographs.

5.2.2. Topographic Layer

Vector contours were digitised at 5-metre intervals using orthophoto sheets of the reserve. Along the western boundary, however, contours were captured at a 20-metre interval due to the complexity of the terrain in this region resulting from the Lebombo Mountain range. This region, however, did not coincide with the areas used for implementing the simulation model.

A continuous topographic layer for the entire reserve was constructed by amalgamating the individual contour coverages. A digital elevation model (DEM), with a pixel size of 25x25m, was then generated by resampling the topographic coverage. A DEM is a raster, or grid, coverage in which each cell contains a value for its elevation. Values for the height of each cell were extracted from the DEM for use in the model.

5.2.3. Ignition Points and Fire Boundaries

Spatial information for the ignition points and resultant fire boundaries was generated by the KZNNCS using Global Positioning Systems (GPS). Three cases of prescribed patch burning conducted in MGR during 1997 were used to implement and verify the simulation model. Further details and maps of each individual fire event will be described in the sections to follow.

5.2.4. Fire Records

Fuel and environmental conditions on the day the burning operation was to be conducted are contained within the fire record compiled by the fire manager. The data are qualitative with most parameters measured in terms of a given index. Furthermore, the fire record generally describes the fuel and environmental conditions occurring at the time of ignition. The location, time and type of ignition, time of extinction and reason for burning are also documented in the fire record.

Fuel conditions include a greenness index, mean fuel height, density and uniformity index whereas environmental conditions include weather conditions – broadly defined for example as cold morning or hot day - wind speed – measured on the Beaufort scale (Table 5.2) - and wind direction – recorded as one of the eight major compass directions.

Table 5.2.

Beaufort scale for estimating wind velocity.

Beaufort Number	Term	Description	Wind Speed	
			km/h	knots
0	Calm	Smoke rises vertically	<1	<1
1	Light air	Smoke drifts slowly; wind vanes not affected	1 - 5	1 - 3
2	Light breeze	Wind felt on face; leaves rustle; ordinary wind vanes move	6 - 11	4 - 6
3	Gentle breeze	Leaves and twigs in motion; wind extends light flag	12 - 19	7 - 10
4	Moderate breeze	Dust and loose paper raised; small branches move	20 - 28	11 - 16
5	Fresh breeze	Small trees sway	29- 38	17 - 21
6	Strong breeze	Large branches in motion; whistling heard in telephone wires	39 - 49	22 - 27
7	Near Gale	Whole trees in motion; inconvenience felt when walking against wind	50 - 61	28 - 33
8	Gale	Twigs broken off trees; progress of walkers impeded	62 - 74	34 - 40
9	Strong gale	Branches broken off trees	75 - 88	41 - 47

5.3. CASE 1: MAHLABENI FIRE

The first case of prescribed patch burning used to implement the simulation model occurred on the 5th October 1997 in the Mahlabeni region of the reserve. Information contained in the fire record indicates that the fire was ignited at 13h00 in the presence of a light, north easterly breeze and continued to burn until its extinction at 18h00 that evening (Table 5.3).

Table 5.3.
Selected information from the fire record for Mahlabeni area of MGR.

Area	Time of Ignition	Time of Extinction	Wind Speed	Wind Direction
Mahlabeni	5/10/97 13h00	5/10/97 18h00	2	NE

The vegetation of the area is characterised by a short grass covering with heavy timber litter, high pocosin, timber (grass and understory) and tall grass in existence (Figure 5.3). The formation of heavy timber litter and understory along the base of the valley and the existence of a road form barriers that constrain the lateral spread of the fire.

Figure 5.4 displays the contours of the Mahlabeni region at 5-metre intervals. The topography of the burned area slopes in an uphill direction from the south east to the north west. Comparing the highest and lowest points of the fire boundary yields elevations of 110m and 65m respectively. This translates into an approximate gradient of 1 in 28, or a slope angle of 2°.

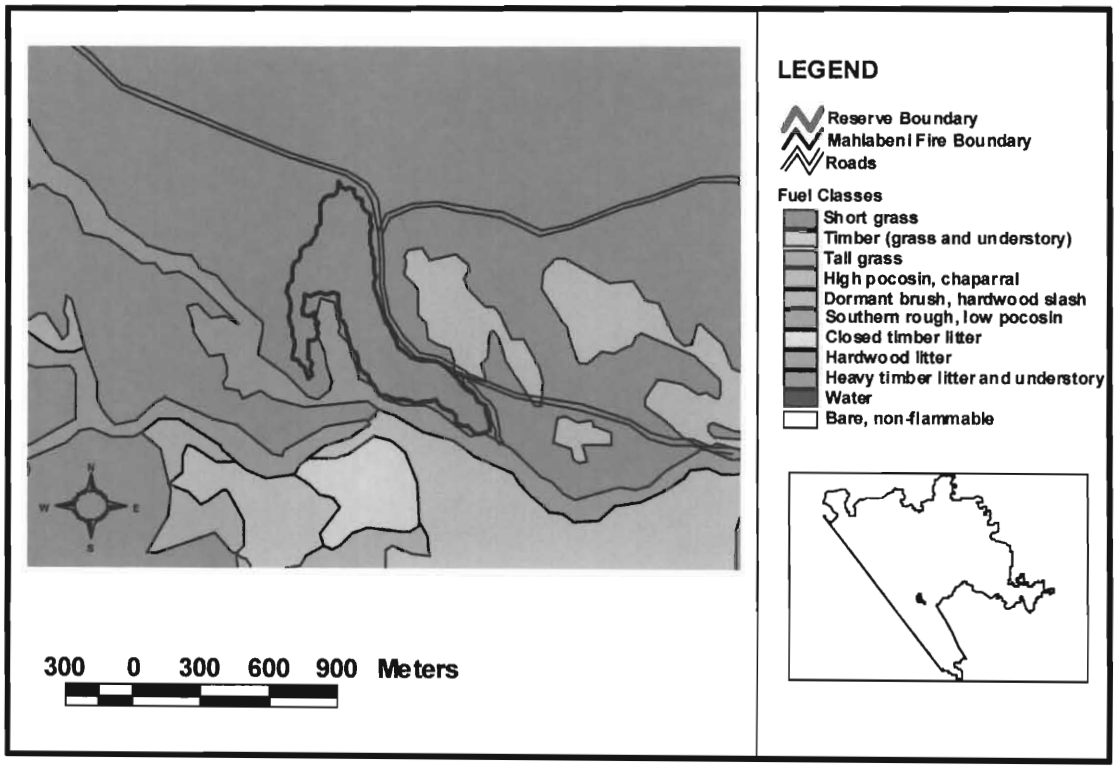

Figure 5.3. Map of fuel classes for the Mahlabeni fire.

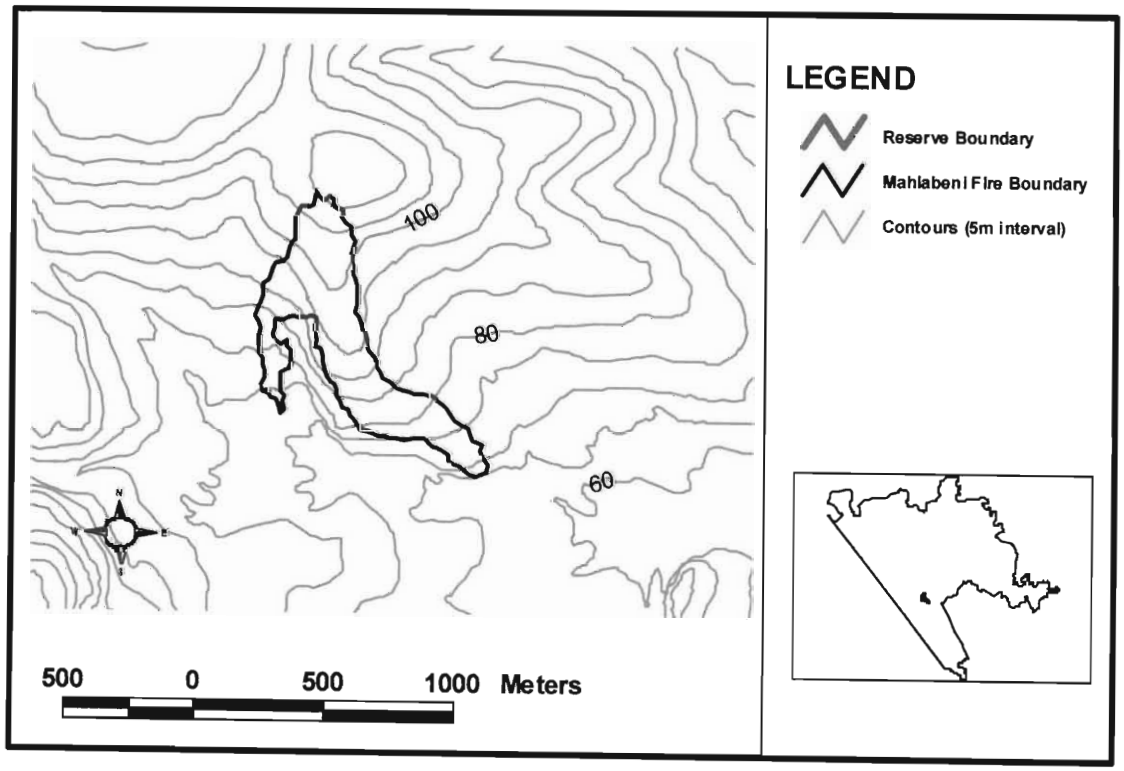

Figure 5.4. Map of contours at 5m intervals for the Mahlabeni fire.

Figure 5.5 is a graphical representation of the fire fronts, displayed at 1-hour intervals, produced by the simulation model for the Mahlabeni fire. The size of the cells was 25x25m. This corresponded to the minimum mappable area of the Landsat TM imagery, which was used to derive the fuel coverage. The simulation time step was 60 seconds. This was sufficiently small to cater for the maximum fire spread rates that occurred. The Weise and Biging flame height model was applied in all simulations with an assumed flame height of 2.8m. The flame height corresponded to the average height recorded for South African grasslands by Trollope (1978).

The fuel moisture content of all fuels was assumed to be 1%. The value for the moisture content was inferred from the fire record, which described the weather conditions at the start of the burn as being a "hot day". Attempts were made to acquire temperature and rainfall information from the South African Weather Bureau (SAWB) and the Computing Centre for Water Research (CCWR) for MGR prior to and including the period of burning. However, only daily recordings were available for weather stations located outside the reserve. Consequently, the information provided little or no assistance with regard to the present study.

In the first three hours, the fire spread in the presence of a light north easterly breeze of 30 $m.min^{-1}$. The rate of spread up the slope, i.e. from the south east to the north west, after one hour was approximately 3.9 $m.min^{-1}$ whereas down the slope spread rate was only 2.4 $m.min^{-1}$ (Figure 5.5a). The rate of head and backfire spread was restricted by the heavy timber litter and understory and the road respectively.

The fire maintained an uphill spread rate between 3.7 $m.min^{-1}$ and 4.1 $m.min^{-1}$ for the next couple of hours. After three hours had elapsed on the simulation clock, the wind speed was assumed be 0. The reduction in wind speed was documented in the unabridged fire record, however, the exact time at which this occurred was not given. This alteration had little effect on the spread rate up the slope between the third and fourth hours, which remained at 3.6 $m.min^{-1}$ (Figures 5.5c and 5.5d). This follows expectation as the fire spreading in a north west direction is influenced primarily by the gradient of the slope rather than the wind, which is blowing at right angles to the slope.

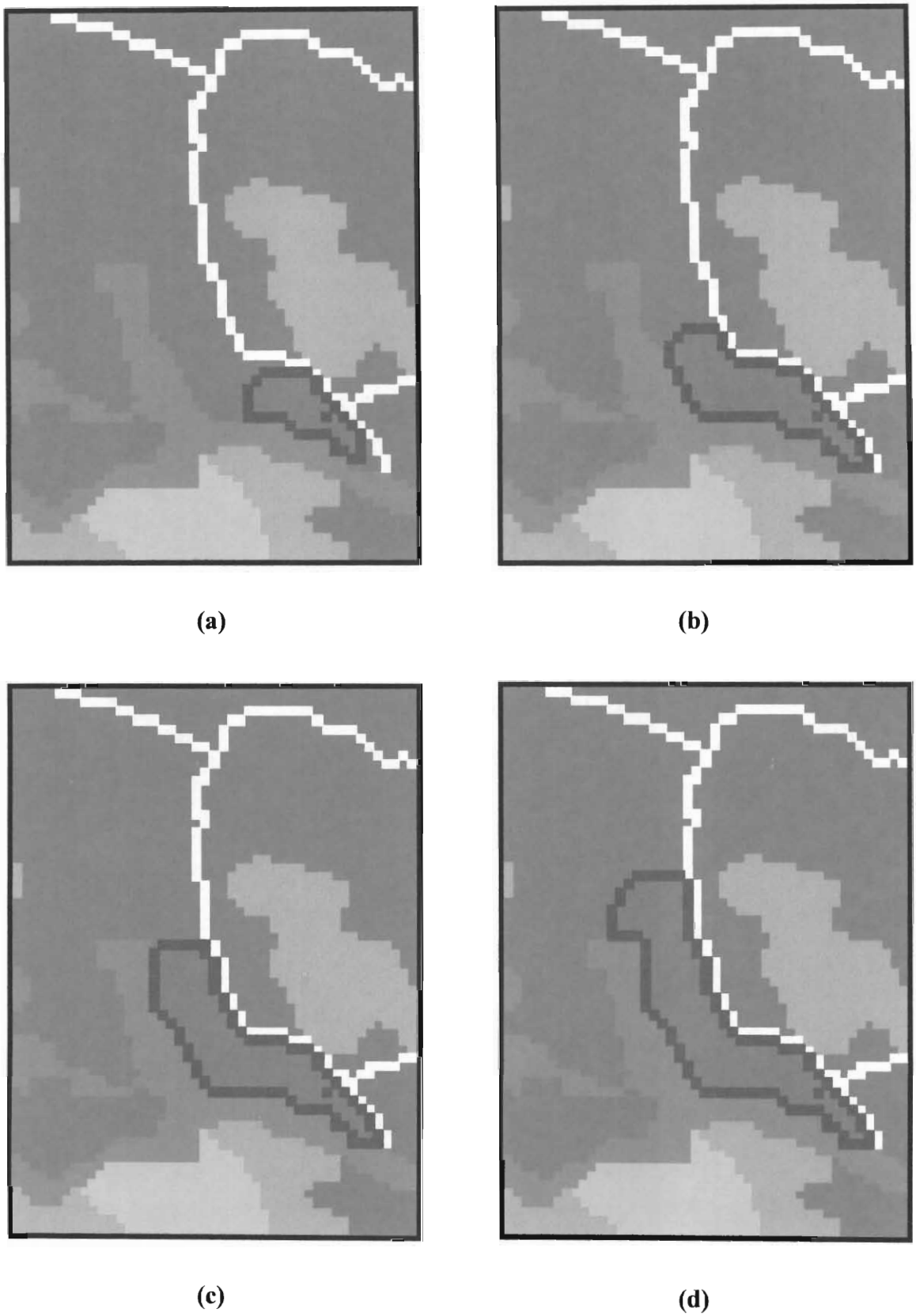

Figure 5.5. Fire fronts generated by the simulation model for the Mahlabeni area of MGR displayed after (a) 1 hour (b) 2 hours (c) 3 hours and (d) 4 hours.

At 18h00, corresponding to 5 hours on the simulation clock, the fire extinguished itself. Goodman (*pers. comm.*, 1999) attributed the fire's extinction to the formation of dew on the ground resulting from a decrease in the air temperature in the late afternoon and early evening. Luke and McArthur (1978) found that dew may contribute to the moisture content of plants and have the effect of delaying the start of fires.

The reduction in the air temperature and the formation of dew was incorporated into the model by adjusting the fuel moisture content of all unburned fuels. In general, the fuel moisture content was assumed to be an approximate inverse linear function of the air temperature i.e. lower air temperatures correspond to higher fuel moisture contents and vice-versa.

For the Mahlabeni fire, the air temperature was assumed to start decreasing at 17h00. Consequently, the moisture content of the short grass, which carried the fire, was increased from its initial value of 1% to 3% after 4.25 hours had elapsed on the simulation clock or 17h15 real time. Thereafter, the moisture content of the short grass was increased linearly, by 3% every 15 minutes. At 18h00 the moisture content reached the extinction level of 12% resulting in the 'burn out' of the fire (Figure 5.6).

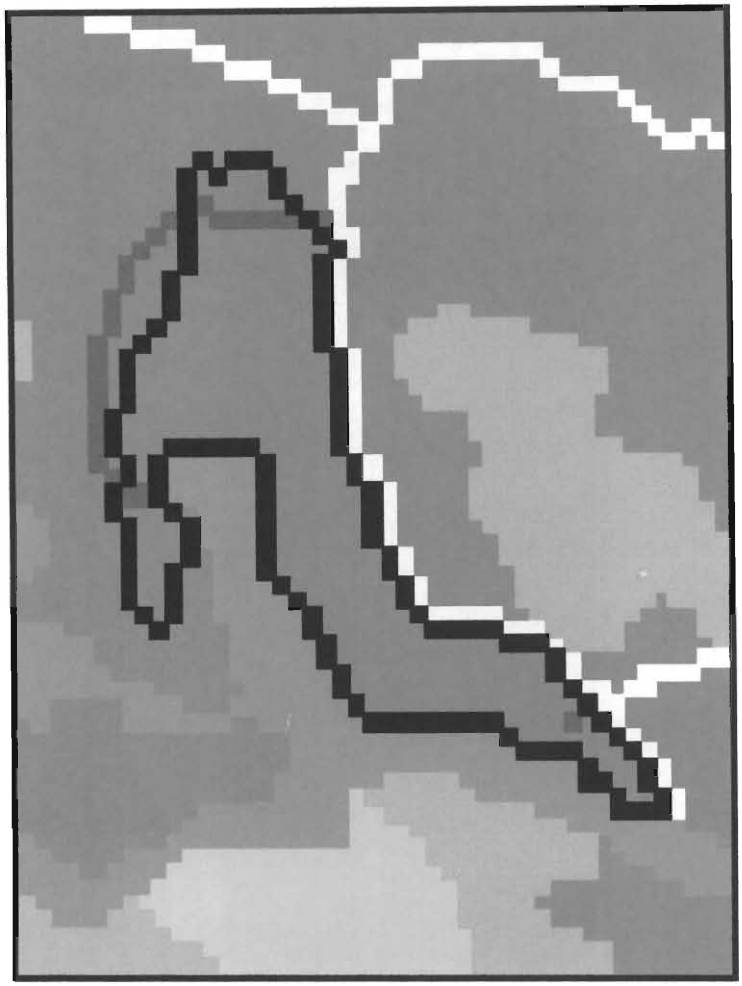

Figure 5.6. Fire boundary after 5 hours generated by the simulation model compared with the observed fire boundary (black cells) for the Mahlabeni area of MGR.

5.4. CASE 2: MAHLALA FIRE

The Mahlala region of MGR was burned on the 28th August 1997 in order to reduce the grass fuel load. The fire was ignited at 12h30 p.m. in the presence of a light north easterly breeze. The time at which the fire eventually extinguished itself was recorded as 22h00 that same evening (Table 5.4).

Table 5.4.

Selected information from the fire record for Mahlala area of MGR.

Area	Time of Ignition	Time of Extinction	Wind Speed	Wind Direction
Mahlala	28/08/97 12h30	28/08/97 22h00	2	NE

The area that was burned consisted primarily of short grass and understory, flanked by hardwood litter and heavy timber litter and understory that restricted the degree of lateral spread of the fire (Figure 5.7).

The topography of the Mahlala region is characterised by a ridge with a long axis sloping gradually in a downward direction from the north east to the south west (Figure 5.8). The ridge, which forms a saddle feature, contains a number of peaks and valleys. The highest point within the observed fire boundary is the summit of a hill in the south west which has a height of 110m whereas the lowest point is approximately 65 m.

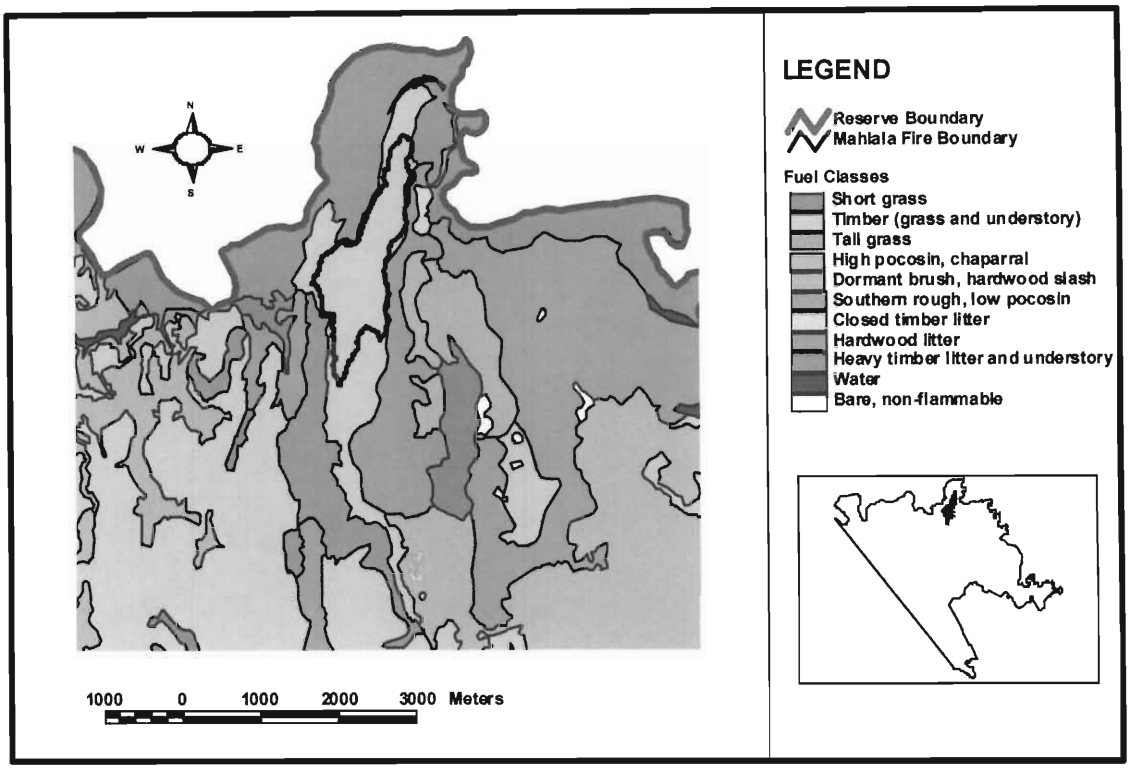

Figure 5.7. Map of fuel classes for the Mahlala fire.

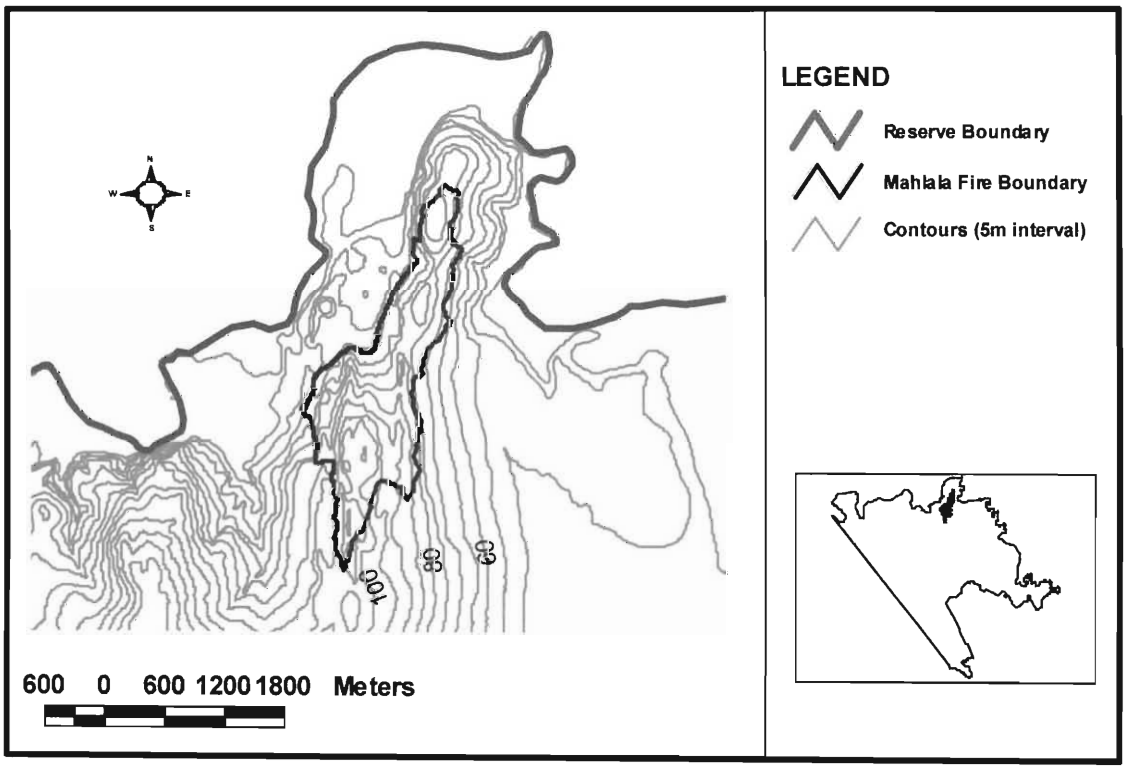

Figure 5.8. Map of contours at 5m intervals for the Mahlala fire.

Figure 5.9 illustrates the fire fronts produced by the simulation model at various time intervals. The model was implemented using a 50x50 m lattice with a simulation time step of 60 seconds. The fuel moisture content of all fuels was assumed to be 3%, and the fire spread in the presence of a constant north easterly breeze of 50 $m.min^{-1}$.

In the first hour, the rate of spread in the north east direction generated by the model was 4.7 $m.min^{-1}$ and was approximately double the rate in the opposite direction (Figure 5.9a). The fire maintained a spread rate in the direction of the wind of between 4.5 $m.min^{-1}$ and 5 $m.min^{-1}$ throughout the entire duration of the simulation, indicating a greater dependence on the magnitude of the wind speed compared with the influence on spread of the underlying topography. In contrast, the backfire rate of spread diminished to 0 as the fire encountered the combined effects of spreading down the slope and against the wind.

Lateral fire spread was constrained by heterogeneous fuels flanking the short grass and understory. The heat produced by combustion of short grass was insufficient to initiate ignition of the surrounding heavy timber litter and hardwood litter.

After 9.5 hours on the simulation clock, corresponding to 22h00 real time, the fire extinguished itself. As with the previous case, the fire's extinction was attributed to the decrease in the air temperature in the evening and the formation of dew on the ground. These effects were implemented by increasing the moisture content of the unburned fuels to the extinction level. In particular, the moisture content of the short grass and understory was assumed to increase from 3% to 6% after 8.75 hours had elapsed. Thereafter, the fuel moisture content was increased linearly by 3% every 15 minutes until the extinction moisture content was attained after 9.5 hours.

The possibility also exists that rain may have caused the fire to extinguish. This phenomenon could be implemented in a similar manner as dew formation. The major difference is that the rate at which the fuel moisture content increases is significantly higher in the former than the latter. However, in the event of rain, it is more probable that the raindrops reduce the flame until a state of extinction is attained.

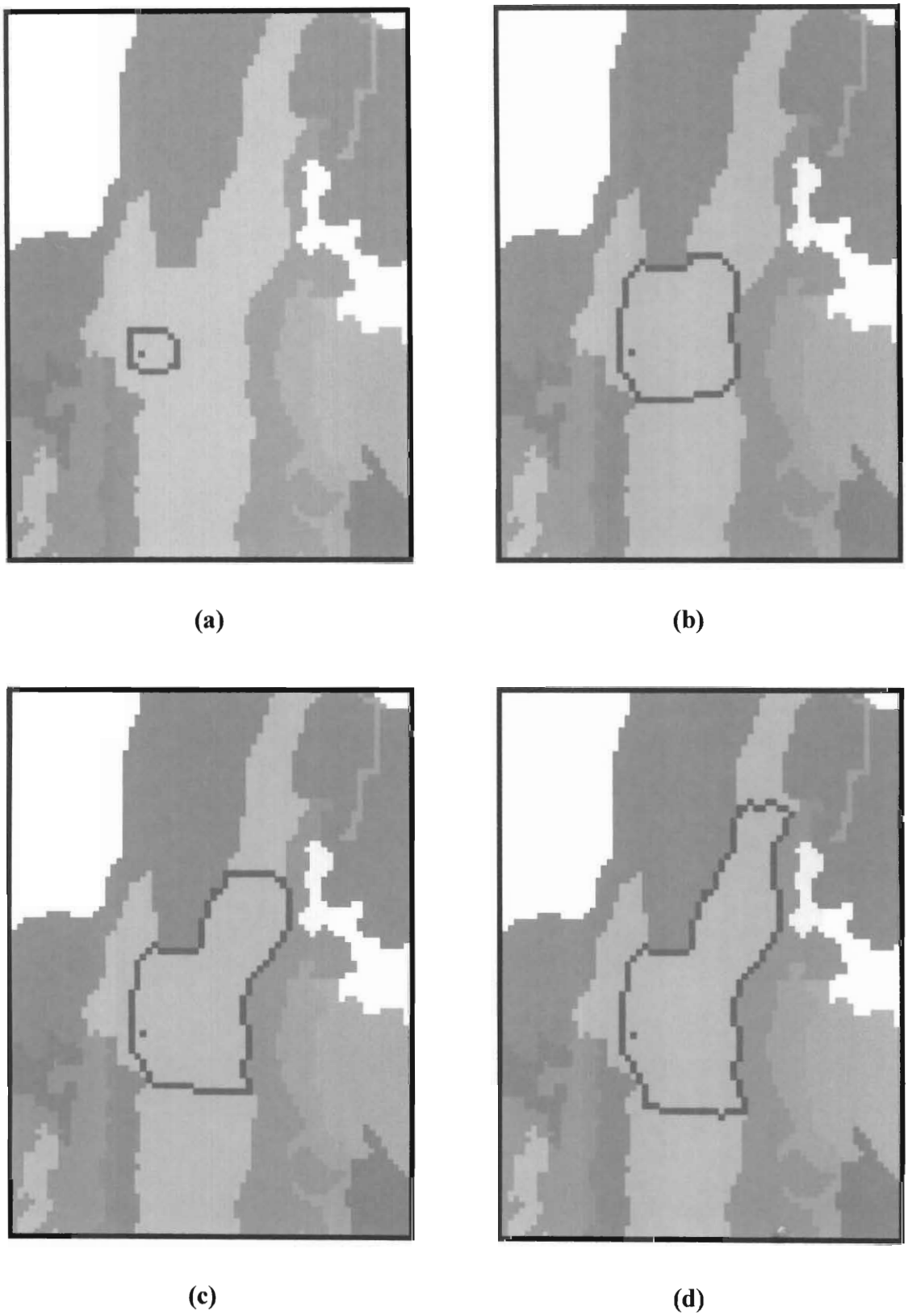

Figure 5.9. Fire fronts generated by the simulation model for the Mahlala area of MGR displayed after (a) 1 hour (b) 4 hours (c) 6 hours and (d) 8 hours.

Figure 5.10 depicts the fire front produced by the simulation model after 9.5 hours compared with the actual fire boundary recorded for the Mahlala fire. Visual inspection of the predicted boundary appears highly correlated to the actual boundary. Comparing areas of the predicted and observed fire boundaries showed 89% coincidence, 7% underestimation and 4% overestimation.

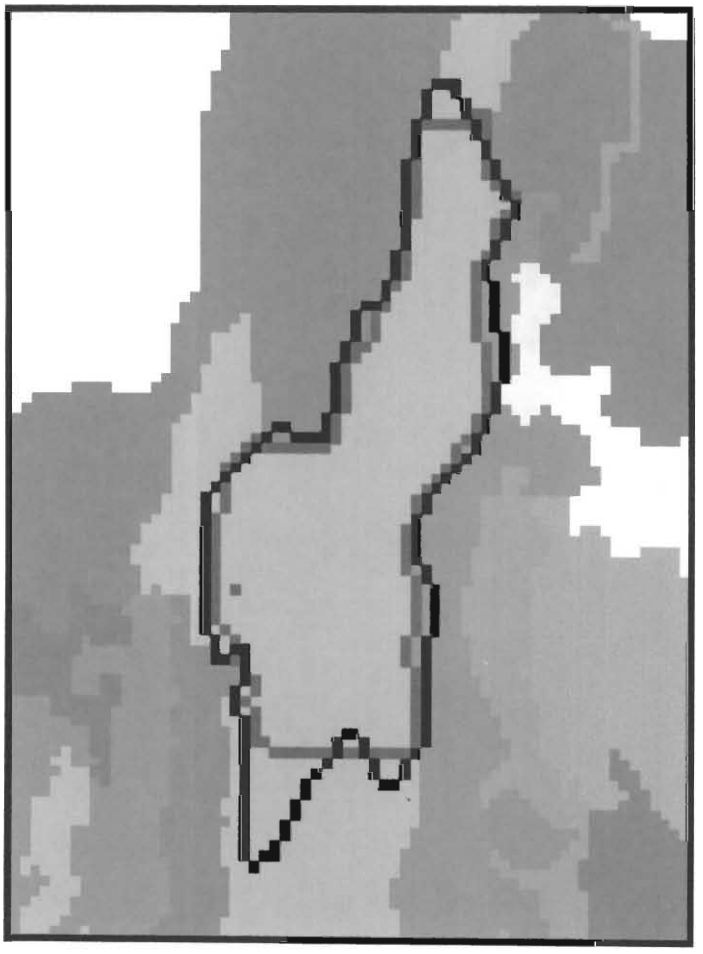

Figure 5.10. Fire boundary after 9.5 hours generated by the simulation model compared to the observed fire boundary (black cells) for the Mahlala area of MGR.

The only significant difference between the two boundaries is the under prediction of the spread rate in the southerly direction. The observed fire boundary in this direction is seemingly strongly related to the shape of the underlying topography. The under prediction by the simulation model is attributed to the dominant effect of the wind compared to slope that was a consistent feature throughout the simulation.

5.5. CASE 3: TRAILS CAMP AND KHONGOLWANE FIRES

The final case of prescribed burning used to implement the model occurred in the Trails Camp and Khongolwane regions of MGR. The burning operation consisted of two fires. The first was ignited in the Trails Camp region, in the south, at 13h00 followed an hour later by a second fire in the northern Khongolwane region (Table 5.5).

Table 5.5.
Selected information from the fire record for the Trails Camp and Khongolwane regions of MGR.

Area	Time of Ignition	Time of Extinction	Wind Speed	Wind Direction
	6/10/97	6/10/97		
Trails Camp	13h00	19h00	2-3	NE-SW
Khongolwane	14h00	20h00	2-3	NE-SW

Both fires had a duration of 6 hours with the Trails Camp fire becoming extinct at 19h00; one hour prior to the Khongolwane fire. The rate and pattern of spread produced by both fires was significantly influenced by the nature of the wind. In their initial stages of development, both fires spread in the presence of a light north-easterly breeze which increased speed and shifted direction by 180° to become a gentle south westerly breeze.

The vegetation of the region is dominated by a short grass and understory covering (Figure 5.11) that has formed on a gradual slope that increases in a direction from east to west (Figure 5.12). Inspection of the observed fire boundary indicates that fire spread was restricted by a combination of physical and environmental factors including wind, topography, roads and spatial heterogeneity.

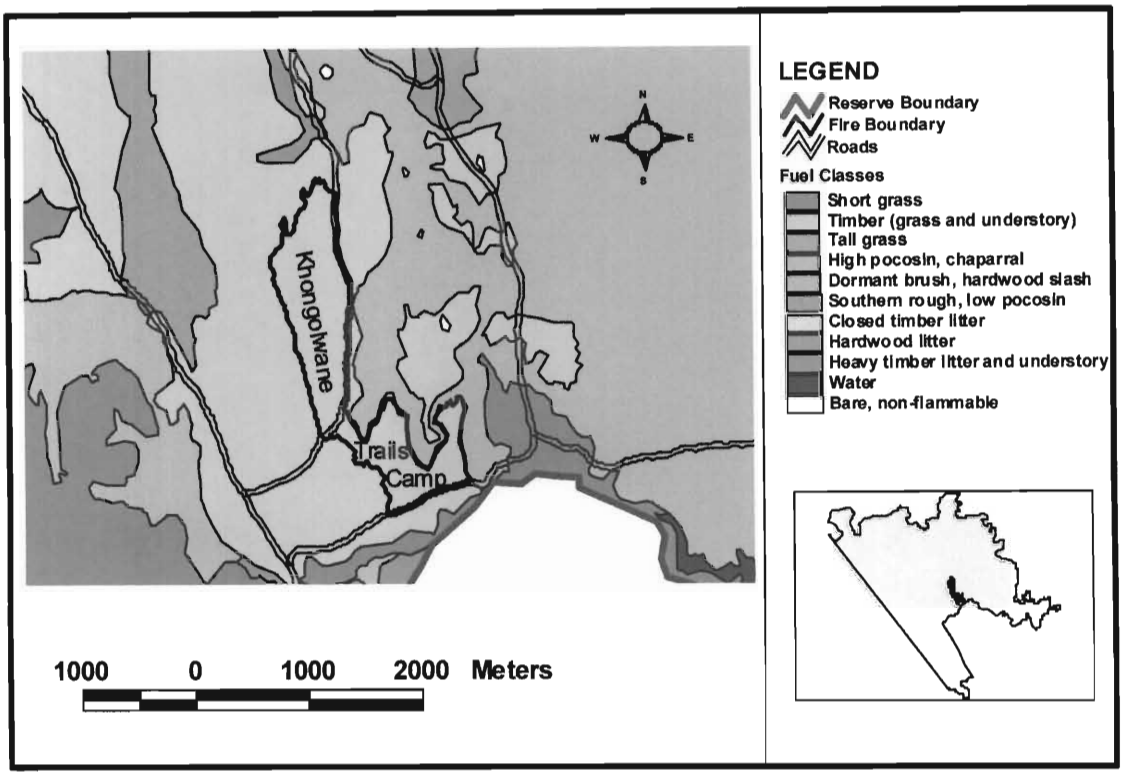

Figure 5.11. Map of fuel classes for the Trails Camp and Khongolwane fires.

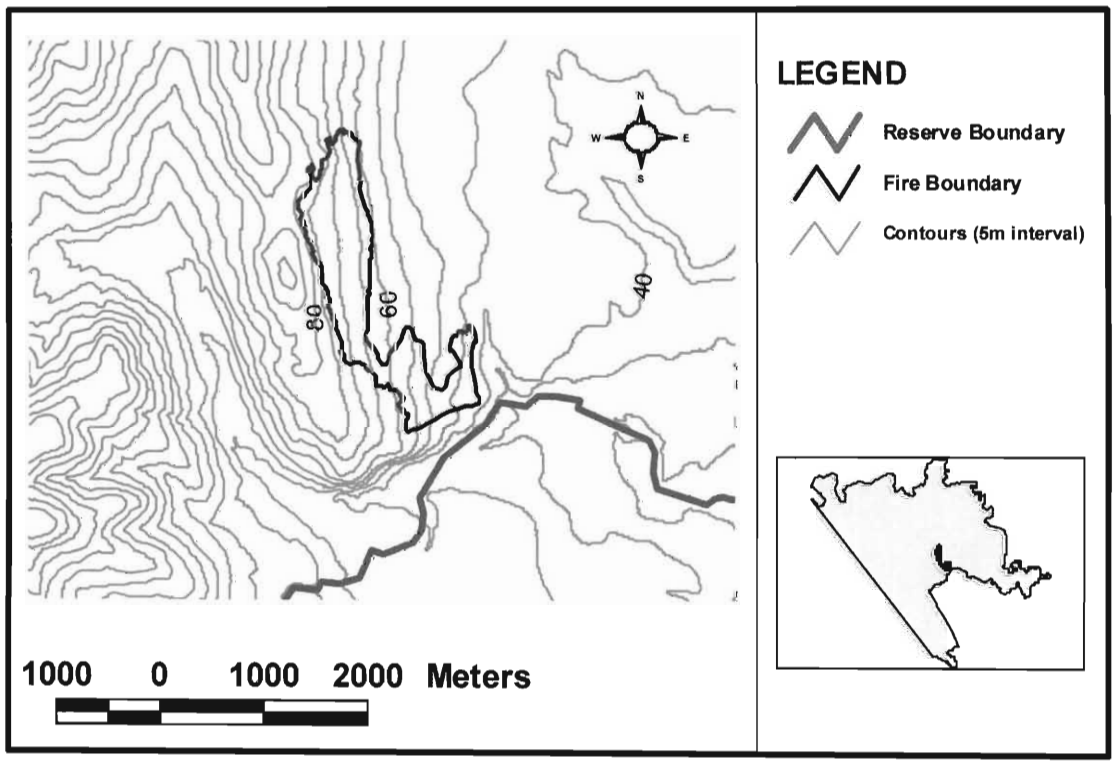

Figure 5.12. Map of 5m contours for the Trails Camp and Khongolwane fires.

Figure 5.13 is a graphical representation of the fire fronts produced by the simulation model for the Trails Camp and Khongolwane fires. Simulations were performed using a lattice with a 50x50 m cell size and a simulation time-step of 60 seconds. The fuel moisture content of all fuels was assumed to be 3%.

The Trails Camp fire was ignited an hour prior to the Khongolwane fire (Figure 5.13a) with a wind of 50m.min^{-1} blowing from the north east. In the first hour, the fire travelled approximately 180 m at a rate of 3 m.min^{-1} as it spread up the slope in the direction of the wind. Conversely, the rate of backfire spread was only 1.86 m.min^{-1}. Lateral spread in the south east and north west directions was contained by the road and the high pocosin fuel respectively.

At 14h00, corresponding to one hour on the simulation clock, the second fire in the Khongolwane region was ignited. The wind speed and direction remained unchanged. During the next hour, the rate of spread of the Trails Camp fire increased in the south west direction to 5.3 m.min-1, primarily as a result of an increase in the gradient of the upslope (Figure 5.13b). The rate of spread in the opposite direction diminished slightly to approximately 1.5 m.min^{-1}. The Khongolwane fire spread approximately 160 m at a rate of 2.6 m.min^{-1} in the direction of the wind compared with only 110 m, at a rate of 1.9 m.min^{-1}, in the opposite direction.

After 2 hours had elapsed on the simulation clock, the wind direction shifted direction from its current orientation of north east to south west whilst the wind speed increased from 50 m.min^{-1} to 60 m.min^{-1}. Consequently, the rate of fire spread in the south west direction diminished for both fires whereas the converse applied to the north and north easterly directions.

Figure 5.13c illustrates the position of the fire fronts after four hours. The rate of spread of the Khongolwane fire increased to approximately 5.4 m.min^{-1} in a northerly direction compared with 4.6 m.min^{-1} in the same direction in the Trails Camp area. The rate of backfire spread in both fires was reduced to approximately 0.9 m.min^{-1}.

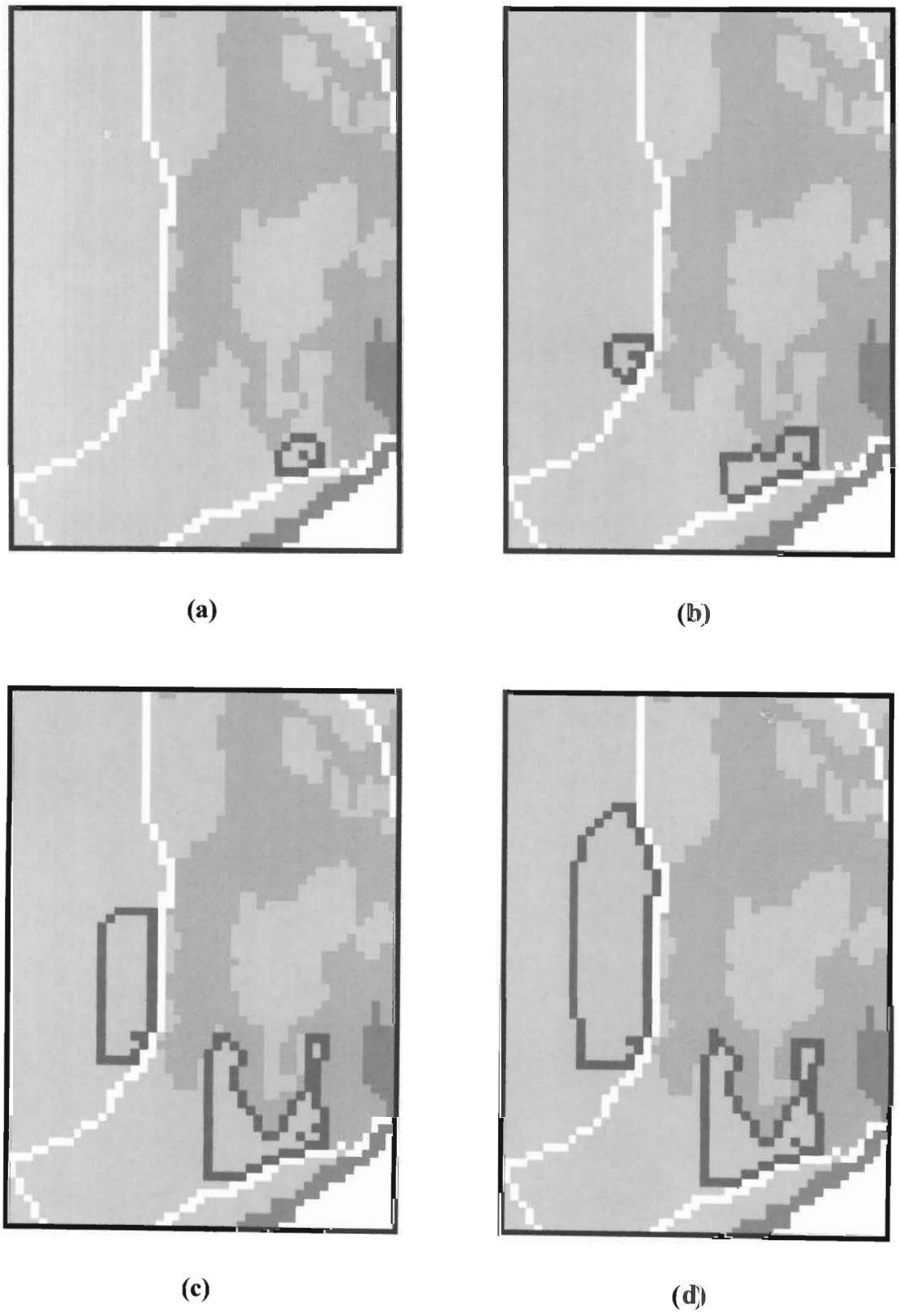

Figure 5.13. Fire fronts generated by the simulation model for the Trails Camp and Khongolwane areas of MGR displayed after (a) 1 hour (b) 2 hours (c) 4 hours and (d) 6 hours.

After 6 hours, or 19h00 real time, the Trails Camp fire became extinct (Figure 5.13d). This resulted from a combination of a change in the wind direction, causing the backfire spread to become insufficiently intense to maintain the combustion process, and the effect of the road and high pocosin fuel that restricted spread in other directions. The Khongolwane fire continued to spread rapidly in the northerly direction at between 4.5 $m.min^{-1}$ and 5.5 $m.min^{-1}$. In contrast, the spread in a direction ranging from the north west to the south west was only approximately $0.8m.min^{-1}$.

The Khongolwane fire extinguished itself after 7 hours on the simulation clock due to a reduction in the backfire spread rate coupled with an increase in the fuel moisture content of all unburned fuels. The latter resulted from a decrease in air temperature and the formation of dew during the early hours of the evening. This was implemented in the simulation by increasing the fuel moisture content of the short grass and understory in 3% increments every 15 minutes commencing at 19h00. At 20h00 the fire 'burned out' as the fuel moisture reached the extinction level.

Figure 5.14 depicts the fire boundaries generated by the simulation model compared with the observed fire boundaries for the prescribed burning of the Trails Camp and Khongolwane areas. The Trails Camp fire tended to underestimate the area of the observed fire primarily as a result of the lack of backfire spread. The area of the predicted fire boundary compared with the observed fire boundary was 400 000 m^2 and 450 000 m^2 respectively, with 88% overlap, 22% underestimation and no overestimation.

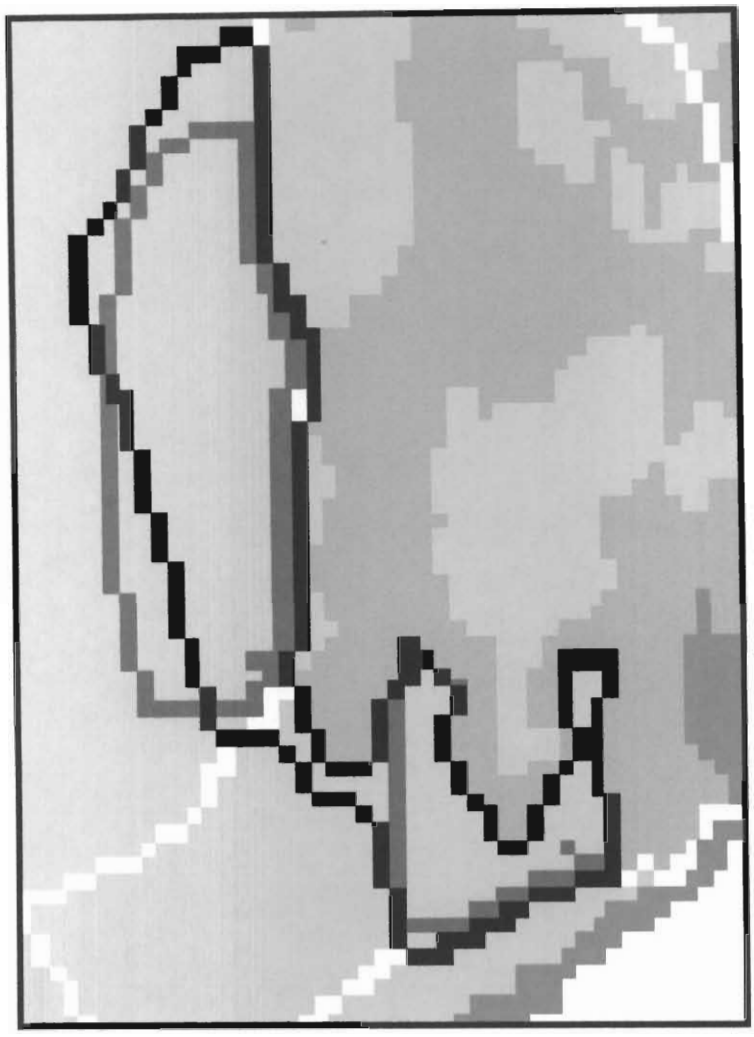

Figure 5.14. Fire boundaries after 7 hours generated by the simulation model compared with the observed fire boundary for the Trails Camp and Khongolwane areas of MGR.

The predicted fire boundary for the Khongolwane area overestimated the degree of spread in the north east direction by 13%. This was possibly due to the influence of the underlying topography, which slopes in an uphill direction from the east to the west, which counteracted the south westerly breeze. Conversely, the rate of spread in the northerly direction was slightly underestimated in comparison with the observed fire boundary. In general, the area of the observed and predicted fire boundaries showed favourable agreement with 83% coincidence, 13% overestimation by the simulation model and only 4% underestimation.

CHAPTER 6

CONCLUSION

A spatial model for predicting fire dynamics in savanna ecosystems has been developed for the purposes of this project. The model integrates spatial fuel and topographic information with temporal weather, wind settings and initial fuel moistures to determine fire behaviour across both time and space. Furthermore, it provides ecosystem managers with a system that has the potential to exceed inventory, monitoring and display and enable the simulation of spatial outcomes of management and policy decisions.

From a scientific perspective, the model provides the basis for predicting the critical physical and chemical releases during a fire. Fire science has developed an extensive body of theoretical and applied physical and chemical research without the benefits of real-time mapping and geographic information management. The model offers the opportunity to observe and test spatial behaviour and intervention hypotheses in addition to the modelling of physical fire parameters.

Implementation of the proposed model to hypothetical landscapes under various scenarios of fuel, wind and topography generated fire fronts that were found to be in good agreement with observed experience of fire spread. In the absence of wind and slope, successive fire fronts in a homogeneous landscape were circular. Fire fronts became elliptical as wind and topographic effects were introduced as a result of increased spread rates in the direction of the wind and in the direction of positive slope. Conversely, fire spreading either downslope or into the wind exhibited spread rates below that generated in windless conditions on level terrain. Analysis of the shape of fire fronts spreading in an *Acacia Nilotica* savanna yielded a relationship for the length-to-width ratio of a fire that was a function of the wind velocity only. The relationship was independent of fuel moisture content.

In a heterogeneous landscape, containing fuel parameters for an *Acacia Nilotica* savanna and a *Themeda Triandra* grassland, fire spread from one fuel type to another

depending on the quantity of heat produced by the combustion of fuel compared with the heat required to ignite the unburned fuel. The heat qualities of each particular fuel were a function of the physical fuel attributes. The rate and pattern of fire spread produced by the model can be practically manipulated by varying, for example, the fuel moisture content. Consequently, the heat qualities of the unburned and/or the burning fuel are subject to changes that critically affect the nature of the resultant fire.

The model was applied to real landscapes using information collected for prescribed burning operations conducted in Mkuze Game Reserve (MGR) during 1997. Layers for fuel, topography, ignition points and fire boundaries used to implement the model were captured into a Geographic Information System. A qualitative description of the environmental conditions at the time of ignition was compiled in fire records. Fuel classification was performed using Landsat Thematic Mapper (TM) imagery of the reserve that provided a rapid, cost effective methodology of generating quantitative fuel information that is of direct benefit to a wide range of conservation activities in South Africa, including fire modelling.

Predicted fire boundaries showed favourable agreement with observed fire boundaries for the Mahlabeni, Mahlala, Trails Camp and Khongolwane regions of MGR. The model accounted for the critical elements governing fire spread including wind, topography and fuel heterogeneity. Inherent characteristics of the simulation model included the prediction of fire containment, by physical constructs such as roads and natural barriers for example vegetation, and backfire extinction. Reproduction of fire boundaries facilitated an improved, holistic understanding of the fire system and its controlling factors.

The fire growth model has the potential for integration with existing models used in ecosystem management including models of bush encroachment and plant-herbivore dynamics. Extension of the model to facilitate economic costs and benefits of decisions made by ecosystem managers may be incorporated through the inclusion of ignition risk, suppression costs and land value. The fire growth model provides the impetus for the development of a decision support system that enables ecosystem managers to apply a holistic approach to formulate optimal strategies.

REFERENCES

ALBINI, F.A. (1976). Combining wind and slope effects on spread rate. Unpublished. Intermt. Fire Sci. Lab., Missoula, MT. 16 pp

ALBINI, F.A. (1981). A model for the wind-blown flame from a line fire. *Comb. Flame*, 43: 155-174.

ALBINI, F.A. (1985a). A model for fire spread in wildland fuels by radiation. *Comb. Sci. Tech.* 42: 229-258.

ALBINI, F.A. (1985b). Wildland fire spread by radiation - A model including fuel cooling by convection. *Comb. Sci. Tech.* 45: 101 pp.

ALBINI, F.A. and STOCKS, B.J. (1986). Predicted and observed rates of spread of crown fires in immature Jack Pine. *Comb. Sci. Tech.* 48: 65-76.

ANDERSON, H.E. (1982). *Aids to determining fuel models for fire behaviour.* USDA For. Serv., Intermt. For. and Range Exp. Stn., Ogden, UT. Gen. Tech. Rep., INT-122: 22 pp.

ANDERSON, H.E. (1983). *Predicting wind-driven wild land fire size and shape.* USDA For. Serv., Intermt. For. and Range Exp. Stn., Ogden, UT. INT-305: 26 pp.

ANDREWS, P.L. (1986). *BEHAVE: Fire behaviour prediction and fuel modelling system - BURN subsystem, Part 1.* USDA For. Serv., Intermt. Res. Stn. Gen. Tech. Rep. INT-194: 130 pp.

ANDREWS, P.L. (1988). Use of the Rothermel fire spread model for fire danger rating and fire behaviour prediction in the United States. In: *Conference on Bushfire Modelling and Fire Danger Rating Systems.* Cheney, N.P. and Gill, A.M. (Eds). CSIRO, Australia. pp 1-8.

BEAUFAIT, W.R. (1965). *Characteristics of backfires and headfires in a pine needle bed.* USDA For. Serv. Res. Note, INT-30.

BROWN, J.K. and DEBYLE, N.V. (1989). *Effects of prescribed fire biomass and plant succession in Western Aspen*, For. Serv. Res. Paper, FSRP/INT-412.

BOND, W.J. and VAN WILGEN, B.W. (1996). *Fire and plants.* Population and Community Biology. Chapman and Hall, London. 14: 188-203.

BURGAN, R.E. (1979). *Fire danger/fire behaviour computations with the Texas Instruments TI-59 calculator: User's manual.* USDA For. Serv., Intermt. For. and Range Exp. Stn., Ogden, UT. Gen. Tech. Rep. INT-61: 25 pp.

BURGAN, R.E. and HARTFORD, R.A. (1988). Computer mapping of fire danger and fire locations in the continental United States. *Journal of Forestry.* 86 (1): 25-30.

BURGAN, R.E. and ROTHERMEL, R.C. (1984). *BEHAVE: Fire behaviour prediction and fuel modelling system - Fuel subsystem.* USDA For. Serv., Intermt. For. and Range Exp. Stn., Ogden, UT. Gen. Tech. Rep. INT-167: 126 pp.

BURROWS, N.D. and SNEEUWJAGT, R.J. (1988). McArthur's forest fire danger meter and the forest fire behaviour tables for Western Australia: Derivation, applications and limitations. In: *Conference on Bushfire Modelling and Fire Danger Rating Systems.* Cheney, N.P. and Gill, A.M. (Eds). CSIRO, Australia. pp 65-78.

BYRAM, G.M. (1959). Combustion of forest fuels. In: *Forest fire - Control and Use.* Davis, K.P. (Ed). McGraw-Hill, New York. pp 61-89.

CATCHPOLE, T. and DE MESTRE, N. (1986). Physical models for a spreading line fire. *Australian Forestry.* 49 (2): 102-111.

CHENEY, N.P. (1981). Fire behaviour. In: *Fire and the Australian biota.* Gill, A.M., Groves, R.H. and Noble, I.R. (Eds). Australian Academy of Science, Canberra. pp 157-175.

CHENEY, N.P (1988). Models used for fire danger rating in Australia. In: *Conference on Bushfire Modelling and Fire Danger Rating Systems*. Cheney, N.P. and Gill, A.M. (Eds). CSIRO, Australia. pp 19-28.

CLARKE K.C., BRASS, J.A. and RIGGAN, P.J. (1994). A cellular automaton model of wildfire propagation and extinction. *Photogrammetric Engineering & Remote Sensing*. 60 (11): 1355-1367.

CONGALTON, R.G., GREEN, K. and TEPLY, J. (1993). Mapping old growth forests on national forest park lands in the Pacific Northwest from remotely sensed data. *Photogrammetric Engineering and Remote Sensing*. 59 (4): 529-535.

DEEMING, J.E., BURGAN, R.E. and COHEN, J.D. (1978). *The national fire danger rating system - 1978*. USDA For. Serv., Intermt. For. and Range Exp. Stn., Ogden, UT. Gen. Tech. Rep., INT-39: 63 pp.

EDWARDS, P.J. (1984). The use of fire as a management tool. In: *Ecological Effects of Fire in South African Ecosystems*. Booysen, P. de V. and Tainton, N.M. (Eds). Springer-Verlag: Berlin. pp 349-362.,

EVERSON, T.M., VAN WILGEN, B.W. and EVERSON, C.S. (1988). Adaptation of a model for fire danger rating in the Natal Drakensberg. *South African Journal of Science*. 84: 44-49.

FINNEY, M.A. (1994a). *Modelling the spread and behaviour of prescribed natural fires*. Unpublished. Sys. for Env. Man., Missoula, MT. 6 pp.

FONS, W.L. (1946). Analysis of fire spread in light forest fuels. *J. Agrc. Res.* 72 (3): 93-121.

FRANDSEN, W.H. (1971). Fire spread through porous fuels from the conservation of energy. *Comb. and Flame*. 16: 9-16.

FROST, P.G.H. (1984). The responses on savanna organisms to fire. In: *International Savanna Symposium*. Tothill, J.C. and Mott, J.C. (Eds). pp 232-237.

GAYLORD, R.J. and NISHIDATE, K. (1996). *Modelling Nature: Cellular Automata simulations with Mathematica®*. Springer-Verlag, New York. 260 pp.

GREEN, K., FINNEY, M., CAMPBELL J., WEINSTEIN, D. and LANDRUM, V. (1995). Using GIS to predict fire behaviour. *Journal of Forestry*. pp 21-25.

GOODMAN, P.S. (1982). The dilemma of artificial water points in Mkuze Game Reserve. In Anonymous (1986). *Mkuze Game Reserve Management Plan*, Appendix 5. Unpublished. Natal Parks Board, Queen Elizabeth Park, Pietermaritzburg.

GOODMAN P.S. (1990). *Soil, vegetation and large herbivore relations in Mkuze Game Reserve, Natal*. Unpublished PhD thesis, Univ. of the Witwatersrand, Johannesburg.

KARAFYLLIDIS, I. and THANAILAKIS, A. (1997). A model for predicting forest fire spreading using cellular automata. *Ecological Modelling*. 99: 87-97.

KOURTZ, P.H. and O'REAGAN, W.G. (1971). A model for a small forest fire...to simulate burned and burning areas for use in a detection model. *For. Sci.* 17 (2): 163-169.

KUSHLA, J.D. and RIPPLE, W.J. (1997). The role of terrain in a fire mosaic of a temperate coniferous forest. *Forest Ecology and Management*. 96: 97-107.

LUKE, R.H. and MCARTHUR, A.G. (1978). *Bushfires in Australia*. Australian Government Publishing Service. Canberra. 359 pp.

MCARTHUR, A.G. (1967). *Fire behaviour in eucalypt forests*. For. & Timb. Bur. Leaflet No. 100.

MERRIL, D.F. and ALEXANDER, M.E. (1987). *Glossary of forest fire management terms*. Natl. Res. Counc. Can. Can. Comm. For. Fire Management. Publ. NRCC-26515.

NELSON, R.M. and ADKINS, C.W. (1986). Flame characteristics of wind-driven surface fires. *Can. J. For. Res.* 16: 1293-1300.

NELSON, R.M. and ADKINS, C.W. (1987). A dimensionless correlation for the spread of wind-driven fires. *Can. J. For. Res.* 18: 391-397.

PUTNAM, A. A.(1965). A model study of wind-blown free-burning fires. In: *Proc. 14th Symposium on Combustion.* Comb. Inst., Pittsburgh. pp 1039-1046.

ROTHERMEL, R.C. (1972). *A mathematical model for predicting fire spread in wildland fuels*. USDA For. Serv., Intermt For. and Range Exp. Stn, Ogden, UT. Res. Pap. INT-115: 40 pp.

ROTHERMEL, R.C. (1983). *How to predict the spread and intensity of forest and range fires*. USDA For. Serv., Intermt. For. and Range Exp. Stn., Ogden, UT. Gen. Tech. Rep. INT-143: 161 pp.

SANDWITH, T.S (1996). *Natal Parks Board protected area management plan - Draft Format.* Unpublished. Natal Parks Board, Queen Elizabeth Park, Pietermaritzburg.

SCHULZE, B.R. (1965). *Climate of South Africa* Part 8, General Survey. South African Weather Beareau. Government Printer, Pretoria.

STOCKS, B.J., LAWSON, B.D., ALEXANDER, M.E., VAN WAGNER, C.E., MCALPINE, R.S., LYNHAM, T..J. and DUBE, D.E. (1988). The Canadian system of forest fire danger rating. In: *Conference on Bushfire Modelling and Fire Danger Rating Systems.* Cheney, N.P. and Gill, A.M. (Eds). CSIRO, Australia. pp 9-18.

THOMPSON, M.W. (1993). *Quantitative biomass monitoring and fire severity mapping techniques in savanna environments using Landsat Thematic Mapper imagery.* C.S.I.R. Div. of For. Sci. and Tech. Rep. FOR-DEA 587: 55 pp.

THOMPSON, M.W. (1995). *A standardised land-cover classification for remote sensing applications in South Africa.* C.S.I.R. Div. of For. Sci. and Tech. Rep. FOR-I 569: 31 pp.

THORNTHWAITE, C.W. (1948). An approach toward a rational classification of climate. *Geographical Review.* 38: 55-94.

TROLLOPE, W.J. (1978). Fire behaviour – A preliminary study. *Proc. of Grassland Soc. of Southern Africa.* 13: 123-128.

TROLLOPE, W.J. (1984a). Fire in savanna. In: *Ecological Effects of Fire in South African Ecosystems.* Booysen, P. de V. and Tainton, N.M. (Eds). Springer-Verlag, Berlin. pp 149-176.

TROLLOPE, W.J. (1984b). Fire behaviour. In: *Ecological Effects of Fire in South African Ecosystems.* Booysen, P. de V. and Tainton, N.M. (Eds). Springer-Verlag, Berlin. pp 199-218.

VAN WAGNER, C.E. (1988). Effect of slope on fires spreading downhill. *Can. J. For. Res.* 18: 818-820.

VAN WILGEN, B.W. (1984). Adaptation of the United States fire danger rating system to fynbos conditions. Part I - A fuel model for fire danger rating in the fynbos biome. *South African Journal of Forestry.* 129: 61-65.

VAN WILGEN, B.J. and BURGAN, R.E. (1984). Adaptation of the United States fire danger rating system to fynbos conditions. Part II - Historic fire danger in the fynbos biome. *South African Journal of Forestry.* 129: 66-78.

VON NEUMANN, J. (1966). *Theory of self-reproducing automata.* University of Illinois, Urbana.

WEISE, D.R. and BIGING, G.S. (1996). Effects of wind velocity and slope on flame properties. *Can. J. For. Res.* 26: 1849-1858.

WEISE, D.R. and BIGING, G.S. (1997). A qualitative comparison of fire spread models incorporating wind and slope effects. *For. Sci.*, 43 (2): 170-180.

WILLS, A.J. (1987). *The "BEHAVE" fire behaviour prediction and fuel modelling system.* Unpubl., Natal Parks Board Rep. 23 pp

WILSON, R. (1980). *Reformulation of the Rothermel fire spread equations in SI units.* USDA For. Serv., Intermt. For. and Range Exp. Stn. INT-292: 6p with errata.

PERSONAL COMMUNICATIONS

GOODMAN, P.S. (1999). Personal communication. Kwa-Zulu Natal Nature Conservation Services, Queen Elizabeth Park, Pietermaritzburg.

KARAFYLLIDIS, I. (1998). Personal communication. Democritus Univ. of Thrace, Dept. of Elec. and Comp. Eng., Xanthi, Greece.

APPENDIX 1

ROTHERMEL FIRE SPREAD MODEL

INPUT/OUTPUT PARAMETERS FOR BASIC EQUATION IN METRIC FORM (WILSON, 1980)

Input

w_n	Ovendry fuel loading, kg/m^2
δ	Fuel depth, m
σ_v	Surface area:volume ratio, cm^{-1}
h	Fuel heat content, kJ/kg
ρ_p	Fuel particle density, kg/m^3
M_f	Fuel moisture content, dimensionless fraction
S_t	Fuel total mineral content, dimensionless fraction
S_e	Fuel effective mineral content, dimensionless fraction
U	Windspeed at midflame height, m/min
tan ϕ	Slope (vertical rise/horizontal run), dimensionless fraction
M_x	Fuel moisture of extinction, dimensionless fraction

Output

R	Spread rate, m/min
I_r	Reaction intensity, $kJ/(min.m^2)$
I_B	Byram fireline intensity, kW/m
L_f	Flame length, m

SUMMARY OF BASIC FIRE SPREAD EQUATION IN SI UNITS

The equations listed below reflect changes by Albini (1976) and the metric formulation by Wilson (1980).

$$R = \frac{I_r \xi (1 + \phi_w + \phi_s)}{\rho_b \varepsilon Q_{ig}}$$

where

$I_r = \Gamma' \omega_n h \eta_m \eta_s$, reaction intensity

$\xi = (192 + 7.9095\sigma_v)^{-1} \exp\{(0.792 + 3.7597\sigma_v^{0.5})(\beta + 0.1)\}$, propagating flux ratio

$\phi_w = C(3.281U)^B \left(\frac{\beta}{\beta_{op}}\right)^{-E}$, wind factor

$\phi_s = 5.275\beta^{-0.3}(\tan\phi)^2$, slope factor

$\rho_b = \frac{\omega_n}{\delta}$, ovendry bulk density

$\varepsilon = \exp\left(\frac{-4.528}{\sigma_v}\right)$, effective heating number

$Q_{ig} = 581 + 2594M_f$, heat of pre-ignition

$\Gamma' = \frac{\left\{\left(\frac{\beta}{\beta_{op}}\right)\exp\left(1 + \frac{\beta}{\beta_{op}}\right)\right\}^A}{(0.0591 + 2.92\sigma_v^{-1.5})}$, optimum reaction velocity

$\eta_m = 1 - 2.59\left(\frac{M_f}{M_x}\right) + 5.11\left(\frac{M_f}{M_x}\right)^2 - 3.52\left(\frac{M_f}{M_x}\right)^3$, moisture damping coefficient

$\eta_s = 0.174 S_e^{-0.19}$, mineral damping coefficient

$\beta_{op} = 0.20395\sigma_v^{-0.8189}$, optimum packing ratio

$$\beta = \frac{\rho_b}{\rho_f}, \text{ packing ratio}$$

$$A = 8.9033\sigma_v^{-0.7913}$$

$$B = 0.15988\sigma_v^{0.54}$$

$$C = 7.47\exp\left(-8.711\sigma_v^{0.55}\right)$$

$$E = 0.715\exp\left(0.010941\sigma_v\right)$$

METRIC EQUATION FOR BYRAM'S FIRELINE INTENSITY

$$I_B = \frac{1}{60} I_r R \left(\frac{12.6}{\sigma_v}\right)$$

METRIC EQUATION FOR FLAME LENGTH

$$L_f = 0.0775 I_B^{0.46}$$